ADAPTATION OF MICROBIAL COMMUNITIES AND THEIR FUNCTIONS TO ENVIRONMENTAL PRESSURES IN AN URBAN WATERWAYS SYSTEM

GOURVENDU SAXENA

NATIONAL UNIVERSITY OF SINGAPORE

2014

ADAPTATION OF MICROBIAL COMMUNITIES AND THEIR FUNCTIONS TO ENVIRONMENTAL PRESSURES IN AN URBAN WATERWAYS SYSTEM

GOURVENDU SAXENA
(M.Sc, NTU)

A THESIS SUBMITTED

FOR THE DEGREE OF DOCTOR OF PHILOSOPHY

DEPARTMENT OF BIOLOGICAL SCIENCES

NATIONAL UNIVERSITY OF SINGAPORE

2014

DECLARATION

I hereby declare that the thesis is my original work and it has been written by me in its entirety. I have duly acknowledged all the sources of information which have been used in the thesis.

This thesis has also not been submitted for any degree in any university previously.

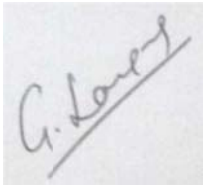

_____

Gourvendu Saxena

(24th January 2014)

ACKNOWLEDGEMENTS

I owe my deepest gratitude to my supervisor A/P Sanjay Swarup, for his persistent guidance, motivation, understanding and patience, without which this thesis would not have been possible.

I would also like to thank my university, National University of Singapore, for providing financial support and excellent research environment. In addition, my deepest thanks to Sustainable Development & Water Alliance, previously known as Singapore Delft Water alliance (SDWA) and The Singapore Centre on Environmental Life Sciences Engineering (SCELSE) for providing research funding.

During this long journey, I got the opportunity to interact with researchers of diverse backgrounds, which helped me gain further insights into microbial ecology. Discussions with Prof. Phanikumar, Mantha, Prof. Peter Steinberg, Prof Stefan Wuertz and Dr. Veronica Rajal were insightful. I appreciate the feedback offered by Dr. Rohan Williams and Dr. Federico Lauro. I thank all my lab members, colleagues from SDWA and SCELSE for all countless discussions with constructive comments and warm encouragements.

My special thanks to Ms. Liew Chye Fong, Ms. Reena Devi and Ms. Priscilla Li for all the help in administration matters.

Last but not the least, I thank my family for being patient and supportive since I began my journey in this world.

PUBLICATIONS

- Gourvendu Saxena, *et al.* and Sanjay Swarup, *Non-anthropogenic factors have major influence on ecogenomics of microbial communities in well-managed canal networks of highly urbanized environments.* (in preparation)
- Gourvendu Saxena, *et al.* and Sanjay Swarup, *Rain perturbations influence sediment associated microbial communities structure and function in tropical urban storm water canals.* (in preparation)
- Gourvendu Saxena, *et al.* and Sanjay Swarup, *Perturbations initiate successional response in sediment associated urban water ways microbial communities: a mesocosm study* (in preparation)

CONFERENCES

- Oral presentation: Gourvendu Saxena, *et al.* and Sanjay Swarup, *Integration of omics and engineering approaches to understand microbial processes in urban waterways*, 2nd Water research conference: 20-23 January 2013, Singapore
- Oral presentation: Gourvendu Saxena, *et al.* and Sanjay Swarup, *Land-use and non-anthropogenic factors influence microbial communities in urban canal networks*. 2014 Water Microbiology Conference, 5-7 May 2014, Chapel Hill, North Carolina, USA
- Oral presentation and poster: Gourvendu Saxena, *et al.* and Sanjay Swarup, *Trends of microbial taxa and functional adaptive responses of sediment microbiome remain conserved in different land use types.* SAME13: 8-13 September 2013, Stresa, Italy
- Poster: Gourvendu Saxena, *et al.* and Sanjay Swarup, *Effects of sediments, water, and land use patterns in shaping microbial community composition and functioning in urban freshwater system.* ISME 14: 19-24August 2012, Copenhagen, Denmark

Contents

Summary

Growing demand for water in cities has led to development of extensive canal infrastructure in cities to capture storm water. While much is known about influences of chemical pressures in contaminated water systems, influence of environmental pressures in urban waterways are highly understudied. Therefore, there is an increasing need to understand how urban waterways can function as an ecological system in highly urbanized environments, with special emphasis on microbial process in these environments. Microbial communities in these waterways provide ecological services, such as primary productivity, organic matter breakdown, mineralization, contaminant degradation, elemental transformation and nutrient cycling, whose understanding can be used to enhance self-cleaning capacities of freshwater systems. This PhD project was designed using a model, well-managed urban canal network, which is efficient in reducing flooding risks by rapidly transporting stormwater from catchment to the reservoirs, to understand 1) relationships of environmental variables in a well-managed waterway 2) influence of inputs from different land-use types on spatial microbial ecology of the catchment, 3) influence of pulse disturbance due to rain on the structure and functional potential of microbial communities of the waterways and 4) the fate of structure and functions of microbial communities after rain.

Regulated contaminants were below their allowable limits and did not affect microbial communities. Only two of 36 physicochemical inputs, aluminum and copper, formed the key drivers for these communities and explained nearly 25% of variation in microbial communities. Fragmentation in the land-use patterns of the catchment due to elevation topology or another land-use type, showed no influence on microbial

communities in the waterways within a given land-use. Such non-fragmented microbial communities can thus be indicators of well-functioning waterways. In addition, as sediment microbial communities were more diverse than in water phase and their functional potential distinguished different land-use types, they seem closely linked to ecological services responding to environmental inputs and can be a better monitoring parameter than those in water phase. Ecological principles can thus be used to identify key practices for managing urban catchments and canal networks.

Perturbation of sediment-associated microbial communities due to rain pulse disturbance could be allowing the microbial communities to reset and start new successional cycle. Such regular cycles could promote higher alpha diversity in waterways sediments. Successional pattern observed in the mesocosm experiment provides evidences of microbial community shifting to anaerobic phase, about week after the rain and preferred nitrate reduction to ammonium as their principle energy harvesting pathway. Despite the differences in the microbial community structure, the successional changes were conserved in the three different land-use types. Relative abundance of active mRNA transcripts also showed similar trends with relatively higher resistance to change. Similar successional trend of microbial taxa irrespective of land-use types provide evidences for core assemblage and conserved functional properties in microbial communities in these environments.

List of abbreviations

Abbreviation	Explanation	Abbreviation	Explanation
RFWR	Renewable freshwater resources	DNA	Deoxyribonucleic acid
USEPA	United States Environment Protection Agency	RNA	Ribonucleic acid
WHO	World Health Organization	PCR	Polymerase chain reaction
ABC	Active, Beautiful, Clean	SS 16s rDNA	Smaller subunit of 16s ribosomal DNA
WUSD	Water Sensitive Urban Design	D/ANRA	Dissimilatory/Assimilatory nitrate reduction to ammonium
^{0}C	Degree Celsius	bp	Base-pairs
km	Kilometer	NGS	Next generation sequencing
cm	Centimeter	T-RFLP	Terminal –restriction fragment length polymorphism
g	Gram	ICP-MS	Inductively coupled plasma-mass spectrometry
mg	Miligram	IC	Ion-Exchange chromatography
L	Liter	HPLC	High performance liquid chromatography
min	Minute	GC-MS	Gas chromatography-mass spectrometry
mL	Milliliter	FGA	functional gene array
µg	Microgram	ANOVA	Analysis of variance
µL	Microliter	PERMANOVA	Permutational multivariate ANOVA
µm	Micrometer	ANOSIM	Analysis of similarity
ppm	Parts per million	CCA	Canonical correspondence analysis
ppb	Parts per billion	NMDS	Non-metric multidimensional scaling
khz	Kilo-hertz	VCP	Variation coefficient portioning

M	Molar		
FU	Fluorescent units	NO_2	Nitrite
s	Second	NO_3	Nitrate
ng	Nano-gram	PO_4	Phosphate
NS	Not significant	SO_4	Sulfate
ND	Not detected	NH_4	Ammonium
rpm	Revolutions per minute		
		Na	Sodium
TDS	Total dissolved solids	K	Potassium
DO	Dissolved oxygen	Mg	Magnesium
TOC	Total organic carbon	Ca	Calcium
ORP	Oxidation-reduction potential	Al	Aluminum
pO_2	Partial-pressure of oxygen	Co	Cobalt
pH	Negative logarithmic concentration of hydrogen ions	Cr	Chromium
Temp	Temperature	Cu	Copper
		Fe	Iron
SPE	Solid phase extraction	Mn	Manganese
BSTFA	N,O bis (trimethylsilyl) trifluoroacetamide	Pb	Lead
HCl	Hydrochloric acid	Cd	Cadmium
PBS	Phosphate buffered saline	Ni	Nickel
PFA	Paraformaldehyde	V	Vanadium
PVC	Polyvinyl chloride	As	Arsenic
		Ti	Titanium
		Zn	Zinc
		Se	Selenium
		Hg	Mercury

List of Tables

List of Figures

Chapter 1: Introduction

Rise in population and subsequent urbanization, driven by recent surge in the economic activity, in tropical (23.5 °S–23.5 °N) and subtropical regions (23.5–35 °S and 23.5–35 °N), has led to expansion of existing cities and emergence of new ones in the region (DeFries and Pandey, 2010; Srinivasan et al., 2013). It is evident from the historical data that transformations in land-use and demography, driven by economic activities are accompanied by higher demand for better living conditions, especially, access to clean water for potable among others (Schneider et al., 2011; Lin and Mele, 2012). The challenge to fulfill the water demand of growing cities is further aggravated by the pressures due to urban land-use on the already scarce water resources available to cities (Tu, 2011; Srinivasan et al., 2013). Several studies show that whereas, rise and non-uniform distribution of population will impact the demand (Buytaert and De Bièvre, 2012; McDonald et al., 2011), climate change will impact the supply of water through phenomena such as skewed spatial/temporal distribution of rain events, longer dry periods (Bender et al., 2010; Elsner et al., 2010; Piao et al., 2010), higher intensity and frequency of extreme events such as storms and cyclones (Bender et al., 2010; Emanuel, 2005; Knutson et al., 2010) and compromised water quality (Vorosmarty, 2000; Whitehead et al., 2009).

The first step in fulfilling water needs is capturing and retaining more water for, which concrete paved urban waterways are been widely used in many cities worldwide (Tortajada and Joshi, 2013). Cities of (sub)tropical region such as Singapore, Jakarta, Kuala- Lumpur and Sydney have developed infrastructure for storm-water collection, transportation and storage to cater the growing water demand which, includes concrete

paved drains, intermediate and large canals (Tortajada and Joshi, 2013; Wong, 2006a). Many other emerging cities are following suit. These waterways penetrate the urban landscape marked with different types of land-use and capture water from the catchment area they cover. They are designed to increase the hydraulic capacity in response to the urbanization and increased imperviousness (Niemczynowicz, 1999; Tortajada and Joshi, 2013; Villarreal et al., 2004; Walsh, 2000) Catchment imperviousness and concrete pavement of the urban waterways not only brings about low stormwater infiltration, high peak flow coupled with short duration turbulence, large stormwater velocity variations, erosion and heterogeneous settlement of sediments but also pressures from local land-use such as sediment load, chemicals and micro-organisms mixed with storm water to the waterways All these factors not only reduce the macro and micro fauna of these freshwater compared to natural bodies, bring poor aesthetics to the canals, frequent dry wet cycles and make stormwater canals a potential reservoir of pathogens (Niemczynowicz, 1999; Walsh, 2000; Wu et al., 2008; Badin et al., 2008), but also facilitate the release of physicochemical variables that could impact the microbial community and its functions in stormwater canals.

Though, impact of anthropogenic sources on microbial communities is well established (El-Sheekh and Hamouda, 2013; Kirchman et al., 2004; Ledin, 2000; Zanaroli et al., 2012a), influences of soft metals on microbial community and its functioning is poorly understood which needs special attention because of their perceived harmless nature, particularly when urban waterways, with longer water residence time, are being transformed to provide self-cleaning ecological services. Novel soft ecological engineering approaches which are primarily driven by micro-organisms, of water sensitive urban designs are being developed and tested in highly urbanized cities such as Singapore, Melbourne (Australia) (Wong, 2006a, 2006b) and Auckland (New Zealand) (Grimm et al., 2008) to improve the utility of waterways and to decrease the risks

associated with them (Wong, 2006a, 2006b). These soft approaches mainly aim to conserve fresh water ecosystem and maximize the self-cleaning capacity by microbial communities.

Sediment-associated microbial communities are the drivers of most of the biogeochemical activity in surface water systems (Canfield et al., 2010; He et al., 2010a; Orcutt et al., 2011; Petersen et al., 2012a; Reese et al., 2013). They form complex communities, which share diverse functions among them including primary productivity, foliage litter decomposition and elemental cycling. Their assemblage based on functional requirements rather than species was recently reported (Burke et al., 2011). The potential for micro-organisms to degrade wide range of organic contaminants, exploitation of small energy gaps from wide range of redox reactions and sequestering heavy metals has been widely studied and documented (Canstein et al., 2002; El-Sheekh and Hamouda, 2013; Ganguli and Tripathi, 2002; Mußmann et al., 2013; Newell et al., 1995; Radwan et al., 2002; Singh et al., 2006). However, the effects of urban pressures and rain perturbation on their assemblage remains poorly understood, especially in tropical environments, largely due to the lack of metagenomics data of urban sediment-associated microbiome. An understanding of the effects of these pressures is important because the former is related to non-uniform distribution of population and the latter is associated with climate change.

Since, the principles governing microbial functioning in other natural systems such as rivers which have less influence from man-made structures cannot be directly applied to the urban waterways systems, similar understanding of microbial functioning in the urban sediment and water systems and the key environmental regulators is necessary. It will further help in optimizing ecologically efficient solutions with low energy regime to be applied to urban systems.

With this motivation, the overall goal of this PhD project was to understand the structure and functions of microbial communities and their associations with environmental drivers in a well-managed urban catchment.

To meet this overall objective following specific objectives were set:

1. To understand the relationships of environmental variables in an urban waterways network
2. To study the spatial microbial ecology and influence of inputs from different land-use types on microbial communities of a well-managed waterway
3. To understand influence of pulse disturbance due to rain on the structure and functional potential of microbial communities of the waterways
4. To study the fate of microbial communities assemblage and their functions after rain.

The overall project was divided into two field studies and one mesocosm study. Field study 1 was further divided into two studies which formed result Chapters 3 and 4, respectively. While field study 1 focused on the first two objectives of the project, field study 2 and mesocosm study concentrated on objectives 3 and 4, respectively.

Chapter 1 gives a general introduction of the project and provides an overview of the thesis organization. Chapter 2 reviews the literature and provides the necessary insights into the current state of research in the field.

The result Chapter 3 explains various aspects of the model catchment and the sampling locations used in the study. It, then, explains the spatial trends of physic-chemical parameters associated with sediment and water samples from the catchment. It also covers the relationships of environmental parameters from sediment and water samples.

The overall organization of the study plan is shown below:

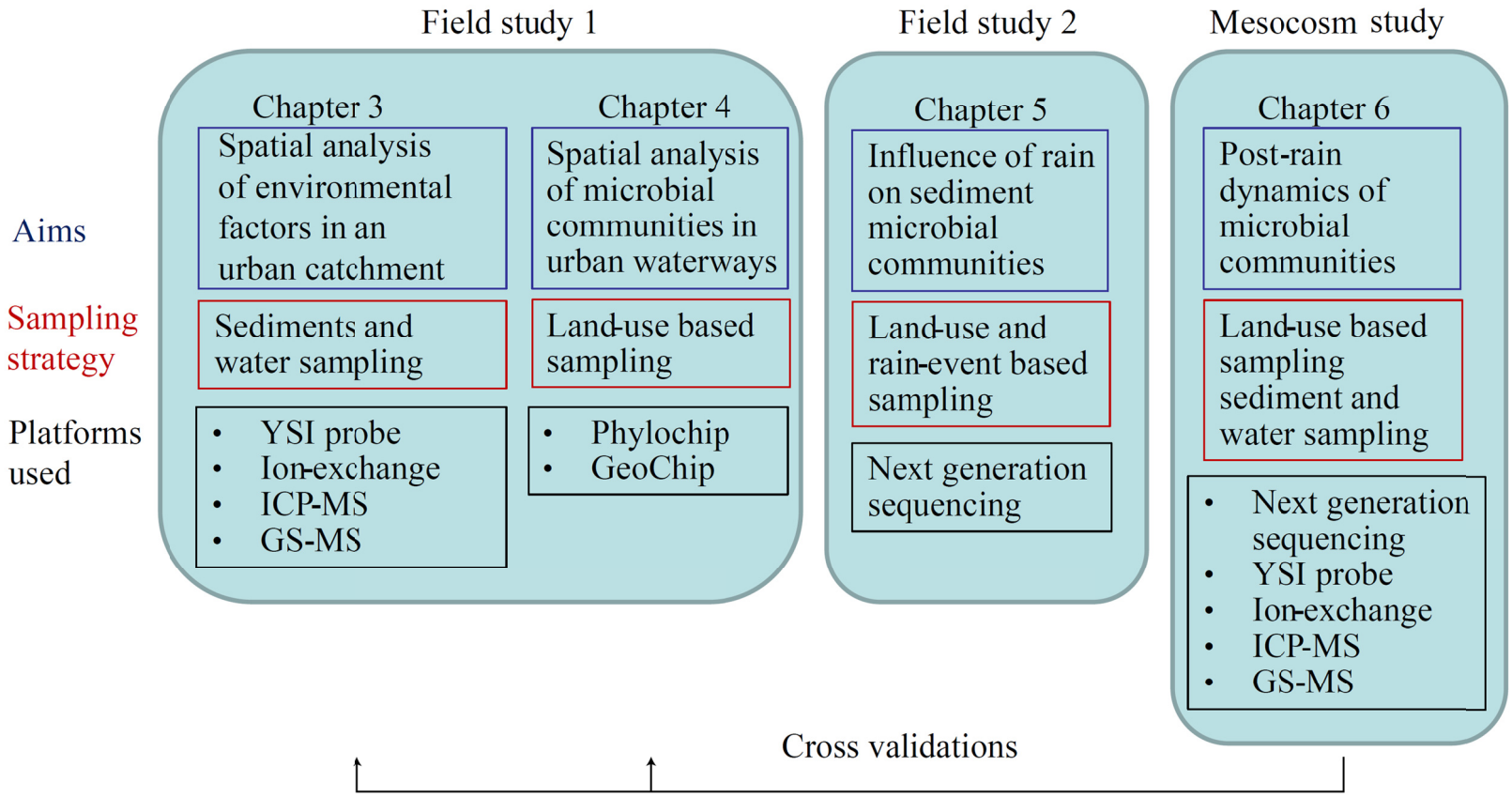

Result Chapter 4, discusses the spatial distribution of sediment and water associated microbial communities in stormwater canals of model catchment. Functional ecology was determined using GeoChip (2.0) which is a hybridization based chip targeting gene variants from different functional gene categories relevant to biogeochemical processes. Taxa based ecology was identified using Phylochip (G2) which is also a hybridization based chip targeting variable regions of 16s rDNA to detect microbial taxa groups.

Result Chapter 5, from field study 2, aims to identify the differences in microbial community taxa structure and functional potential due to pulse rain disturbance in two land-use types, residential and industrial. The results are based on metagenome sequencing data with annotation using NCBI database for taxa identification and KEGG/SEED databases for functional genes annotations.

Result Chapter 6 explains the mesocosm study, focusing the 4th objective of the project. The study explains the taxa and functional successions of sediment-associated microbial communities from three sediment types, residential, industrial and mixture of two, after a rain-event.

Finally, Chapter 7 summarizes the major findings and highlights further questions, which can be addressed in next studies.

Chapter 2: Literature review

Urbanization and its implications

Urbanization which is the natural outcome of industrialization and demographic transition, has intensified in the past few decades due to recent rise in economic growth, especially in emerging economies. In future, as world population grows further, more urban centers will emerge and attract increasing number of people migrating from rural areas in search of better living standards. United Nations report on world urbanization prospects (2007) shows that since 1950, the world urban population has increased more than thrice and it is predicted that such trend will continue in future. By the end of 2050, 6 out of 10 billion people will live in cities. By the year 2008 (2050), ≈50% (67%) of the world population was living in urban areas with 47% (64%) of less developed and 78% (86%) of more developed regions being urbanized. While, the population in rural areas of more developed regions is already lower than urban areas and declining, urban population in these regions is on the rise.

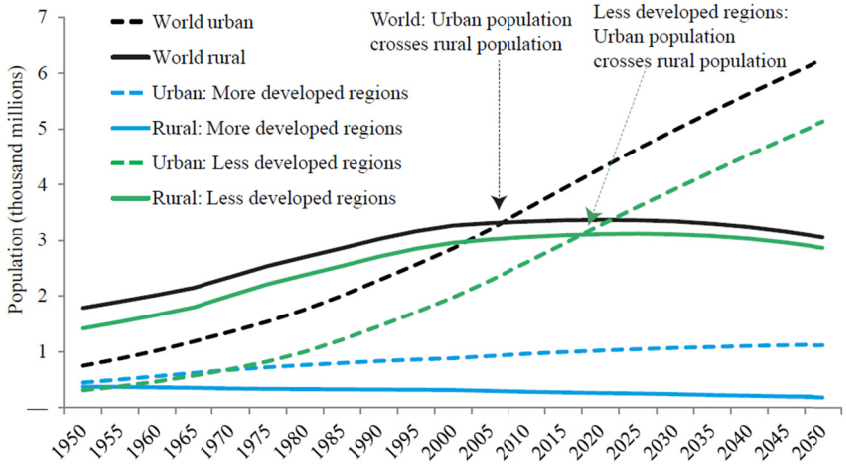

Figure 2.1. World urban and rural population trends (Data source: United Nations DESA/Population Division World Urbanization Prospects: The 2011 Revision)

The population trends in less developed regions, indicate that currently urban population in these areas is lower than rural population but it is growing fast and will exceed the rural population before 2020 ("United Nations, DESA (Population Division) World Urbanization Prospects: The 2007 Revision (1st February 2008) ESA/P/WP/205") (Fig. 2.1). Interestingly, many urban agglomerations are concentrated in tropical and subtropical making them hotspots for urban activities in near future. Consistent with this, the number of cities with population more than 1 million has increased exponentially. There were 83, 160, 348 and 441 cities with more than 1 million inhabitants in the years 1950, 1975, 2000 and 2010, respectively. Megacities which by definition means metropolitan agglomeration with population size of more than 10 million, have also increased substantially. In 1950, there were only two megacities, New York and Tokyo. In 1980, four cities crossed the benchmark. However, by the end of 2011, this number increased to 23 and by 2025, there will be 35 megacities with most new entries from Asia (Fig. 2.2). Currently, about 10% world population lives in these megacities and by 2025, it will increase 13.6%. The increase in urban centers and concentration of population in these areas clearly indicates that disproportionate colonization of human beings will continue in the 21st century.

Collectively, cities across the globe represent 2% of the surface area, inhabit about 50% of population and utilize 75% of the world resources ("United Nations, DESA (Population Division) World Urbanization Prospects: The 2011 Revision (1st August 2012) ST/ESA/SER.A/322"). Such disproportionate colonization and utilization of resources by human population due to rapid urbanization, has not only posed sustainability challenges in sectors such as food security (Chen, 2007; Rosegrant and Cline, 2003; Stage et al., 2010) and health (Freudenberg and Galea, 2008) but also highlighted the necessity to ensure water security across many parts of the world

especially in emerging megacities of developing countries (Srinivasan et al., 2013; Varis, 2006a; Varis et al., 2006). Rise in demand for better quality food and water are reported to be closely linked to both population growth and urbanization (Satterthwaite et al., 2010; Stage et al., 2010).

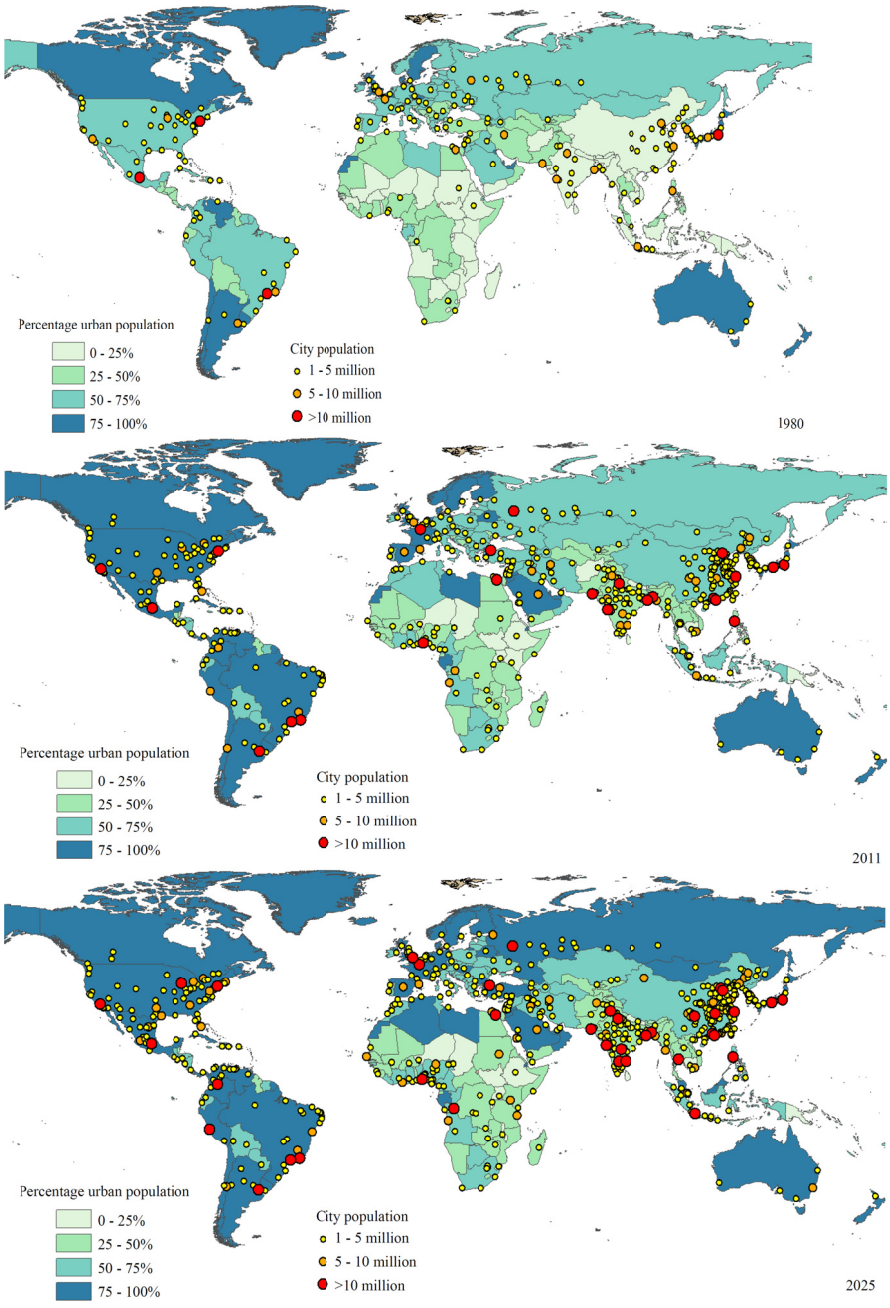

Figure 2.2. Increasing trend of urbanization across the world over time. (Source: United Nations, Department of Economic and Social Affairs, Population Division: World Urbanization Prospects, the 2011 Revision. (New York 2012) http://esa.un.org/unup/Maps/maps_urban_2011.htm)

Water demand and scarcity

Global fresh water discharge (Renewable Fresh water Resources) is about 45,000km^3/year, which flows through the rivers and aquifers annually. Out of which about 3,900 km^3 is withdrawn for human use annually (Oki and Kanae, 2006). This may give the impression that there is plenty of available water for exploitation but because of uneven distribution, both of water resources and human population, pockets of high water stress areas have been inhabited by human population. In addition, due to requirements for natural environmental and ecological processes and seasonal/annual variations, catchments withdrawing more than 10% water for human use are categorized as water stressed. A value more than 0.4 (water stress index, R_{ws}) which is indicative of 40% of available water withdrawal, is an indication of high water stress (OKI et al., 2001). An account of distribution of water stressed countries can be found at Water Resources Institute (WRI), Washington, DC 20002, USA and Oki and Kanae, 2006 (Lehner et al., 2008a; Oki and Kanae, 2006). The distribution of water scarcity areas clearly indicates because of combined effects of high economic growth and limited water resources, many areas will be highly water stressed in coming future (Fig. 2.3).

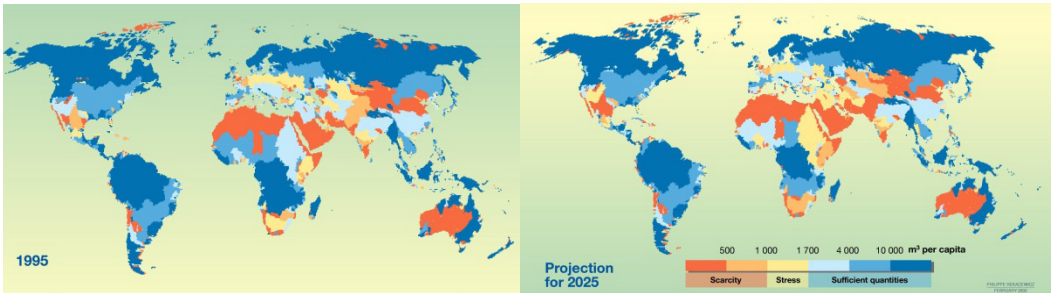

Figure 2.3. Global distribution of water scarcity and projections for 2025 (Source: United Nations Environment Programme, An Overview of the State of the World's Fresh and Marine Waters - 2nd Edition – 2008)

Global water demand which can be divided into four broad categories, namely, demand from 1) industrial sector 2) domestic use 3) live-stock and 4) irrigation, is predicted to

increase from 3,900 km^3 to 4,794 km^3 (IMPACT-WATER projections). For developing countries, it will increase from 2,762 km^3 to 3,528 km^3. The demand for domestic and industrial use, especially from urban areas from developing countries, is set to more than double from 110km^3 and 62 km^3 to 221km^3 and 121 km^3, respectively (Cai and Rosegrant, 2002; Rosegrant and Cai, 2002). The steep increase in future domestic and industrial water demand will have adverse effects on available water resources, especially for cities such as Singapore which has a growing population, high economic growth compounded with limited options for available water resources (Tortajada, 2006). Given that the increase in global fresh water runoff will marginally increase (<10%) in the coming 30 years (Jackson et al., 2001), ensuring water security for the growing population, especially in the urban centers, has emerged as an important issue for policy makes across the world. Therefore, in order cater for the needs of the growing population, it is important that the per-capita availability of water remains unchanged. To achieve this, enhancing the efficiency of water management practices is given high importance, worldwide (Varis, 2006b; Varis et al., 2006). Singapore, with its innovative initiatives in managing freshwater, has demonstrated that even for a highly urbanized and fast growing city, keeping constant per capita requirement of water is an achievable objective (Tortajada, 2006).

Water demand and supply in Singapore

Singapore is an island city with a total land area of 700 km^2 and a population of about 5.4 million (http://www.singstat.gov.sg/statistics/latest_data.html#14), making it one of the highly densely populated countries in the world. Past decade of high economic growth has led to the economic prosperity and resulted in a gradual improvement in the quality of life of its people. However, maintaining high economic growth rates with one of the

highest density of population with high quality standard of living puts enormous pressure on the already scarce water resources of this island country. Singapore, with the stress index of >0.4 (R_{ws}) (a ratio of water withdrawal to total renewable water), is categorized as highly water stressed country (Rosegrant and Cai, 2002). Despite of an annual rainfall of 2400mm, Singapore's water scarcity is due to limited land area to store water. Therefore, withdrawal of water from the available water resources is estimated to be more that 80% (Lehner et al., 2008b). Singapore recognized this problem earlier and since 1980, tremendous efforts have been made to ensure water security to support growth and high living standards.

Current approaches

The current water demand of Singapore is about 380 million gallons of water per day. Lack of perennial natural water streams led to the water managers and policy makers of Singapore to develop new resources of water and diversify the available ones. Quest to develop new resources for to meet the current demand and sustainable supply for future, resulted in 4 national water tap policy. The four taps which are aimed at fulfilling water demand with diversified sources are as follows: 1) local catchment 2) imported water 3) reclaimed and purified water known as NEWater and 4) desalinated water ("MOEWR (2006) The Singapore Green Plan 2012, 2006 edition, (http://www.pub.gov.sg)").

Local catchment: Water is collected from catchment through two separate networks. Storm-water is collected through dense network of large, intermediate canals and small drains (8,000km). The sewer lines are separated from storm-water canals. Therefore, the possibility of stormwater getting contaminated by fecal pollution is minimal. Singapore also has 32 small rivers flowing across the island. The water collected through the waterways and rivers, is stored in 17 different reservoirs and used by water purification

agencies to treat water for potable use. With the inclusion of Marina, Punggol and Serangoon Reservoir in 2011, more than 60% of the land area has been brought under catchment which makes Singapore one of the model countries to showcase large-scale rain-water harvesting and its managing its supply (http://www.pub.gov.sg/water/Pages/LocalCatchment.aspx).

Imported water: Before its independence in 1965, Singapore had signed long-term bilateral agreements with Johor state of Malaysia in 1961 and 1962, to import water at a price of 1 cent per 1000 gallons, till 2011 and 2061, respectively. Following the expiry of 2011 agreement, Singapore initiated efforts to extend the second agreement beyond 2061 without much success. Because of, which, Singapore developed the plan to gain self-sufficiency in water sector post 2011. After the expiry of first agreement on 2011, the current imported water is about 250 million gallons per day from the Johore River, Malaysia (Tortajada, 2006).

NEWater: Water conservation is the key to sustainable water supply. With this aim, initiative was taken in May 2000 to recycle the used instead of discharging it in the sea. Encouraged with the initial successes, Public Utilities Board (PUB) started treating all the collected used-water and converting it to highly purified NEWater. Currently, Singapore operates 4 NEWater plants covering 30% of the water demand. At present, NEWater is primarily for non-potable purposes. It is supplied to industries such as wafer fabrication, electronics and power generation for industrial and commercial processes. A small fraction of this water is also returned to the reservoirs for it to re-enter the water cycle of potable use (Routledge, 2013).

Desalination: Desalination has significantly augmented and diversified the available options of water resources for Singapore. Started in 2005, Singapore now operates two

desalination plants, with a total capacity of 100 million gallons water per day, covering 25% of the total water demand of Singapore (http://www.pub.gov.sg/water/Pages/DesalinatedWater.aspx).

Future goals

The current water demand of Singapore stands at 380 million gallons per day, which is expected to more than double in next 50 years. Major fraction (70%) of the demand will come from non-domestic sector, while the rest will be from domestic use (Tortajada, 2006). As it is clear that the water import agreement with Malaysia will expire in 2061, Singapore has developed the strategy to enhance water security and self-sufficiency by increasing the capacity in all the available water resources.

Local catchment:

With the current battery of 17 reservoirs, more than 60% of land-area of Singapore is under catchment. However, from the viewpoint increased of water demand in future, Singapore plans to increase the land-area under catchment from current 60% to 90% by including the remaining streams and rivulets near the shoreline. The plan includes technology development to treat water with variable salinity (http://www.pub.gov.sg/water/Pages/LocalCatchment.aspx).

In addition, Singapore has initiated a program called Active, Beautiful, Clean water program with an overall objective of transforming the current concrete paved urban waterways into naturally looking clean streams with good water quality suitable for human interaction and recreational purposes (MOEWR (2006) The Singapore Green Plan 2012, 2006 edition, (http://www.pub.gov.sg)). The objectives will be achieved by introducing previously explained soft approaches (please see section 3.2) to the drains, canals and reservoirs and integrating them with the surrounding environment. The major

solutions in the list are reduction in the peak flow of captured stormwater, allow the natural microbial communities and plants to clean the water as it flows through the streams and transform the concrete paved canals into natural streams with soft sediment bed. Finally general public will be encouraged to come close to these waterways. A comparison between the canals at Geylang River (ABC site) and Jurong East (no ABC work) is shown in fig. 2.4.

Figure 2.4. View of canals before and after implementation of ABC program. (A) Picture taken on 23rd November 2012 showing current view of stormwater canal at Jurong east. (B) Geylang River after completion of pilot ABC project. (Panel B: With kind permission from Public Utilities Board, Singapore (PUB)) (http://www.pub.gov.sg/mpublications/Pages/PressReleases.aspx?ItemId=397)

NEWater: Keeping the water cycle closed and circulating as much water as possible mitigates the risk of variability associated with natural resources such as rain. Consistent with this, Singapore plans to expand it NEWater capacity to meet 55% of the future demands. Currently it covers about 30% of the current demand (http://www.pub.gov.sg/water/newater/Pages/default.aspx).

Desalination: As Singapore is surrounded by sea from all directions, seawater is available in abundance. It, therefore, serves as another source with minimal risk in variation in supply. Therefore, desalination capacity will also be expanded from current 100 million gallons per day (25% of current demand) to ≈230 million gallons per day (30% of future demand) (http://www.pub.gov.sg/water/Pages/DesalinatedWater.aspx)

Fulfilling water demand

An efficient water management system is the key to mitigate water security threat. Two primary ways which are "classical engineered approaches" and "ecology based approaches" have been proposed and tried to manage the water supply (Wolff and Gleick, 2002).

Classical engineering based approaches

Water was traditionally considered as an abundant resource and therefore, engineered structures (grey) based water-supply dominated the twentieth century. The engineered based approaches of water management aims to maximize the water supply through centralized infrastructure such as dams, reservoirs, concrete channels/ pipelines and water treatment facilities (Wolff and Gleick, 2002). Cities around the world such as Amsterdam, Century city at Cape Town, Delft, Jakarta, Mexico, Sydney, Tokyo, Venice and Singapore have built the canal and reservoir infrastructure for rain water collection and its storage and reduced their water stress to an extent. Apart from the canal infrastructure, other strategies included in the engineered based approaches are desalination, centralized purification of grey water and long-distance water transport from water-surplus areas. While such approaches have effectively mitigate water scarcity, they are overloaded with huge capital-cost, highly energy intensive and threat to natural ecosystems and biodiversity (Vörösmarty et al., 2010) which makes them environmentally unsustainable in a longer run.

Ecological approaches employing microbial communities

The path to meet water demand starts from capturing and retaining more water for, which concrete paved urban waterways have been widely used in many cities worldwide

(Tortajada and Joshi, 2013). However, another objective to meet the water security challenge is maintaining acceptable water quality which is directly linked to the urban engineering associated with canal infrastructure and local land use development. The anthropogenic pressures from different types of land use patterns, artificial fragmentation created within and between catchments coupled with poor management of waterways could lead to deteriorated water quality and thus, the urban lifestyle (Badin et al., 2008). Therefore, meeting the challenge to provide sufficient clean water to current population and upcoming generations will require scientific understanding of soft approaches which are not only economically efficient but also environmentally friendly and socially acceptable. The ecological approaches include different ways to sustainably manage, both, demand and supply of water. The methods used in these approaches include focusing on meeting the water related need of people than merely supplying water, decentralization of water harvesting and storage, engaging the general public in water conservation and maintaining the ecological health of the waterways among others. Unlike engineered centered approaches, ecological approaches emphasize on natural structures (green) for the same purpose (Wolff and Gleick, 2002). Novel soft ecological engineering approaches of Water Sensitive Urban Designs (WSUD) are being developed and tested in highly urbanized cities such as Singapore, Melbourne (Australia) (Wong, 2006a, 2006b) and Auckland (New Zealand) (Grimm et al., 2008) to improve the utility of waterways and to decrease the risks associated with them. The concept of WSUD is defined by the inter-government agreement on a National Water Initiative as "The integration of urban planning with the management, protection and conservation of urban water cycle which ensures that urban water management is sensitive to natural hydrological and ecological processes". The emphasis on integration of urban planning and sensitivity on both hydrological and ecological processes showcases the inter-government recognition of importance of natural processes in providing sustainability

and stability to the urban fresh water systems. The framework of the integration is shown to achieve ecologically sustainable development by integrating water conservation, waste-water minimization, storm-water quality improvement and flow control. The results after 15 years of initiation of the project indicate varied success. Although, the project succeeded in capturing water and maintaining good aesthetics of the waterways, it faced few structural failures including clogging of drainages (Wong, 2006a, 2006b). , which might be due to project's limited focus on the microbial ecology of the waterways system.

Conserving the ecological health, especially microbial ecological health, of the waterways system is important because these systems provide ecological based self-water-purification services ranging from natural geochemical cycles such as primary productivity, foliage litter decomposition and elemental cycling to contaminant degradation and sewage treatment (Ducklow, 2008), which can be used to clean the water as it flows through the canals (Table. 2.1).

Table 2.1 Ecological services by microbial communities

Group	**Processes**	**Services**
Heterotrophic bacteria	Organic matter breakdown, mineralization	Decomposition, nutrient recycling, climate regulation, water purification
Heterotrophic bacteria	Extracellular polymer production	Carbon sequestration
Photoautotrophic bacteria	Photosynthesis	Primary production
Chemoautotrophic bacteria	Specific elemental transformations (e.g. sulfate reduction, iron oxidation)	Nutrient recycling, climate regulation, water purification
Unicellular phytoplankton	Photosynthesis	Primary production
Archaea	Specific elemental transformations (e.g. methanogenesis, nitrification)	Nutrient cycling, atmosphere and climate regulation
Protozoans	Consumption and mineralization of other microbes	Decomposition, nutrient cycling, soil formation
Fungi	Organic matter consumption and mineralization	Decomposition, nutrient cycling, soil formation
Fungi (mycorrhizal)	Nutrient recycling	Primary production (indirect)
Viruses	Lysis of hosts	Nutrient cycling

Microbial communities in surface freshwater systems

Surface freshwater systems, which are the principle source of water for human needs are broadly divided in two major categories, natural freshwater systems and artificial urban fresh water systems.

Microbial biofilms in freshwater environment

It was recently understood that biofilm mode of living enables microbial communities to resist the environmental pressures and allow them to function as a single unit (Lee et al., 2013; Singh et al., 2006). Biofilms in natural environments are complex agglomeration of microbial communities embedded in exo-polymer matrix (EPS). The EPS provides both, structural and protection, to the inhabiting microbial community. EPS allows the movement of nutrients, metabolites, enzymes and also in the disposal of waste products outside and inside of a biofilm matrix (Sheng et al., 2010). In addition, biofilm mode also provides diverse survival strategies to inhabiting microorganisms against environmental stresses such as toxic contaminants and nutrient scarcity For example, biofilms provide enhanced metabolic cooperation, intracellular communication and horizontal gene transfer, increased availability of nutrients for growth, increased synthesis of protective matrix, increased binding of water molecules and higher structure and functional diversity of bacterial population and proximity to progeny and other bacteria (Please see review: Percival et al., 2011).

Combined with the diversity of functional potential, microbial communities, which are resistant to harsh environments, function as a single unit and cover almost all the habitats with all the biogeochemical functions (El-Sheekh and Hamouda, 2013; Ledin, 2000; Newton et al., 2011; Pernthaler, 2013; Petersen et al., 2012b; Radwan et al., 2002; Singh et al., 2006; Wang et al., 2009, 2010; Wilhelm et al., 2013). Therefore,

occasional environmental perturbations to microbial communities could be helpful (rather than damaging) in enhancing the diversification of their metabolic potential.

Natural freshwater systems

Natural freshwater systems, which are responsible for majority of circulating renewable freshwater resources (RFWR) flux (Oki and Kanae, 2006), differ from artificial ones in many respects. These systems mainly include rivers, streams, lakes ponds and reservoirs, which can have varying depths, flow velocities and water discharge rates. In this context, natural freshwater systems are further classified as lentic or lotic systems. Whereas, lenthic water systems show vertical stratification due to depth dependent light penetration and oxygen content, are characterized as stagnant water, lotic systems have moving water and are characterized by continuous mixing of water due to velocity variations and turbulence.

Microbial communities in natural fresh water systems

It is worth noting that, most studies done on the microbial ecology of freshwater systems, so far, are from temperate regions. In addition, studies, done till date, have mostly focused on the easily accessible epilimnetic layer and are highly descriptive in nature (Newton et al., 2011). Because of which, an understanding of microbial communities and their ecological dynamics in the sediment and surface-water habitats tropical regions, is largely missing. Nevertheless, it is understood from the available literature that natural freshwater systems provide habitat to many aquatic organisms and that, microbial communities constitute significant part of the biomass in these systems, thus, they maintain significant aquatic macro, as well as, microbial ecology (Besemer et al., 2013; Jiang et al., 2006; Jones et al., 2013; Krumins et al., 2013; Menon et al., 2013; Morrissey et al., 2013; Newell et al., 1995; Pernthaler, 2013; Wilhelm et al., 2013).

Multiple point and not-point sources, such as, farm-lands, urban catchments and frosted regions, serve as the entry-point of new microbial communities along with different physicochemical parameters to these systems and contribute to the gradual or abrupt longitudinal transitions in the microbial community structure and biogeochemical characteristics such as respiration, primary productivity and degradation of organic contaminants of the systems (Kirchman et al., 2004; Winter et al., 2007). Transitions in the structure and functions of microbial communities are thus indicators of influences from local environment and highlight the importance of the local entry-points. Similarly, temporal successions in microbial communities could also be explained by the gradual shifts in the available resources for microbial communities in the system. Functionally, the natural freshwater systems, with microbial communities as a driver of most biogeochemical processes, could influence climate at local as well as global scale by playing a critical role in global biogeochemical cycling, carbon cycling in particular, despite the small fraction (<1%) they occupy on the Earth (Cotner and Biddanda, 2002; Tranvik et al., 2009). Microbial biomass in the natural freshwater systems serves as the largest sink of carbon, comparable to the marine environments, through respiration (Ask et al., 2009). In addition to carbon cycling, they are involved in wide range of biogeochemical processes, such as, primary and secondary production, nutrient cycling, carbon sequestration, litter decomposition, organics degradation, methanogenesis and fermentation among many others (Ducklow, 2008) and have colonized even in the most challenging environments ranging from Arctic dry valley to hydrothermal vents (Chan et al., 2013; Wang et al., 2009).

Urban freshwater systems

Urban waterways generally include, concrete paved canals, drains, dams and storage reservoirs. While these waterways are designed to increase the hydraulic capacity in

response to the urbanization and increased imperviousness (Niemczynowicz, 1999; Tortajada and Joshi, 2013; Villarreal et al., 2004; Walsh, 2000), they are associated with several challenges, which include low infiltration, high peak flow (Fig. 2.5), erosion and heterogeneous settlement of sediments, frequent dry wet cycles, potential reservoir of pathogens, poor aesthetics and negligible freshwater ecology compared to natural bodies (Badin et al., 2008; Characklis and Wiesner, 1997; Leopold, L. B. 1968; Niemczynowicz, 1999; Walsh, 2000; Wolman, 1967; Wu et al., 2008). Such characteristics differentiate the urban waterways significantly from the natural river systems, thus limiting the direct transfer of principles of river ecology and management system to these systems.

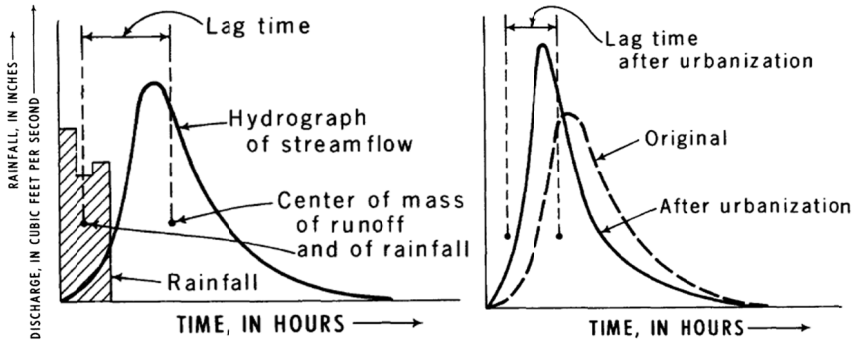

Figure 2.5. Hydrograph relating shifts in peak-flow time lag after rain. Left panel: rain and peak-flow in pre-urbanized conditions; Right panel: comparison between pre and post urbanized state. (Source: Leopold, L. B. 1968)

Urban waterways in tropical regions are of particular significance because of high frequency of heavy rains in the region, which poses a constant risk of flash floods in these regions. Therefore, the primary threat perception of stormwater among urban planners is flood risk and thus, the focus of managing urban waterways has mostly been on improving their efficiency to quickly transport water from catchment to downstream sink. Studies done on impact of urbanization on hydrology of the concrete waterways capturing stormwater (Paul and Meyer, 2001) indicate that coverage of canal infrastructure in the catchment and increase in catchment imperviousness are the hallmark and exclusive features of urbanization. Water discharge due to stormwater

runoff in the waterways after rain is directly related to catchment imperviousness and area under drainage. Studies show that for a catchment, 100% served with the stormwater drainage, a 10-20% increase in imperviousness can double the water discharge when compared to no imperviousness (Arnold and Gibbons 1996, Leopold, L. B. 1968.). Although, not many studies on impact of rain on water hydrology are available from (sub)tropical urban regions, an important inference can be made from a study done in Minnesota, USA (Brezonik and Stadelmann, 2002). The study shows that the runoff volume is highly correlated to the rainfall and imperviousness. Other studies show that higher runoff is directly associated with high peak flow, turbulence and high flow velocity and increase in sediment load, which brings wide range of organic and inorganic pollutants to the canals (Lao et al., 2010; Memarian et al., 2012; Sutherland et al., 2012; Zhao et al., 2010).

The level of pollutants, however, differs for areas with different histories of land-use. For example, heavy metal levels were found significantly different in the sediments of different land-use types in China (Xia et al., 2011). Due to these factors, the water-quality and ecological processes in the waterways systems could experience regular shifts during the rain events. However, the studies on understanding the effects of physicochemical urban inputs brought by stormwater runoff to the receiving waters are limited because continuous pollution of urban waterways with sewage in the past century, the research remained limited to on study the effects sewage pollution on the quality of receiving waters. It was until the last few decades of 20^{th} century, that the degrading nature of stormwater runoff to the receiving waters was recognized (Heaney and Huber, 1984). Therefore, although, the hydrological properties of the waterways in relation to urbanization are well understood, influences of pressure from urban land-uses on the water-quality are understudied.

Microbial communities in urban freshwater systems

Like water-quality, the microbial ecology of the concrete paved urban waterways ecosystem which comprises of two main habitats, sediment and water phase, is also influenced by multitude of factors in an urbanized environment. These factors include, fragmentation due to space, elevation and engineered structures in the stormwater channels (Francis and Chadwick, 2013), physicochemical inputs from different types of land-use (Badin et al., 2008; Characklis and Wiesner, 1997; Jørgensen and Halling-Sørensen, 2000), urban heated effects (Arnfield, 2003), dry-wet cycles and pulse physical perturbations such as rain which not only brings chemicals and new microbial communities washed with the stormwater (Cregger et al., 2012; Cruz-Martínez et al., 2012; Sutherland et al., 2012; Walker et al., 1999), but also affects the ecology by acute velocity variations and turbulence after rain. Though, impact of anthropogenic sources on microbial communities is well established, influences of non-anthropogenic sources on microbial community and its functioning are still poorly understood. The understanding of microbial functioning in relation to their associations with non-anthropogenic factors needs special attention because of their perceived harmless nature.

The structure and functions of microbial communities could also experience permanent shifts in different land-use types and regular temporary shifts during the rain events. Many studies done in the past, clearly show the effects of fragmentation on macro-ecology, with varying degree, in urban environments (Gibb and Hochuli, 2002; Goddard et al., 2010; Tigas et al., 2002). However, for microbial ecology, the studies have recently started to emerge. For example, a recently conducted study in River Ybbs, Austria indicated that the tributaries (headwaters) harbor higher diversity than receiving water (Besemer et al., 2013) in fluvial systems, indicating that the terrestrial area directly in contact with upstream headwaters augment the alpha diversity but selection pressures in downstream local environments and competition tend to reduce it.

Research Gap

Role of microbial communities in providing ecological services to the freshwater systems is well-established (Ducklow, 2008). Such ecological services can be employed to enhance the inherent self-purification capacities of the urban waterways, which have traditionally been used solely for rapid transportation of stormwater. However, not much emphasis was given in the past century to the ecosystems, for example waterways, in urban systems (Grimm et al., 2008). As a result, our knowledge of urban ecosystems is very limited and hence urban problems, such as water quality in the waterways, largely remain unaddressed. In order to develop novel strategies using ecological principles, a thorough understanding of structure and functions of microbial communities and their interactions with the local and regional environmental factors is necessary. We adopted a previously used ecogenomics approach, by which we characterize the structure and functions of microbial communities and combined it with environmental metadata analysis (Debroas et al., 2009; Kim et al., 2012; Kirchman et al., 2004; Wang et al., 2009; Zhang et al., 2013), to fill this gap.

Approaches used in understanding microbial communities

Hybridization based technologies provide high-throughput screening of target genes with full coverage of reported genes in the databases and reproducible results at relatively cheaper price. They allow parallel detection of multiple target genes with better estimation of structure and composition of target genes of interest than molecular methods such as cloning.

DNA figure printing (T-RFLP)

Terminal –Restriction Fragment Length Polymorphism (T-RFLP) is widely used to detect the changes in the microbial community structure and composition (Osborn et al., 2000). The technique relies on the assumption that different microbial species have polymorphism in the position of a restriction site of a restriction enzyme. Hence, SS 16s rDNA variable region (of choice) is amplified with fluorescent labeled primers and digested with a combination of restriction enzymes. The resolving power of T-RFLP can be enhanced by using fluorescent labels on both forward and reverse primers (Schütte et al., 2008). In addition, more number of restriction profiles can be generated by using higher number of restriction enzymes. The profile of the restriction fragments is recorded using capillary electrophoresis. The resulting profile of fragments is the signature of microbial community of interest. Similar principle can also be used to monitor the microbial processes by targeting the functional genes (Morrissey et al., 2013).

GeoChip 2.0

Functional gene abundance of the microbial communities was determined using whole genome hybridization based functional gene array (FGA) known as GeoChip. The array is developed by United States based Institute of Environmental Genomics at University of Oklahoma. The first version of the array called GeoChip 2.0 was released in 2007 (He et al., 2007). The chip covers more than 400 functional gene groups from gene categories such as antibiotic resistance, organic contaminant degradation, metals resistance, carbon, nitrogen, sulfur and phosphorous cycling, with 35,669 (50mer) probes. GeoChip 2.0 and its advanced version GeoChip3 which came later, have been extensively used and revealed functional insights of many habitats around the world, including some of the very extreme environments such as Arctic dry valley and deep sea hydrothermal vents

(Chan et al., 2013; He et al., 2010b, 2007; Liang et al., 2011; Orcutt et al., 2011; Wang et al., 2009), indicating the robustness and global acceptability of GeoChip.

Table 2.2 Probe information for GeoChip 2.0

Gene category	# Genes	# Probe	# Sequence specific probes	# Group specific probes	# Covered CDS
Carbon cycling	41	5196	1765	3431	10573
Carbon fixation	5	1165	270	895	2794
Cellulose degradation	4	305	151	154	484
Lignin degradation	4	330	274	56	419
Other carbon compounds degradation	25	3142	998	2243	6434
Methane oxidation	2	118	87	31	193
Methanogenesis	1	136	2148	52	249
Nitrogen cycling	16	3763	764	1615	7353
Nitrogen fixation	1	1124	764	460	2277
Nitrification	2	111	69	42	257
Denitrification	5	1543	1061	482	2995
Other nitrogen processes	8	885	254	631	1824
Phosphorus cycling	3	599	183	416	1220
Sulfur cycling	4	1504	1083	421	2024
Sulfite reduction	3	1309	1017	292	1703
Sulfur oxidation	1	195	66	129	339
Energy processing	2	508	410	98	671
c-type cytochromes	1	384	370	14	398
Hydrogenases	1	124	40	84	273
Metal resistance	41	4870	603	4267	10962
Arsenic	3	392	59	333	814
Mercury	6	291	77	214	620
Chromium	1	543	65	478	1292
Other metals	31	3644	402	3239	8236
Organic contaminant degradation	172	8609	2160	6449	16948
Aromatics	124	6192	1654	4538	12416
Chlorinated solvents	5	203	41	162	449
Herbicides and Pesticides	16	1104	172	932	2286
Other organic contaminants	27	1110	293	817	1797
Antibiotic resistance	11	1539	263	1276	2784
Beta-lactamases	4	353	146	207	554
Transporters	5	1182	103	1021	2103
Others	2	62	14	48	127
Phylogenetic markers (gyrB)	1	1318	947	371	1777
Pathways for human microbiomes	136	7763	6958	805	12601
Total	438	35669	16520	19149	66931

Phylochip

The structure of microbial community was determined using another small subunit 16s rDNA probes based microarray called Phylochip (G2) (Brodie et al., 2006). The chip contains more than 50,000 (25mer) probes with more than 11 probes per taxa, covering more than 8,700 taxa groups from 63 phyla of Bacteria and Achaea. The array used three SS 16s rDNA databases, namely, NCBI - Genbank, Michigan State - Ribosomal Database and LBNL -Greengenes for probe design which cover most of the reported microbial taxa. PhyloChip allows reliable of identification of microbial communities because whole complex microbial community is detected in a single assay using multiple probes with identical and hierarchical levels of specificity. Phyochip has also been used extensively to profile and monitor microbial communities across various habitats (Brodie et al., 2007, 2006; Weinert et al., 2011).

Next-generation sequencing (NGS)

Next generation sequencing (NGS) has advantage over Sanger method due to its high-throughput ability. Otherwise the basic theory is more or less similar (Mardis, 2008). The generic flow of events includes shearing of metagenomic DNA into smaller fragments and ligated with adapter sequences. Single stranded DNA fragments are attached to inner surface of the flow-cell. Adapter sequences serve multiple purposes, such as, they help in the attachment of DNA fragment to the surface, serve as primers attachment sites and work as sequence barcodes in case of multiplexing more than one samples to be run in a single flow-cell. Once the DNA fragments are attached to the surface, they are amplified to emit enough signals. Finally as they re-synthesized, each chemistry cycle emits a unique signal (one for each type of nucleotide) with each new nucleotide addition. The signals from all DNA fragment are recorded in parallel at each chemistry cycle (http://www.illumina.com/technology/next-generation-sequencing/sequencing-

technology.ilmn). The sequence data is then assembled into larger contigs and annotated using database search.

In this study, Illumina HiSeq and MiSeq systems were used for sequencing DNA and RNA samples. Whereas, MiSeq system gives a read length of 250bp and generates about 25 million reads per flow cell, HiSeq system gives a read length of 150bp and generates about 3 billion reads per flow cell. Hence, Miseq gives data, which is easy to assemble but HiSeq provides data with high coverage (http://www.illumina.com/pages.ilmn?ID=203).

Advantages and disadvantages of chip based methods and NGS

Table 2.3 Comparison between chip and NGS based microbial community analysis

Chip based	**Next-Generation Sequencing (NGS)**
Quickly and accurately	Accurate but not quick
Analyzes microbial DNA samples from any environmental source	Analyzes microbial DNA samples from any environmental source
Detects known microorganisms (>8000 strains)	Simultaneously detects all known and unknown organisms. Sequences can be binned based on similarity
Can analyze the RNA to study metabolically active strains and functions in a sample	RNA samples can be analyzed
Detects low-abundance organisms	Detects low-abundance organisms
Identifies trends in microbial community shifts	Identifies trends in microbial community shifts
Efficiency and Specificity are fixed	Efficiency and Specificity are a function of depth and stringency in post processing

Chapter 3: Relationships among environmental variables

Background

Rise in pollutants level during the past few decades of excessive industrialization in urban areas (Badin et al., 2008) has led to increased environmental pressures. However, the studies focusing on understanding the effects of environmental pressure on ecological systems have traditionally been restricted to the pristine environment or heavily contaminated areas (El-Sheekh and Hamouda, 2013; Ledin, 2000). Understanding effects of natural and anthropogenic pressures in a well-managed urban area, such as Singapore, is important from two viewpoints. Firstly, the present business as usual scenario can be evaluated and, if the adverse effects are minimal then the management principles can be extended to developing economies. Secondly, new ways to develop sustainable, low energy and self-cleaning systems can be explored for future requirements.

Urban waterways which are designed to increase the hydraulic capacity, are often concrete-paved. This brings about low stormwater infiltration, high peak flow coupled with short duration turbulence, large stormwater velocity variations, erosion and heterogeneous settlement of sediments. All these factors not only reduce freshwater macro and micro fauna compared to natural bodies, bring poor aesthetics to the canals, frequent dry wet cycles and make stormwater canals a potential reservoir of pathogens (Badin et al., 2008; Characklis and Wiesner, 1997; Niemczynowicz, 1999; Walsh, 2000; Wolman, 1967; Wu et al., 2008), but also facilitate the release of physicochemical pressures, both anthropogenic and non-anthropogenic in nature, which could impact the ecological health of stormwater canals.

In the first field study, the aim is to understand the relationships of environmental parameters in sediment and water phases of urban canal system and their associations with microbial communities. Part 1 focuses on the relationships of environmental parameters in sediment and water phases for, which a sub-network of Ulu-Pandan catchment was adopted, as a model system which is well-managed as indicated by low levels of organic contaminants and its ability to mitigate floods.

Materials and methods

Catchment map

ArcMap 10.1 module of ArcGIS from ESRI (USA) was used to create the Ulu-Pandan catchment map of Singapore. Shape files for Singapore border, Ulu-Pandan catchment, land-use types, canals and drains, reservoirs, roads and digital elevation were obtained from Public Utilities Board (PUB), Singapore. The files were imported as layers and superimposed to create the map.

Sediment and water sampling

The storm water canals in Singapore are separated from the sewer lines. Therefore catchment catchments do not get seed micro-organisms from the sewer lines and therefore makes an ideal case to study the natural microbial processes in an urban catchment. Ulu-Pandan catchment which lies south-west of Singapore (Fig 3.1) and drains water in Pandan reservoir, was used as a model area for this study. Its total land area is roughly 25km^2. In order to avoid the bias, random sampling approach was chosen. This resulted in a total of 38 samples (19 water and 19 sediment) from the catchment. The samples were collected during a storm event in the last week of April, 2009, close to the small drains in intermediate and large canals from the catchment. The major land use type in the catchment include residential areas in Bukit Batok, Pandan gardens and

Clementi, industrial areas near Jurong east, forest patches near Bukit batok and Holland village and commercial areas near Buona vista area. Because of larger land occupied by residential and industrial areas, more samples came from these land use types. For each sample, sediment/water was collected from five points at the same location and composite was made.

Samples were collected about 2 hours after rain. Sediment samples were collected from five random spots within the diameter of 5 meters and pooled. About 5mL of overflowing water was added on the top of sediment samples. The collected sediments were stored on ice to be transported back to the lab. Separate tubes of sediment samples were prepared for nutrient analysis, metals analysis, organic contaminants and pharmaceutical drugs analysis. Water samples for organics and pharmaceutical drugs analysis, were collected in separate clean 1L glass bottles and filled to the top. Water samples for metals were collected in clean 50mL falcon tubes. Samples were stored in ice box and transported to the lab for further processing.

In-situ testing of water samples

Water samples were tested for physicochemical parameters such as temperature, pH, conductivity, salinity, dissolved oxygen, oxidation-reduction potential (ORP) using 556 multi-probe system and 650MDS data recorder from YSI.

Nutrients and metals analysis

Loosely attached metals and nutrients from sediments, soluble in pore water and bioavailable to the microorganisms were measured. The protocol to extract the water soluble fraction of metals and nutrients was adapted from previously reported method (Meers et al., 2006). Extractions of 1g of sediment samples were performed and 20mL of mili-Q water (18.2 MΩ cm) was added to the samples. The samples were shacked at 200

rpm, overnight to detach the sediment surface-associated inorganic compounds. Extracted ions and metals in the supernatants were filtered using 0.2 μm membrane syringe filters. 10 mL of supernatant was used to analyze nutrient ions using Dionex ICS-3000 IC machine (Dionex, USA). Rest of the 10mL of water was acidified (500μL of analytical grade nitric acid) for metals analysis using ICP-MS. Canal water samples were filtered through 0.2 μm membrane syringe filters (Milipore) and analyzed for nutrient ions. For metal analysis the samples were acidified using 500μL of analytical grade nitric acid in 10mL water sample before being analyzed on ICP-MS.

Organics and pharmaceutical drugs analysis

This analysis was done with Mr. Niyang Nyi Nyi from MSSE Lab, Dept. of Chemistry, NUS. Toluene, xylenes, styrene, pinene, limonene, naphthalene, fluorene, atrazine, lindane, anthracene, chloramphenicol, penincillin G and nalidixic acid were purchased from Sigma-Aldrich (St. Louis, MO, USA). Individual standard solutions of all the compounds were prepared in methanol (at concentrations of 1000 mg L-1 each), except for the antibiotics, which were prepared in acetone. HPLC grade methanol was obtained from Tedia (Fairfield, OH, USA). Acetone, dichloromethane and derivatization agent N,O bis (trimethylsilyl) trifluoroacetamide (BSTFA) were purchased from Merck (Darmstadt, Germany). For solid phase-microextraction, the fibre (carboxen/polydimethylsiloxane, 75 μm) was purchased from Supelco (Bellefonte, PA, USA). Ultrapure water was produced on a Purelab Option-Q (Bucks, UK) system. The HyperSep C18 SPE cartridges were obtained from Thermo-Fisher Scientific (Waltham, MA, USA) and Oasis-HLB SPE cartridges were purchased from Waters (Milford, MA, USA). Whatman GF/B filter was obtained from Whatman International Ltd (Maidstone, England)

To test antibiotics in water samples, the HyperSep C18 cartridges were conditioned with 5mL of methanol and 5mL of ultrapure water before use. The 300mL of water sample previously adjusted to pH 2 with HCl was passed through the SPE cartridge at ~10 mL/min. The cartridge was subsequently washed with 3mL of methanol-water (10:90 v/v). Finally, 2mL of acetone was used to elute the antibiotics. The volume of acetone was reduced to dryness using a gentle stream of nitrogen gas. The extract was reconstituted with 150 µL of acetone (with 10 µL of BSTFA) and derivatization was allowed to take place for 10 min at 60ºC in a water bath, after, which a 1-µL aliquot was injected into the GC-MS system.

For sediments, 5g of sample was mixed with 25mL of acetone and sonicated for 15 minutes. The extraction was repeated twice. The combined extracts were filtered through Whatman filter paper and pre-concentrated to 5mL on a rotary evaporator at room temperature. The extract was subjected to clean-up with an Oasis-HLB SPE cartridge, which was preconditioned with methanol:water (1:5) mixture. After loading, the sample was washed with 5% methanol in water and antibiotics were subsequently eluted with 2mL of acetone. Finally, the extract was pre-concentrated with gentle stream of nitrogen to dryness. It was then reconstituted with 150 µL acetone. The derivatizing process with 10 µL BSTFA was the same as in 2.1. 1 µL of derivatized extract was injected into the GC-MS system.

For organic pollutants in water samples, a 10-mL amber colored vial was filled with 6mL of water sample. Automated SPME was applied to the sample. The vial was placed in the agitator, which temperature was set at 60º C. The agitating time for complete extraction was 15 min with the speed of 500 rpm. Finally, the fibre was automatically introduced to the GC injection port for a desorption time of 3 min.

For sediment samples organic pollutants, ultrasonication was used to extract the organic pollutants. 25mL of methanol was added to the 5 g of sediment sample and then

ultrasonicated. The extraction and clean-up procedure was the same as in 2.2. 2mL of methanol was used to elute the analytes. The pre-concentration process under nitrogen stream was carried out to the dryness. The extract was reconstituted in 150 µL of methanol and 1 µL aliquot was injected into the GC-MS system.

Statistical analysis

Non-parametric correlations were used to identify the associations between different variables. Kendall tau's coefficient was used to calculate non-parametric correlations (Newson, 2002). The significance (with Benjamini Hochberg false discovery rate correction) of correlation was tested by a two tailed t-test. The correlations were computed and plotted in R.

Results

Land-use and canal network characteristics

Sungei Ulu Pandan catchment which lies in the south-west region of Singapore (Fig. 3.1) and drains water to the Pandan reservoir, was used as a model area for this study. With an area of 25km^2, Sungei Ulu Pandan catchment is 3.5% of total area of Singapore and encompasses four major land uses which are residential (10.7 km^2), industrial (5.4 km^2), commercial (0.66 km^2) and forested (5.7 km^2) (Table 3.1).

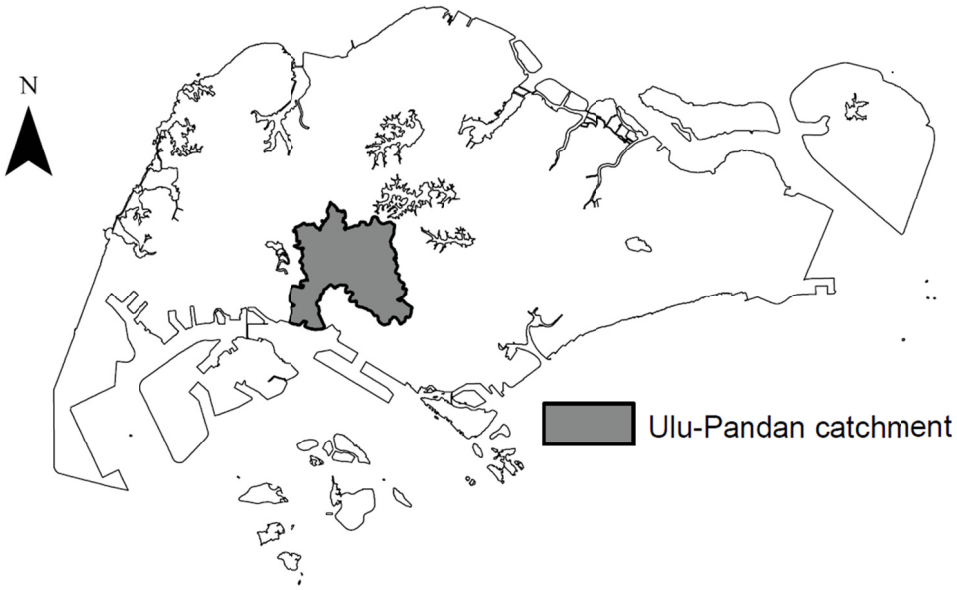

Figure 3.1. Ulu-Pandan catchment in Singapore. The catchment lies in the south-western region of Singapore and spreads across 25km^2

The regions in the catchment are divided by a combination of elevation topology, urban engineering and land-use types. For example, two land-use types namely, residential and forested regions (Residential regions 1, 2, 3 and forested regions 1, 2) had two regions each that were fragmented. Whereas industrial region separated residential regions 1 and 3, elevation topology separated first and second regions of residential and forested land-

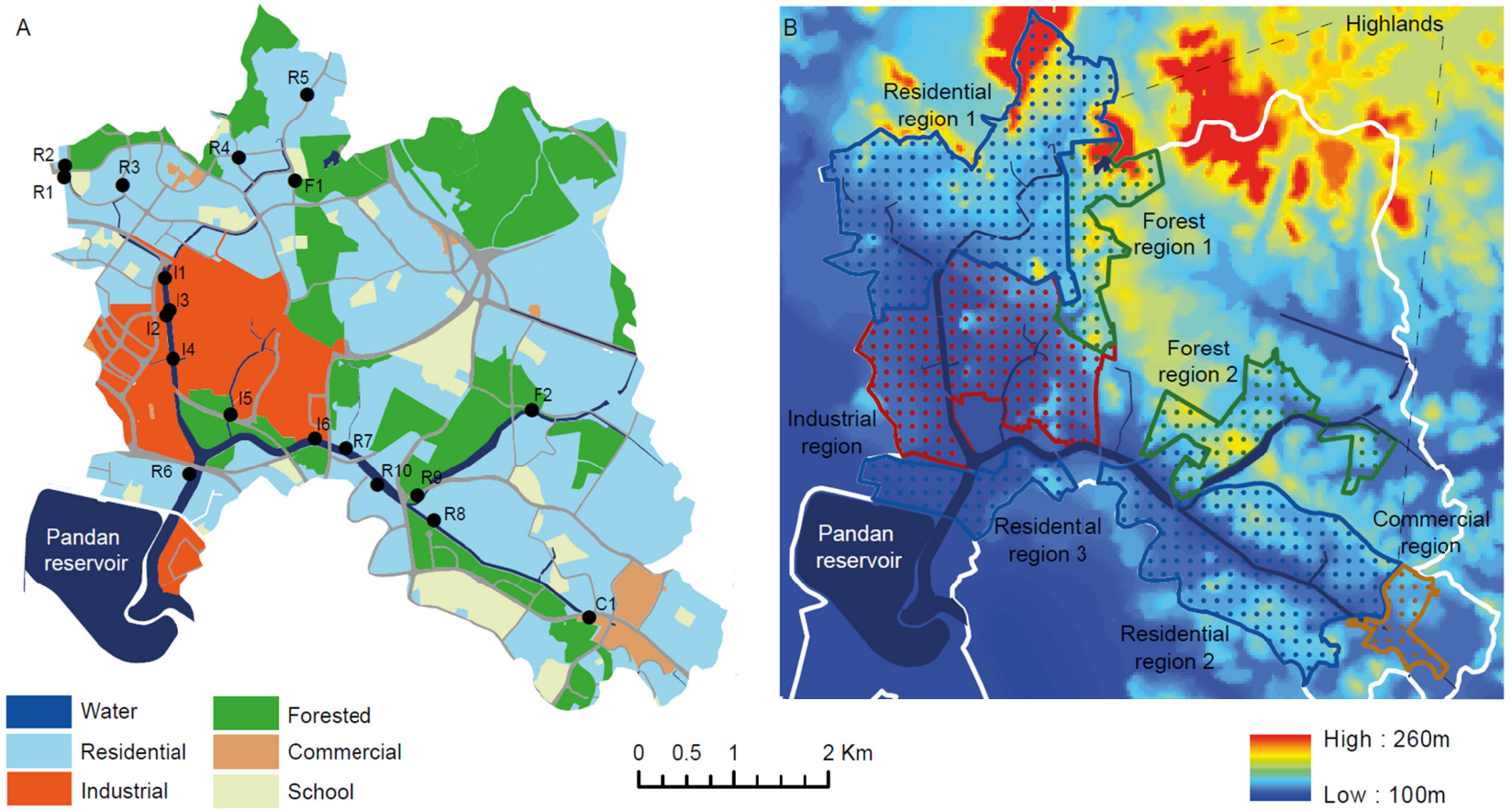

Figure 3.2. Land-use distribution in Ulu-Pandan catchment. (A) Sediment and water samples were collected from 19 locations distributed non-uniformly across the drains and canal network, which serves different land-use types, mainly residential and industrial (see color legends). (B) Ulu-Pandan canal network is shown in context of natural elevation confounded with land-use patterns. The catchment is divided into three residential, two forested and one region each from industrial and commercial land-use based on their geography.

use types (Fig 3.2B). The industrial region is developed at lower elevation with industries such as ware houses, industrial storage and water treatment plant.

The canals and drains system serving the catchment is separated from the sewage lines. Therefore it does not get seed micro-organisms from the sewer lines. This extensive sub-network consists of more than 16,000 meters of big and intermediate canals (>20m wide) and a dense network of small drains of length more than 300 km which collect stormwater from the local catchment and drains it into Pandan reservoir (Table 3.1). The catchment supports a total population of about 0.4 million with an overall density of more than 20,000 people/km^2. Big canals serve a population density of more than 28,000 people/km whereas small drains serve 1,500 people/km. Residential areas which support most of the population (36,000/km^2), are extensively covered with more than 8 km of big and intermediate canals and more than 200 km of small drains. The density of population supported by the big canal and drain network in residential areas is more than 46,000 people/km and 1,800 people/km respectively. However, industrial and forested regions are covered with relatively thin network, which could be due to relatively less population they support.

Landscape developments as well as natural factors have fragmented the catchment into different regions. For example, the residential, forested and commercial regions in the eastern side are segregated by the highlands (Fig. 3.2B). Water from the eastern front of forested region 1 travels eastwards and enters the main Sungei Ulu Pandan canal after passing through the residential and forested region 2. Water from the forested region 2 is moved to the eastern arm of Sungei Ulu Pandan canal. However, the water from western front of forested region 1 travels through residential and industrial regions on western side and ends up in the reservoir through the western arm of Sungei Ulu Pandan canal.

Table 3.1. Canal network characteristics of Ulu Pandan urban waterways

Land use type		**Area (Km^2)**	**Canal length**		**Canal density**		**Ratio: small\large canals**
Primary	**Subtype**		**Large canals (km)**	**Small drains (km)**	**Large canals (m/km^2)**	**Small drains (km/km^2**	
Residential	**Total**	10.73	8.35	205.91	778.37	19.19	24.65
	Res region 1	2.5	3.53	75.01	1.41	30.00	21.22
	Res region 2	1.9	2.54	42.83	1.33	22.54	16.85
	Res region 3	0.64	0.49	12.46	771.87	19.47	25.23
	Uncovered	5.69	1.78	75.59	312.82	13.28	42.47
Industrial	**Total**	5.4	4.86	65.79	901.29	12.18	13.52
Forested	**Total**	3.31	2.46	15.35	433.56	2.69	6.22
	For region 1	1.68	NA	5.39	NA	3.21	NA
	For region 2	1.63	2.46	9.95	1.51	6.10	4.04
	Uncovered	2.38	NA	NA	NA	NA	NA
Commercial	**Total**	0.66	0.38	12.283	575.75	18.61	32.32

Therefore, highlands in the middle of the catchment clearly fragment the catchment and prevent the mixing of water and sediments within the catchment. In addition, forested regions are at high elevation with minimal concrete infrastructure. Minimal imperviousness in forested regions allows shallow and deep infiltration of rainwater and thus an increase in residence time during peak-flow and reduced flooding risks. Excess water, collected from forested areas is guided towards the residential regions where an extensive network of small drains in ensures the efficient collection of all the storm water during peak-flow. Water from residential areas then flows to the downstream industrial areas because of, which upstream regions remain unaffected from contaminants originating from industrial regions.

Patterns of physical parameters in catchment surface water

The physical parameters were tested *in-situ* for water samples. The temperature remained fairly constant with mean of 26.6°C for all the samples and coefficient of variation of about 2.5%. Dissolved oxygen (DO) varied from 2.4 to 13.2 mg/L, which is about 30 to 160% saturation shows good amount of oxygen supply in surface waters for microbes. Water at small drains, such as, region 1 and 3 of residential areas and region 1 of forested areas was found to highly turbulent (on site observation) and mostly saturated with dissolved oxygen (>73%). However, water in larger canals such as industrial, commercial, and region 2 of residential and forest areas was low in DO (<70% saturation respectively). The pH ranged from 6.7 to 10.9. The highest pH of 10.9 happens to be the location with highest DO. The pH and DO correlated well (Pearson's correlation coefficient: 0.65). Although, oxidation-reduction potential (ORP) remained in range for tropical environments, it showed considerable variation across the catchment (142.2 ± 24.2). It varied between 71 to 170 mV which is fairly optimal range in tropical environments. Total organic carbon (TOC) and total dissolved solids (TDS) ranged between 2-7ppm and 0.03-0.5g/L. Conductivity, salinity and total dissolved solids (TDS) showed strong correlation (> 0.98) but the coefficient of variation was more than 65% for all the three across the catchment (Table A1.1).

Trends of nutrient ions in catchment surface water and sediments

Major nutrient indicators, such as nitrites, nitrates, ammonium, sulfates and phosphates were estimated for both water (Fig. 3.3; Table A1.2a) and sediment samples (Fig. 3.3; Table A1.2b). Nitrites and phosphates were undetected for most of the samples. The non-detection may be due to the already low phosphorous levels in well oxygenated waters. Further, the samples were collected during a storm event, which further diluted the

samples. Whereas, nitrates were found to be dominant among nitrogen species in the surface water of Ulu Pandan catchment, sediment showed partitioning of nitrogen species in favor of more reduced form, ammonium. Nitrates in sediments ranged between 0.77 mg/L at location R2 and 5.17 mg/L at location R7 with an exception of location R5 where high levels (27.77 mg/L) of nitrates were detected. While, the concentration of nitrogen species was less in sediment samples, most of it was in reduced form of ammonium ions. Interestingly, sulfates levels were higher, when compared to nitrates, in water as well as sediment samples. Water sulfate levels ranged between 0 and 18.39 ppm with an average of 6.5ppm and standard deviation of 5.3ppm. In sediments, they ranged between 0.08 and 9.33 µg/g of wet sediment.

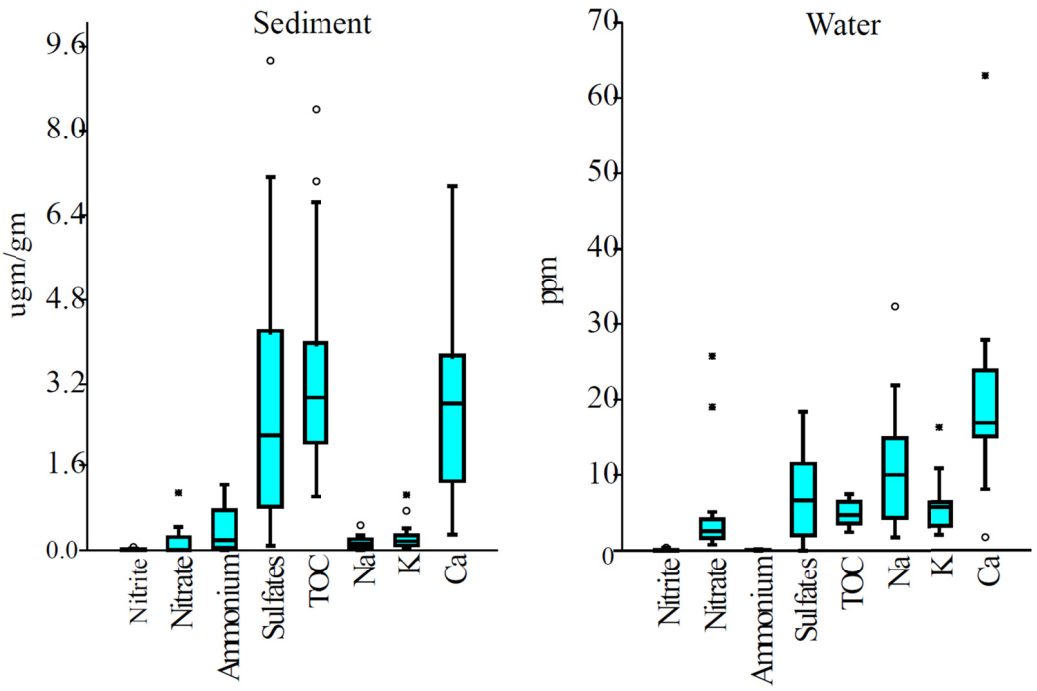

Figure 3.3. Box plot of levels of nutrient ions in sediment and water samples across the catchment. For each sample, box represents 25-75% quartiles. The median is shown by horizontal line in the box. The whiskers (vertical lines) represent data point less than 1.5 times the box height from the box (the "upper inner fence"), above and below the box. Circles show values outside the inner fences but less than 3 times the box height from the box. Values outside the inner fence (the "outer fences") are shown as stars

Metals levels in catchment surface water and sediments

A set of 13 metals was tested in sediment (Fig. 3.4; Table A1.3b) and water (Fig. 3.4; Table A1.3a) samples across the catchment. Metals remained below the maximum allowable limits. Some, however, exceeded the limits. For example, mercury touched the limit of 2ppb at an industrial site I1 and crossed at F1 in water samples. Magnesium and aluminum were among the highest in water as well as in sediments. The average levels in water for both were 1.7 ppm and 0.14ppm respectively and in sediments the average values were 38 and 21ng/g. Their high abundance could be due to their natural abundance in earth crust and non-toxic nature. Though, Zinc never exceeded the allowable limits, it was detected in highest concentration among the regulated metals. The average concentration was found to be 277ppb in water samples and 0.77 ng/g sediment samples.

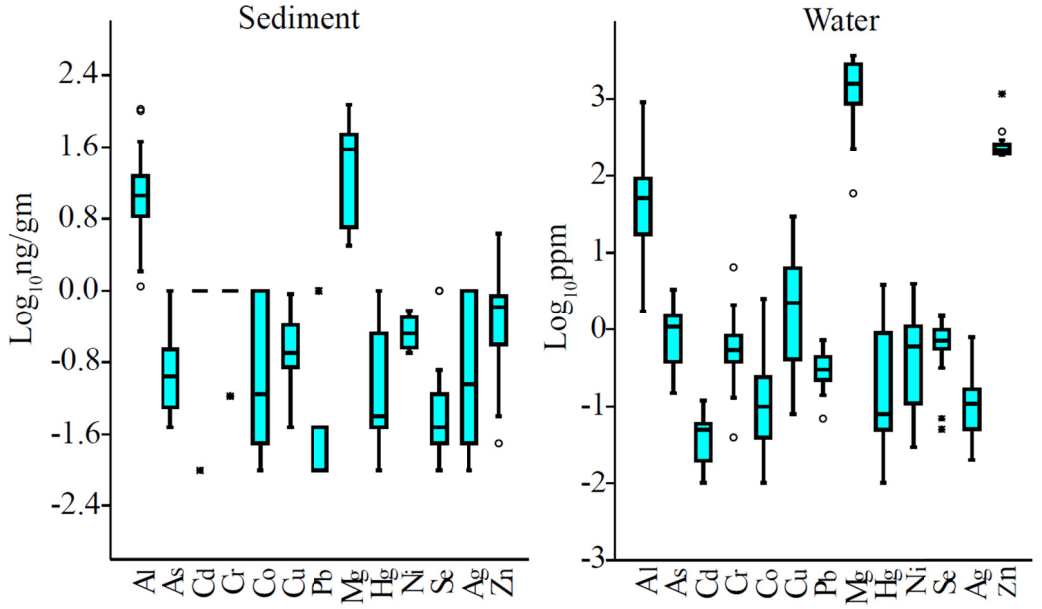

Figure 3.4. Box plot of levels of metals in sediment and water samples across the catchment. For each sample, box represents 25-75% quartiles. The median is shown by horizontal line in the box. The whiskers (vertical lines) represent data point less than 1.5 times the box height from the box (the "upper inner fence"), above and below the box. Circles show values outside the inner fences but less than 3 times the box height from the box. Values outside the inner fence (the "outer fences") are shown as stars

Trends of organics in catchment

Although, organics which included 10 solvents and 3 antibiotics, were in detectable range but were found to be well below their allowable limits in sediment (Fig. 3.5; Table A1.4b) and water samples (Fig. 3.5; Table A1.4a). High variations were detected among all the solvents and antibiotics across catchment in sediments as well as water samples. Three common antibiotics, Penicillin, Chloramphenicol and Nalidixic acid were found in higher concentration in sediments when compared to solvents. However, in water samples, toluene, among the solvents, was detected in higher concentration compared to other solvents or antibiotics.

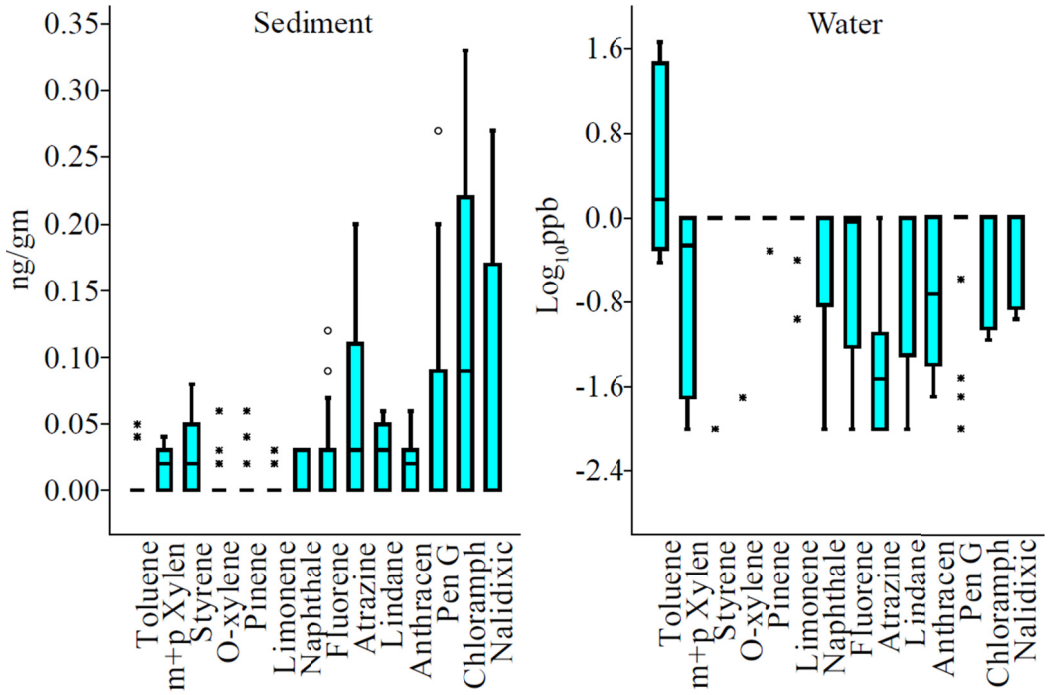

Figure 3.5. Box plot of levels of organics in sediment and water samples across the catchment. For each sample, box represents 25-75% quartiles. The median is shown by horizontal line in the box. The whiskers (vertical lines) represent data point less than 1.5 times the box height from the box (the "upper inner fence"), above and below the box. Circles show values outside the inner fences but less than 3 times the box height from the box. Values outside the inner fence (the "outer fences") are shown as stars

Correlations between environmental variables in catchment

Kendal tau relationships were calculated for 36 parameters in sediments and 43 parameters in water samples from 19 locations. Water samples dissolved oxygen showed inverse correlation with water temperature (Fig. 3.7; Table A1.5a). Two large blocks of relationships stood out in correlation matrix (Fig. 3.7 & 3.8; boxed areas) that showed different trends in sediment and water samples. In the first block (red box), ten organic compounds, which included solvents and pesticides showed positive correlations with each other in water but not in sediments. The second block (green box) of relationship was that of metals and nutrient ions where positive correlations were picked in sediments and negative in water. Among metals and nutrient ions block, whereas, ammonium showed negative correlations with metals in water, it showed positive correlation except aluminum in sediments. Aluminum, on the other hand, showed mostly negative correlations with other metals in sediment as well as in water samples. In addition, it showed positive correlation with temperature and pH in water and with nitrates in sediments. Interestingly, ammonium also showed strong positive correlation with sulfates in water ((Fig. 3.6 and 3.7).

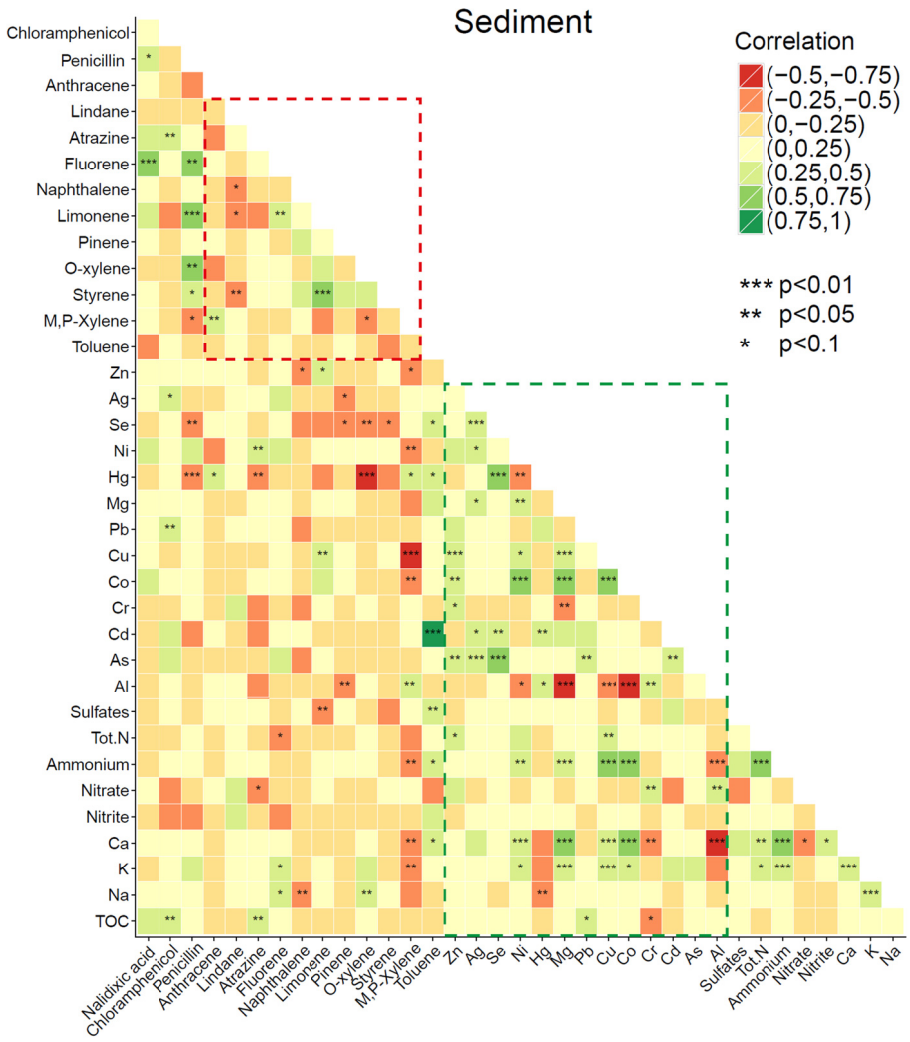

Figure 3.6. Spatial relationships of environmental stressors in sediments. Kendal Tau correlations among 36 parameters for sediment samples are shown. Stars depict the two-tailed probabilities that the parameters are uncorrelated. Boxes represent broad groupings of traits that show different correlation patches (red, organics; green, metals and nutrients).

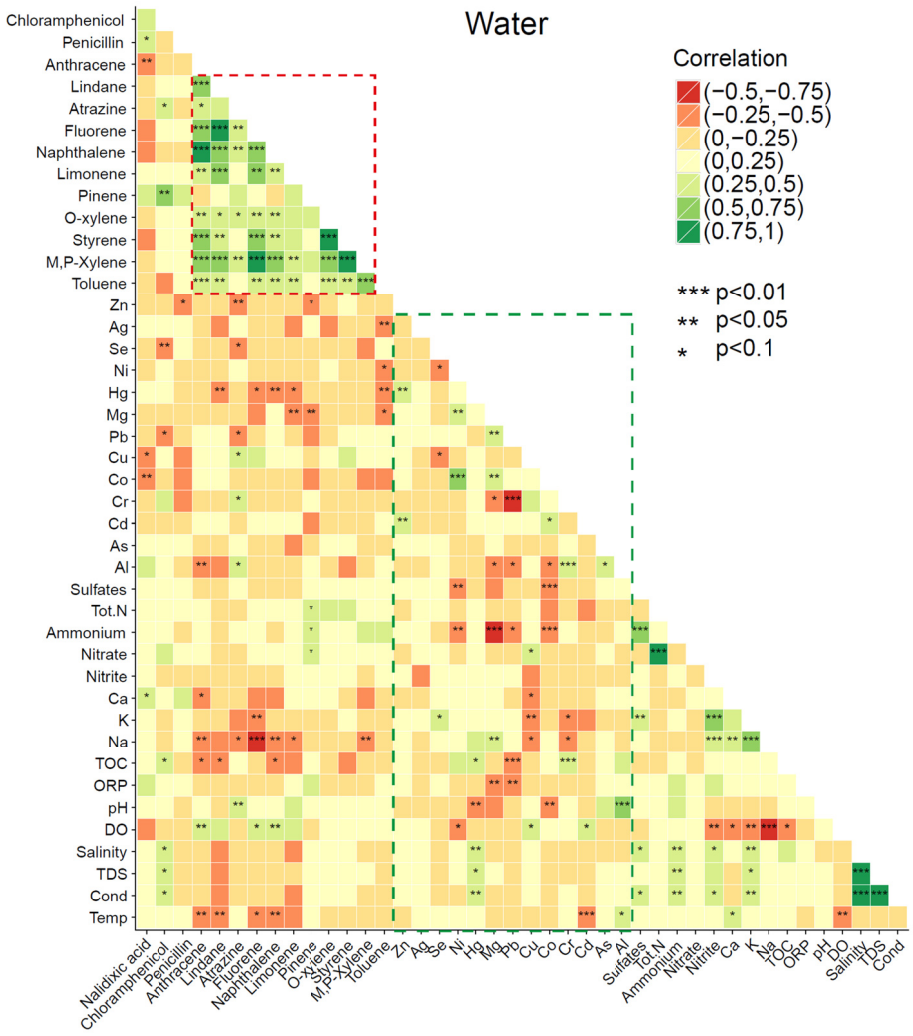

Figure 3.7. Spatial relationships of environmental stressors in water. Kendal Tau correlations among 43 parameters for water samples are shown. Stars depict the two-tailed probabilities that the parameters are uncorrelated. Boxes represent broad groupings of traits that show different correlation patches (red, organics; green, metals and nutrients).

Discussion

This study was conducted with the aim of understanding relationships of environmental variables in well-managed urban waterways. Though ecologically sustainable waterways development may seem ambitious, the current study shows that a well-managed urban stormwater canal system can coexist with high density of human population.

A survey of land-use and canal network data showed that the forested land-use type is located at higher elevation with minimal imperviousness and canal infrastructure. Water in these areas, therefore, percolates through soil and reaches groundwater. Residential areas are settled at lower elevation to forested areas. Storm water is captured using a dense network of small drains and transported to industrial areas with larger canals. This can be substantiated by the fact that density of big canals is higher in industrial areas than residential areas and opposite is true for small drains. Further, industrial regions are located after residential areas in the direction of water flow and thus are away from chemical pressures originating from industrial areas. Therefore, it seems that the canal infrastructure is planned to keep the residential areas unaffected from pollution originating from industrial areas. However, high variation in water velocity during basal and peak flow emphasize that the waterways are designed to transport water quickly after rain and avoid flooding and not to maintain a healthy microbial ecosystem. Such variations in hydrodynamics could result in the release of contaminants from the local catchment.

Physicochemical parameters were tested to evaluate the performance of model urban waterways system used in this study at 19 different location spread across the catchment. Basal levels of water reached within 4-5hrs after typical rain event that ranged between 27 and 64 mm per hour ("National University of Singapore, https://inetapps.nus.edu.sg/fas/geog/ajxdirList.aspx," 2013). This supports the

effectiveness of canal structure for water drainage. However, high variations in water velocity could release solutes from soil and add suspended solids to the canal water.

Both physical and chemical parameters of water quality, especially the organics and metals remained largely within the limits as specified by USEPA (USEPA, 2013) which has more comprehensive list of contaminants and is more stringent than WHO (World Health Organization, 2003). However, local commercial activities could affect the water quality. For example, TDS and TOC were higher at sites where either construction activity was going on or where open unpaved area was present (location: R7). Similarly, water DO gradually goes down from upstream open areas to downstream larger canals. This might be due to multiple factors such as oxygen consumption by micro-organisms, limited oxygen transfer due to reduced turbulence and higher water temperature (significant correlation between temperature and DO, Fig. 3.7). In addition, temperature in canal water was found to be in narrow range and higher than natural systems by 2-3^{0}C (Fera et al., 2013). The increase in water temperature could be attributed to shallow depth and heat transfer from paved surface to overflowing water. Similarly, availability of metals, such as, aluminum and copper is also linked to turbulence and velocity variations in water (Yanful et al., 2000).

Correlation analysis showed two major relationships. First interaction group observed was significant positive correlations among organic solvents in water samples indicate that the water phase has limited capacity to degrade organic contaminants. Compared to water phase, levels of organic solvents in sediments samples did not significant correlations indicative of a reverse trend in sediments. This can be explained by the presence of diverse microbial processes in sediments over water phase.

Second major interaction was between metals and nutrient ions. Metals showed largely, positive correlations among themselves and nutrient ions in sediment samples.

Except aluminum, other metals showed inverse trend in water samples. It was interesting to find association of aluminum with ammonium and nitrates in sediment samples. Aluminum showed significant positive correlation with nitrates but negative correlation with ammonium in sediments, indicating possible interactions between aluminum and nitrogen species. Strong correlation between ammonium and sulfate in water samples indicate that apart from aerobic pathways where, oxygen is used as terminal electron acceptor, nitrate reduction and sulfur oxidation could be operating in the canal system as an alternative energy harvesting pathway.

Conclusions

This study concludes that in well-managed stormwater systems of a highly urbanized environment, pressures from organic contaminants can be minimal while pressures from inorganic chemical constituents such as soft metals can be the major drivers of water-quality, which could affect ecology of these waterways and in-turn the its ecosystem services to keep such canal networks clean in low energy regime.

Chapter 4: Spatial distribution of microbial communities

Background

Though, impact of anthropogenic sources on microbial communities is well established, influence of soft metals on microbial community and its functioning is poorly understood. The understanding of microbial functioning in relation to their associations with soft metals factors needs special attention because of their perceived harmless nature.

Based on unique nature of urban waterways and the potential of sediment-associated microbial communities to influence the physiochemical characteristics of the water systems in the canals, a field study was designed to understand the microbial ecology of the canal sediment and water system (Please refer to Fig. 3.2A for sampling locations). A sub-network of Ulu-Pandan catchment was adopted, as a model system for this study which is well-managed as indicated by low levels of organic contaminants and its ability to mitigate floods. This network receives water from 25km^2 catchments, represents 3.5% of total land area of Singapore comprising four different land use types and supports 10,000 residents per km^2 ("Statistics Singapore - Population and Population Structure," 2013). Ecogenomics approach, combined with environmental metadata analysis were adopted to understand the microbial community and functions and asked two broad questions, firstly, do pressures from different land-use types influence the functional ecology of microbial communities? And secondly, are the influences of environmental pressures distributed or skewed towards few of them? Here we report analysis of spatial analysis of microbial communities and their functions and their associations with 43 environmental parameters.

Materials and methods

Sediment and water sampling

A random subset of all 38 samples collected, were used for microbial community structure (Phylochip) and functions (GeoChip) analysis. Analysis of this subset was statistically sufficient to answer our research questions and that this subset was representative of the full set of samples. 18 samples (10 water and 8 sediment) were used for functional genomics studies using GeoChip, while 26 samples (14 water and 12 sediment) were used for microbial specie analysis using Phylochip. Samples were collected about 2 hours after rain. Sediment samples were collected in clean 50mL falcon tubes, using sterilized spatula, from five random spots within the diameter of 5 meters and pooled. About 5mL of overflowing water was added on the top of sediment samples. The collected sediments were stored on ice to be transported back to the lab. Water samples for genomic DNA extraction were collected in 1L clean glass bottles and stored on in ice box for transportation.

Genomic DNA extraction

Genomic DNA was extracted from the samples immediately after sampling. Sediments were dewatered and DNA was extracted by a combination of mechanical, chemical and thermal lysis and chloroform-isoamyl alcohol purification using protocol described by (Zhou et al., 1996a). Removal of co-precipitated humic substances was achieved by OneStep™ PCR Inhibitor Removal Kit from Zymo Research Corporation (USA) following manufacturer's protocol. DNA was suspended in nuclease free water quantified using nano-drop and pico green. Extraction of genomic DNA from water samples was similar to sediment DNA extraction except few steps, which were added to filter biomass

from water. 1L Water was filtered through 47mm 0.2 μm pore size membrane filters (Milipore). The filter papers were cut into small pieces using sterilized scissors.

GeoChip and Phylochip microarray hybridization

Functional gene array (FGA), GeoChip 3.0 was used to detect the functional gene abundance of microbial communities in the catchment. The information on probe and covered sequence is available elsewhere (He et al., 2010b). Labeling of genomic DNA sequences, hybridization of labeled sequences and array image scanning are performed as described in (He et al., 2005). Phylochip (G2) was used to analyze the microbial community structure in the catchment following the previously described procedures (Brodie et al., 2006).

Statistical analysis.

Shannon Weiner diversity index, Buzas and Gibson's evenness and the dominance index (Wagner, 2000) for microbial community structure profiles for each sample were calculated using PAleontological Statistics (PAST) version 2.15. The definitions and formulas are as follows:

- Shannon diversity index: $H = \sum_{1=1}^{s} P_i \times \log P_i$ (S: total number of species; Pi: relative cover of ith species)
- The Dominance index: $D = \sum_i \left(\frac{n_i}{n}\right)^2$ (ni is number of individuals of species I, n is the total number of species)
- Buzas and Gibson's evenness: 1-Dominance

Grouping of samples were visualized by Non-metric Multidimensional Scaling (NMDS) plots (Kruskal, 1964) and Hierarchical clustering (Murtagh, 1983). For NMDS analysis, functional gene abundance data was first standardized across samples and square root

transformed. Community structure data was binary in nature; therefore, no transformation was applied. Bary-Curtis dissimilarity matrix was created for functional gene abundance data, Jaccard distance matrix was created for microbial community structure data (P/A). This matrix was then used for multidimensional ordination plots such as NMDS and hypothesis testing such as PERMANOVA and ANOSIM (Anderson and Walsh, 2013). Kruskal stress was calculated determine minimum stress with 50 restarts in NMDS analysis (Kruskal, 1964).

Hierarchical clustering was chosen for cluster analysis. Hierarchical clustering heat-map of variable abundance was plotted using Spearman rank correlation for creating distance matrix and average linkage method for generating clusters. The data was square root transformed, median centered and normalized across samples and variables. Heat-map of clusters was viewed in Treeview (http://rana.lbl.gov/EisenSoftware.htm).

PERMANOVA design was created with independent fixed factors land-use type (residential/industrial dominated groups) for functional gene abundance data and phase (sediment/water). PERMANOVA was performed with 9999 permutations of residuals under reduced model. One-way ANOSIM was performed on microbial community structure data separated by phases as factor. *p*value was estimated based on 9999 permutations to test null hypothesis.

Mantel test (Anderson and Walsh, 2013) was used to find out the correlation between a subset of 12 environmental variables (Fig. 4.4A) and the genes which showed variation. The data was normalized across samples before creating the distance matrix. Bray-Curtis distance was used to create the distance matrix for functional gene data while Euclidian distance was used to create the distance matrix for environmental data.

To identify the associations between microbial community and environmental parameters, Variation Coefficient Portioning (VCP) (Peres-Neto et al., 2006) based on

Canonical Correspondence Analysis (CCA) was used (Cajo J. E ter and Piet E M, 1995). Test of significance was calculated using 9999 permutations.

PERMANOVA and ANOSIM were performed in commercially available software PRIMER6 (version 6.1.13) with PERMANOVA+ add on (version 1.0.3) from PRIMER-E Ltd (USA). Cluster analysis was performed in CLUSTER 3.0 from Stanford University and University of Tokyo and viewed using TreeView 1.16r4 (Saldanha, 2004). Correlations were calculated using software PAST 2.17c from University of Oslo. CCA was performed using Canoco4.5 and Canodraw4.14 from Wageningen UR. VCP was performed using MATLAB based codes described previously (Peres-Neto et al., 2006).

Results

Sediment harbor more diverse microbial community than water phase

Based on Phylochip analysis, total of 35 phyla were detected comprising of species belonging to 2,110 sub families (Table A 2.1). Proteobacteria was the most prevalent phylum accounting for 29.4% (620 out of 2,110) of the sub families detected, followed by Firmicutes and Bacteroidetes, which accounted for 16.3% and 11.7% respectively. Out of total 2,110, sub-families, around 225 families were significantly responsible for variation between sediment and water samples, out of, which 43 (≈2%) were more represented in in water phase and 182 (≈9%) in sediment phase (Fig. 4.1A) Different diversity indices, calculated at phylum level, showed significantly high diversity (Shannon's diversity index) for sediment and greater dominance for water samples (Fig. 4.1B). Differential analysis at phylum level showed that Chloroflexi, Planctomycetes and Verrucomicrobia, from less dominant phyla were significantly different and higher in sediment phase ($p<0.01$) whereas Firmicutes and Bacteriodites belonging to dominant phyla were significantly different and higher in water phase and (Fig. 4.1C). Among Proteobacteria, only Gammaproteobacteria showed significant difference between sediment and water phase and was higher in water samples than sediments.

Hierarchical clustering using spearman rank correlation average linkage method showed clear difference between the microbial communities of water and sediments phases (Fig. 3.2A). One way ANOSIM and single factor PERMANOVA results showed significant difference ($p<0.01$) between the sediment and water samples (Table A2.3). Within the sediment cluster, separated regions of residential (region 1, 2 and 3) clustered as one group and forest (region 1 and 2) as another (Fig 4.2A). Clustering on taxa showed three visibly distinct clusters, two with taxa enriched in sediment and water phases and

one with taxa in both phases (Fig. 4.2A). Subfamilies appearing in cluster water (W) and both (B) generally belonged to dominant phyla (with respect to number of sub-families detected across the catchment) such as Proteobacteria, Bacteroidetes, Firmicutes and Actinobacteria while subfamilies appearing in cluster sediment (S) belonged to less dominant ones. Particularly, taxa from Gemmatimonas, Cyanobacteria and Chloroflexi were detected in high numbers in sediment (S) cluster than the other two. Most Cyanobacteria subfamilies were either unclassified or showed similarity to chloroplast lineage. Others common ones belonged to Oscillatoria (Nostocales) and Prochlorococcus (Prochlorales) and Stigonematales. Acidobacteria which is detected with high number of subfamilies in the catchment, was also found more in cluster sediment (S) (Fig. 4.2B).

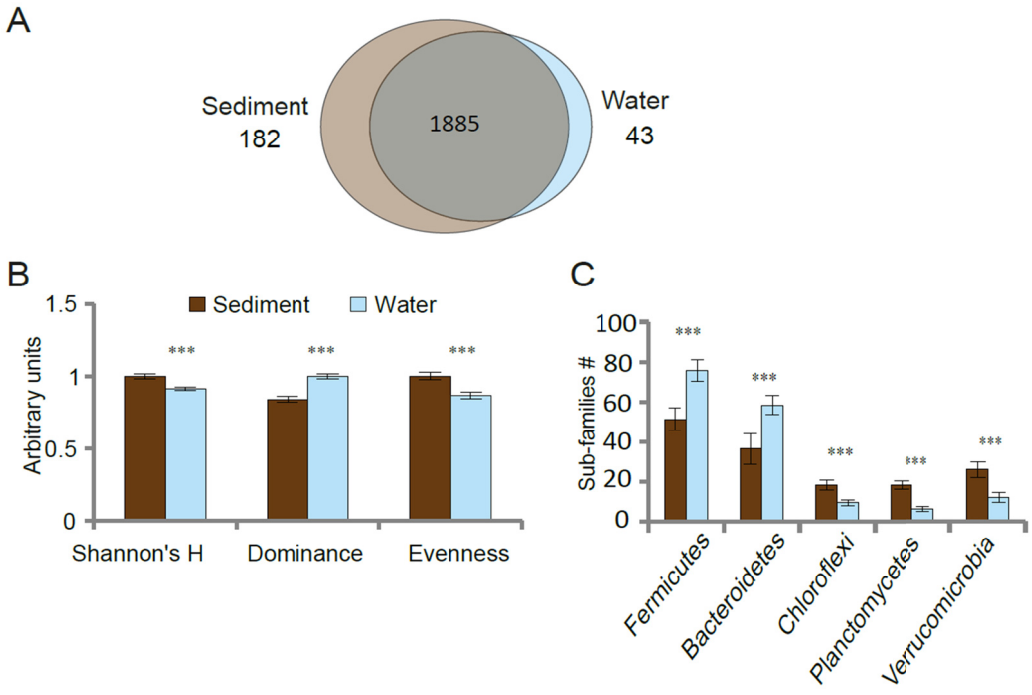

Figure 4.1. Differences in microbial communities in the sediment and water phase of urban waterways. (A) Distribution of significantly different taxa at sub-family level between sediment and water phase (t-test, $p<0.05$). (B) Diversity indices calculated on number of taxa detected in phylum for sediment and water samples. Significance for differences were tested using t-test, ***$p<0.05$ (C) Phyla (# taxa detected in phylum), which showed significant difference in sediment and water samples are shown. Bars show the standard error from mean for water and sediment samples.

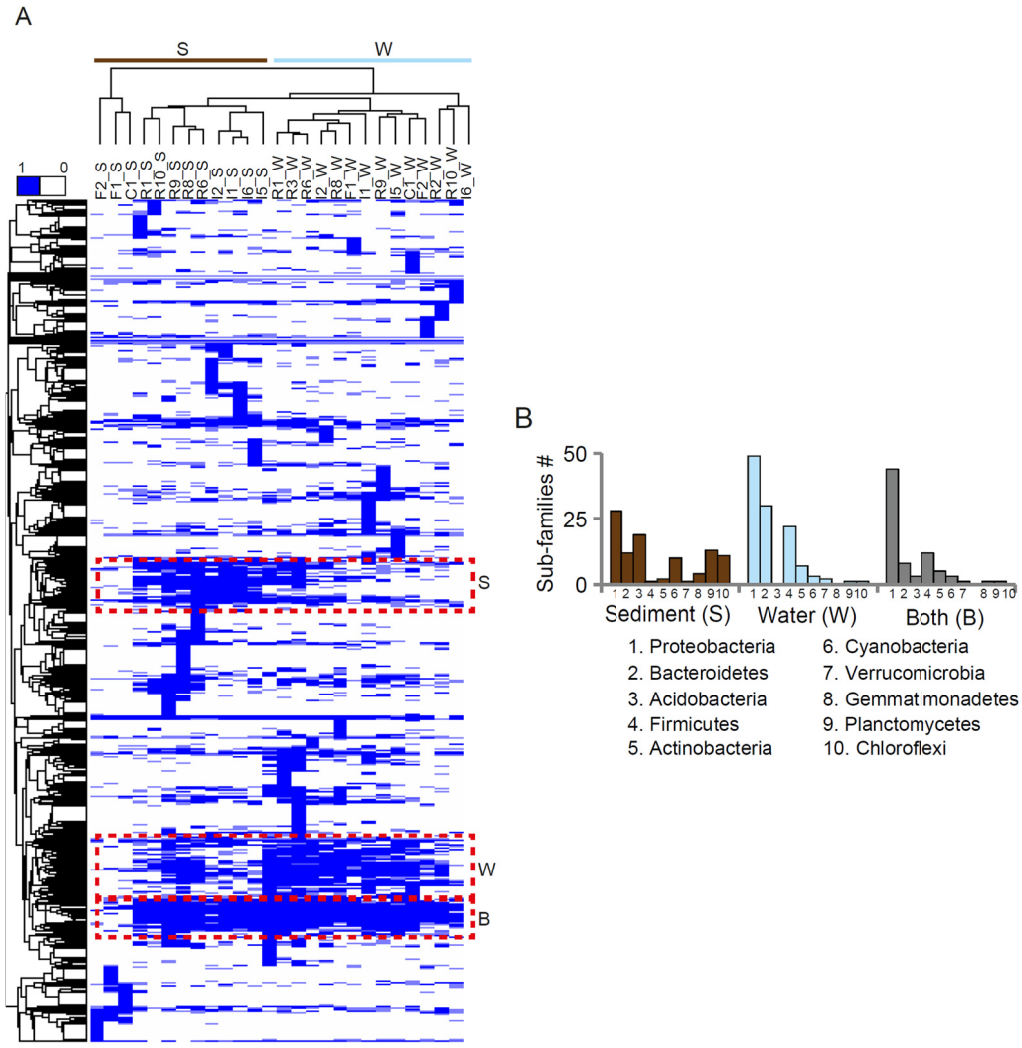

Figure 4.2. Structure of Microbial communities in the sediment and water phase of urban waterways. (A) Hierarchical clustering of Phylochip presence/absence data. Spearman's rank similarity was used to create similarity matrix and clustering was done using average-linkage method. Taxa and samples were median centered and normalized across rows and columns. Two major clusters belonging the sediment and water phase are shown with brown and blue bar (B) Top ten phyla based on high number of sub-families detected, enriched in cluster sediment (S), water (W) and both (B) are shown.

Functional genes differentiate land-use patterns

Total and relative functional gene abundance was calculated for all the locations. 11,848 gene variants from different functional gene categories were detected across the catchment. The total number of genes in each gene category was normalized against total genes present in corresponding gene category on the chip (He et al., 2010c). Genes involved in antibiotic resistance, organic remediation and metal resistance gene categories were highly abundant and represented between 45-50% of genes in respective gene categories on the chip. Other gene categories such as energy processes, phosphorus, sulfur, nitrogen and carbon cycling were between 30-40% (Table A2.2). Hierarchical clustering of gene intensity data (Spearman rank correlation with average linkage) showed two groups: one dominated by industrial samples while the other by residential samples (Fig. 4.3A). One way ANOSIM and single factor PERMANOVA results showed that the two groups were significantly different from each other ($p<0.05$) (Table A2.3). Samples from forested areas grouped with samples from residential areas. The trend remained similar when genes from individual gene categories were clustered. Non-metric multidimensional scaling (NMDS) showed that most samples from different regions remained confined to their respective land-use (Fig. 4.3B). Regions of residential and forested land-use types separated by elevation topology or other land-use type (Fig. 3.1B) were grouped together (Fig. 3.1C).

Differential analysis showed 328 gene variants to be significantly different in the two groups (Bonferroni corrected unpaired-ttest: $p<0.01$) and about 1500 genes at (uncorrected $p<0.05$). The most abundant gene category among varying genes were organic remediation and metal resistance followed by carbon and nitrogen cycling (Table A2.2). Gene variants from antibiotic resistance, gyrase B, phosphorous cycling, energy processes and carbon fixation were enriched in residential type (Fig. 4.3C) while organic remediation and metal resistance were enriched in industrial areas (Fig. 4.3D). Among

gene categories, small molecule resistance (*smr*) gene in antibiotic resistance gene category, *endochitinase*, *Pcc* and *amyA* in carbon cycling, *AceB* in carbon degradation, *cytochrome* and *hydrogenases* in energy processes, *CopA* in metals, *nifH* in nitrogen cycling, *pimF* in organic remediation and *dsrA* was detected in high numbers in sulfur cycling.

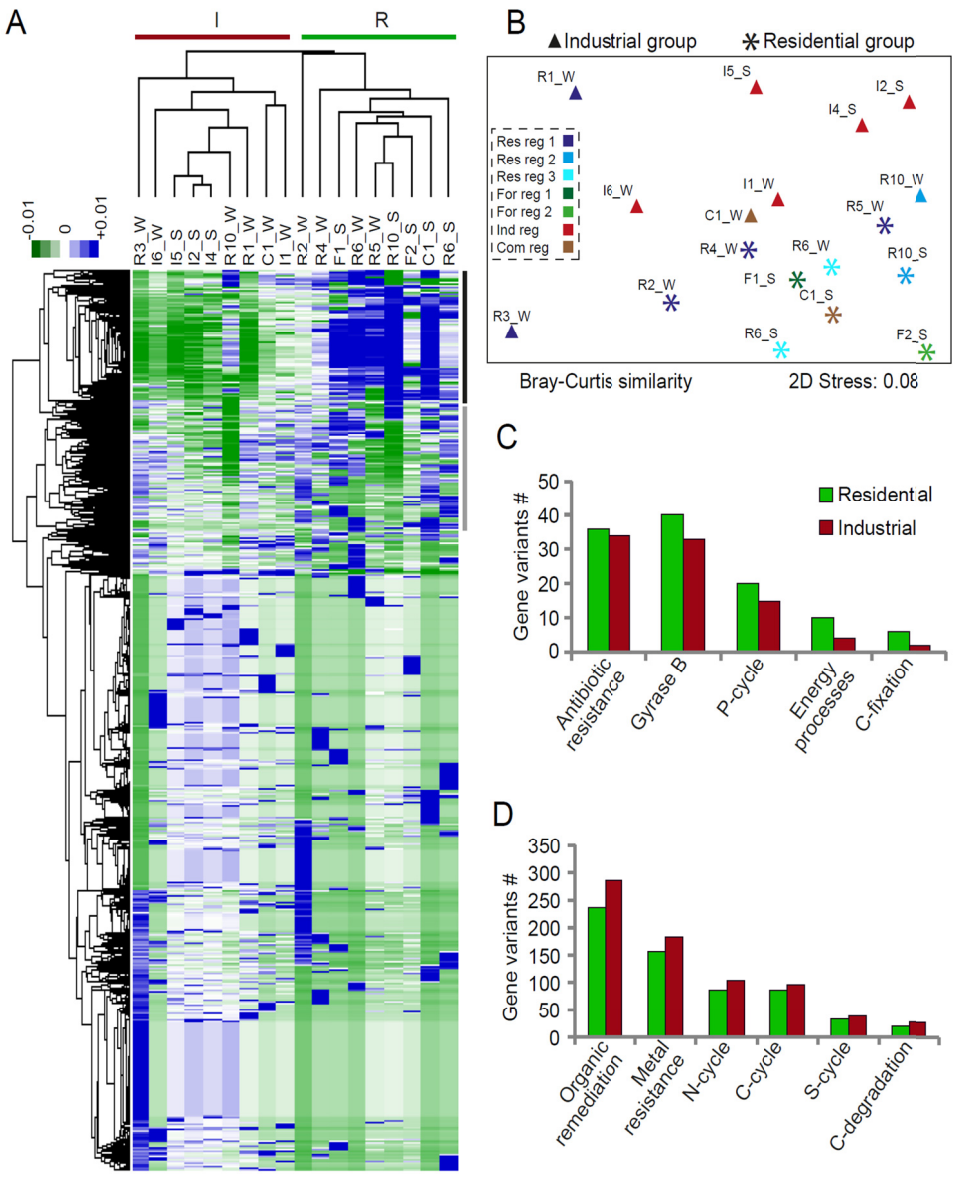

Figure 4.3. Distribution of functional genes abundance in different land-use patterns. (A) Hierarchical clustering heatmap of functional gene abundance. Spearman rank similarity matrix and average-linkage method was used generate clusters of the samples. The genes and samples were median centered and normalized across rows and columns. Clusters belonging to industrial and residential dominated groups are shown by red and green horizontal bars respectively. Gene clusters enriched in the two groups are shown by vertical black and grey bars. (B) NMDS plot of functional gene abundance. The two groups are marked by symbols and land-use regions are shown by colors. The functional gene abundance was standardized against maximum intensity and square root transformed before creating Bray-Curtis distance matrix for NMDS analysis (C) Gene categories with number of gene variants significantly higher in residential and (D) industrial group are shown. Antibiotic resistance, phosphorous cycle, energy processes and carbon fixation were higher in residential group and organic remediation, metal resistance, nitrogen, carbon and sulfur cycle and carbon degradation were found to be higher in industrial group.

Correlations among environmental parameters and functional genes.

Mantel test analysis showed no significant correlation (Pearson's R) between functional genes and associated 36 environmental variables (Bray-Curtis distance matrix). However, Mantel test, which estimates the correlation coefficient between two distance matrices (please see statistical analysis section in materials and methods for details) showed that a set of 12 environmental variables (Fig 4.4A) showed significant correlation of 0.4 ($p<0.01$). As the correlation was high, significance of individual parameters was next assessed. Partitioning of variation in functional gene abundance was explained most by aluminum (15.2%) and copper (14.1%) with a significance level of $p<0.05$. Between the two variables, nearly a quarter of variation in functional gene abundance was significantly explained (Fig. 4.4A). Individual contributions of other environmental variables which are mostly anthropogenic environmental pressures, to the variations in functional gene abundance were insignificant and ranged between 2 to 8%. About a quarter of variation remained unexplained. As aluminum and copper explained majority of the variation in functional gene abundance, their relationship with the functional gene categories were explored. Kendal tau correlations between aluminum and number of gene variants in functional gene categories from water samples did not show significant trends. However, sediment samples showed strong positive correlations. In the case of copper, negative correlations were observed between copper levels and number of gene variants in functional gene categories. Aluminum and copper levels in sediment samples from residential and industrial group were also found to be significantly different (Kruskal-Wallis, $p<0.05$). Aluminum was high in residential areas whereas copper was high in industrial areas sediment samples. Number of carbon cycling, organic remediation and metal resistance gene variants in functional gene categories showed highest positive correlations with aluminum levels whereas, number of antibiotic

resistance and nitrogen cycling gene variants in functional gene categories showed highest negative correlations with copper levels in sediment samples (Fig. 4.4B).

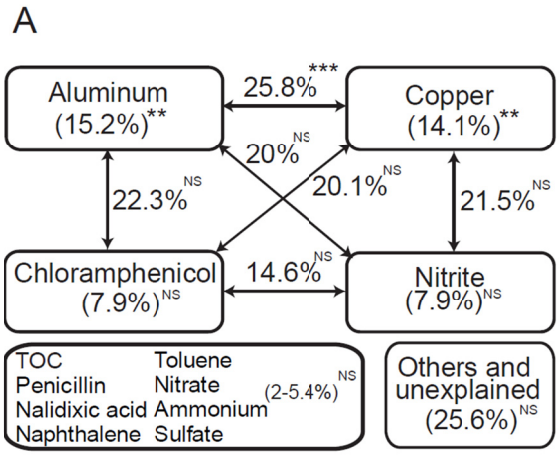

B

Kendal Tau correlation	# gene variants in watershed	Al	Cu
Carbon cycling	1888	0.79***	-0.47NS
Organic remediation	4172	0.79***	-0.47NS
Metal resistance	2148	0.79***	-0.47NS
GyraseB	390	0.79***	-0.47NS
Antibiotic resistance	755	0.71**	-0.55*
Nitrogen cycling	1341	0.71**	-0.55*
Sulfur cycling	549	0.71**	-0.25NS
Phosphorous cycling	238	0.69**	-0.37NS
Energy processes	196	0.57**	-0.40NS

Figure 4.4. Associations of environmental stressors with functional gene abundances. (A) Variation in functional gene abundance explained by individual (boxes) and combination (bidirectional arrows) of environmental variables. *** denotes $p<0.01$; **, $p<0.05$; *, $p<0.1$ and NS, not significant. (B) Kendal tau correlation coefficient between number of gene variants in gene categories with respective aluminum and copper levels (top variables contributing to the variation in functional gene abundance) in sediment samples.

Discussion

This study was conducted with two aims, firstly, to understand the spatial distribution and the influence of catchment and land-use on microbial communities and their functions and secondly, to identify the key environmental parameters and their influence on the functional potential of microbial communities. Our findings of strong influence of copper and aluminum on microbial communities are consistent with these properties of engineered waterways described in Chapter 3.

As the contributions from organic contaminants were minimal, aluminum and copper stood out as they contributed to the largest extent towards shaping microbial functions of sediment microbiome. Copper is among the top three metals involved as cofactors in enzymes (Lehninger, 1950; Linder and Hazegh-Azam, 1996; MacPherson and Murphy, 2007), hence it is likely to have broad ranging effects on microbiomes. In

contrast, not much is known about the biological role of aluminum in microorganisms or higher forms of lives (Greger, 1993; Piña and Cervantes, 1996). Studies done on yeasts and selected plants show widespread effects of aluminum on core metabolism, such as central carbon metabolism, nitrogen metabolism, signal transduction, oxidative stress and pathogen defense (da Cruz et al., 2011; Drummond et al., 2001; Nasr et al., 2011; Ramírez-Benítez et al., 2011). A study done on yeast showed that alterations in citrate metabolism affected it's aluminum tolerance capacity (Anoop, 2003). Hence, both the influencing metals seem to affect core metabolism and stress response functions.

But, does the waterways network create isolated and thus fragmented microbial communities within and between land-use types in the catchment? Our study demonstrates that if catchments are managed using uniform set of practices, such as using similar soil for tree plantation in a given land-use, then microbial communities do not get fragmented into different groups within same land-use types, despite the presence of engineered structures or elevation differences (Fig 3.2B, 4.2A and 4.3B). However, between different land-use types microbial community structure was more distinguished based on gene abundance than taxa. Microbial functions based on gene abundance clearly resolved two dominant categories of residential and industrial land-use types. These results of function-based grouping more than taxa based grouping to explain differences between microbial communities in a given environment are consistent with other studies (Burke et al., 2011; Debroas et al., 2009; Wellington et al., 2003). This indicates that while microbial communities in the catchment are similar, their functions are adapted to the local pressures. Based on such ecological principles, where microbial community assembly is based on functions more than taxa within a given land-use, it should be possible to influence the functions of microbial communities in the waterways through management interventions to control the local environments.

Lastly, the microbial communities were clearly distinguishable in the two phases, sediment and water. Consistent with other cases (Teske et al., 2011) high diversity and evenness was present in sediments than in water phase. As the sediment microbial community has high abundance of bacteria that are involved in utilization of wide range of complex sugars, reduction of nitrates and nitrites without denitrification, dehalogenation and degradation of halogenated organic compounds and phosphate removal, it makes the sediment microbial community highly suited for survival in urban waterways (DeBruyn et al., 2011; Ward et al., 2009; Zanaroli et al., 2012b; Zhang et al., 2003).

Conclusions

This study concludes that in well-managed stormwater systems of a highly urbanized environment, pressures from organic contaminants can be minimal while sources such as natural metals can be the major drivers of microbial communities that provide ecosystem services to keep such canal networks clean in low energy regime.

By understanding the spatial distribution and functioning of microbial communities of urban stormwater systems, it is possible to identify few key environmental variables that can be incorporated in the current management practices. If such well-managed systems can be scalable, different land-use types in a city plan can potentially support somewhat uniformly structured microbial communities, thus allowing development of common management practices on large scales.

Chapter 5: Influence of rain perturbation

Background

Several studies show that whereas, rise and non-uniform distribution of population will impact the demand (Buytaert and De Bièvre, 2012; McDonald et al., 2011; Vorosmarty, 2000), climate change will impact the supply of water through phenomena such as skewed spatial/temporal distribution of rain-events, longer dry periods (Arnell and Reynard, 1996; Bender et al., 2010; Easterling et al., 2000; Elsner et al., 2010; Piao et al., 2010), higher intensity and frequency of extreme events such as storms and cyclones (Bender et al., 2010; Emanuel, 2005; Henderson-Sellers et al., 1998; Knutson et al., 2010) and compromised water quality (Vorosmarty, 2000; Whitehead et al., 2009).

The climate in (sub)tropical regions is characterized by longer and rainy hot periods and milder cold periods. Although, not many studies are available from (sub)tropical regions, an important inference can be made from a study done in a temperate city of Minnesota, USA (Brezonik and Stadelmann, 2002). The study shows that the runoff volume is highly correlated to the rainfall and imperviousness. Other studies show that higher runoff is directly associated with high peak flow, turbulence and high flow velocity and increase in sediment load, which brings wide range of organic and inorganic pollutants with them (Lao et al., 2010; Memarian et al., 2012; Sutherland et al., 2012; Zhao et al., 2010). The level of pollutants, however, differs for areas with different histories of land-use. For example, heavy metal levels were found to be significantly different in the sediments of different land-use types in China (Xia et al., 2011). Due to these factors, the microbial community structure and functions could

experience permanent shifts in different land-use types but regular temporary shifts during the rain-events.

Therefore, given that landscapes will continue to transform for urban land-use and storm events will be affected due to climate change, it becomes important to study their impact on sediment microbial community structure and function. In this study the hypothesis is tested that physical perturbation due to rain coupled with pressures from land-use will bring shifts in microbial community structure and functional potential. Urbanized Ulu-Pandan catchment of Singapore was chosen as the study area with two types of land use, residential and industrial. Two locations were covered for each land-use type to collect sediments samples before and after rain for two rain-events from each location of both land-uses. Each sample was collected in triplicates.

Materials and methods

Experiment design

In order to capture the effects of rain perturbation and pressures from land-use on microbial community and its functioning, a nested ANOVA based experiment was designed. Land-use (residential and industrial) and rain perturbation (pre and post rain) were chosen as fixed factors with two levels each. Two locations were selected as random factor nested within land-use. Samples were collected in triplicates at two separate rain-events (random factor orthogonal to all other factors). This resulted in a total of 48 sediment samples for analysis (Fig 5.1).

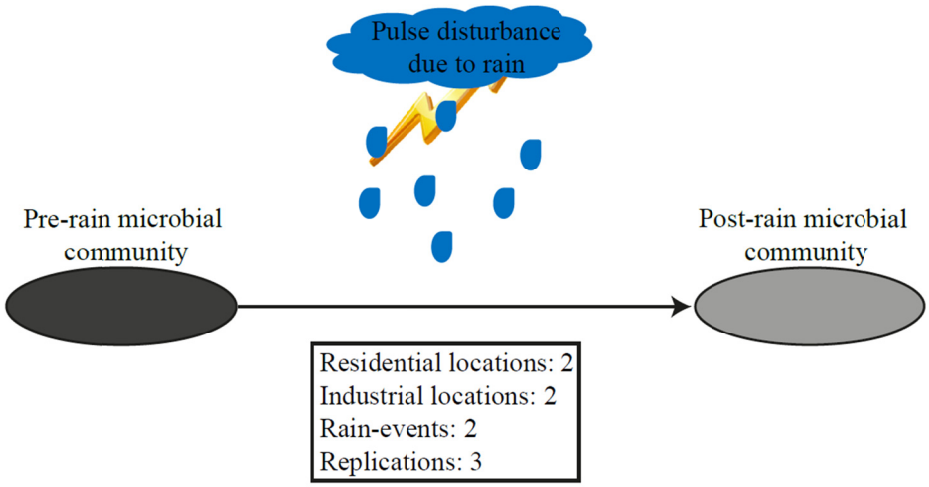

Figure 5.1. Nested ANOVA based experiment design for studying influence of rain perturbation on microbial communities

Study site description and sample collection

Locations from two land-use types in Ulu Pandan catchment of Singapore were chosen for this study. Ulu-Pandan catchment lies in the south-western region of Singapore (Fig. 5.2 A) and drains water in Pandan reservoir. Its spread is about 25 km^2 and comprises residential and industrial as two major land-use types. Two locations were chosen each from industrial area (Location1: 1.337775, 103.748776; Location 2: 1.334632, 103.749212) and residential area (Location 1: 1.334632, 103.749212; Location 2: 1.319401, 103.770213) (Fig. 5.2 B). Sediment samples were collected about 2 hours after rain, first from residential locations and then from industrial locations with a time lag of about 30 minutes. First sampling was done on 15th January 2012 (Rain event 1, ≈16mm rain in 4.5hrs) and second one was done on 20th January 2012 (Rain event 2, ≈16mm rain in 1.25hr). Dry period prior to the first rain event was about 10 days but for second rain event, it was about 5 days. Sediment samples were collected in 50mL clean nuclease free falcon tubes using autoclaved spatula. Sediment samples were collected from five random spots within the diameter of 5 meters and pooled. About 5mL of overflowing water was added on the top of sediment samples. Three replicates were collected for each

sample without repeating the same spot. The samples were immediately transferred in the ice box and transported to lab for DNA extraction. The time for transportation from last sample collection to the beginning of DNA extraction is about one hour.

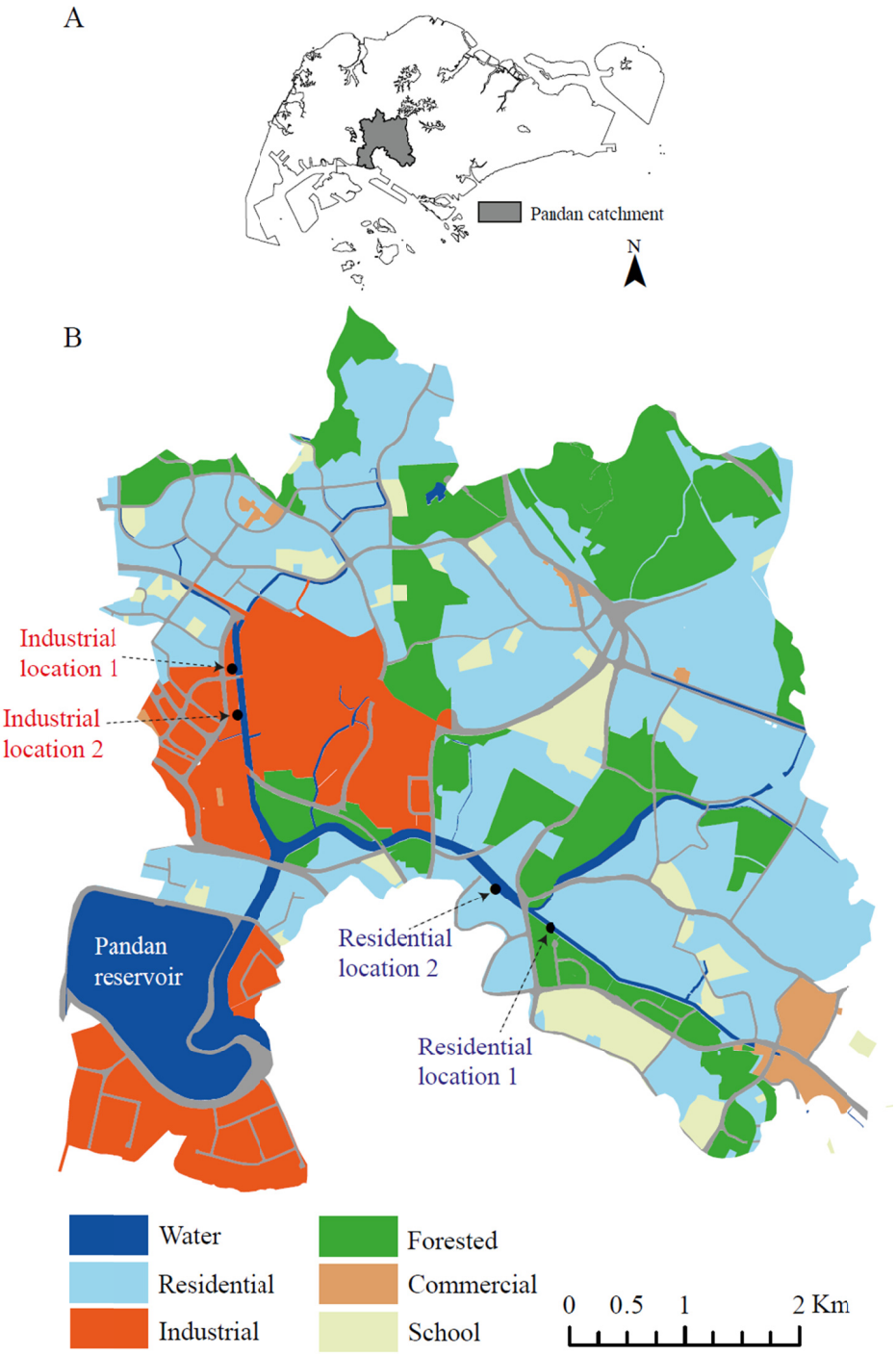

Figure 5.2. Pandan catchment map (A) Ulu-Pandan catchment in context of Singapore (B) Sampling locations in residential and industrial areas of Ulu-Pandan catchment

DNA extraction and cleanup

Sediment samples were thoroughly mixed using clean spatula prior to weighing. Sediments mixed with water were siphoned off in 2mL tube and centrifuged to discard the pore water. Sediments were then weighed to 200±20 mg for extracting DNA. DNA extraction was done using FastDNA™ SPIN KIT for soil from MP Biomedicals (USA) with slight modifications from manufacturer protocol. For example, homogenization and lysis of sediment-associated microbial communities was done at speed 5m/s for 30 seconds instead of 6m/s for 40 sec, prescribed by the manufacturer. Capturing of DNA binding matrix was carried out at 10,000g for 5min to avoid damage to filter membrane. Washing step was repeated. DNA was eluted in nuclease free water and cleaned using OneStep™ PCR Inhibitor Removal Kit from Zymo Research Corporation (USA) following manufacturer's protocol. Nano-drop assay and gel runs were performed to check quality and quantity of DNA.

Sequence data generation

A total of 48 genomic DNA samples were submitted to The Singapore Centre on Environmental Life Sciences Engineering (SCELSE), Cluster 2, Genomics group (Dr. Daniela Drautz) for sequencing. Samples were stored in -80^{0}C after submission till further processing. Quality checks of DNA samples were done using Qubit® dsDNA HS Assay on Qubit® 2.0 Fluorometer from Life Technologies Corporation and 2100 Bioanalyzer System from Agilent Technologies before processing the samples for library preparation. Standard pipeline of Illumina HiSeq sequencing was adopted. Briefly, Genomic DNA was sheared to obtain mean fragment size of 150bp. Samples were separated into 8 different groups of 6 samples each. DNA fragments each of the six samples from a group were attached with adapters connected to a unique barcode. The samples from each group were then pooled (multiplxed) and run on single lane of the

sequencing flow-cell. Hence, 8 such lanes were used to run all the 48 samples. The fastq-files generated were then processed with standard HiSeq data processing pipe-line for sequence alignment. This resulted in an average of 30 (±9 SD) million reads per samples. Resulting contigs were annotated through MEGAN 5 (Huson et al., 2011) using NCBI database for taxa and using KEGG/SEED databases for functions.

Statistical analysis

Normalized sequence abundance data (using total number of reads), at different taxonomic and functional level, for taxa and functional genes, respectively, was exported from MEGAN 5 (Huson et al., 2007) (http://ab.inf.uni-tuebingen.de/software/megan5/) in text format. Later, the data was standardized across samples (abundance of individual variable/sample total (maximum among all samples)*sample total (minimum among all samples)) and transformed. Two transformations were tested, square root and presence/absence transformation. Followed by standardization and transformation, dissimilarity matrix based on either Bary-Curtis or Jaccard distance was created. Bray-Curtis dissimilarity was used with abundance data to calculate compositional dissimilarity whereas, Jaccard distance was used to calculate structural dissimilarity of the microbial community by counting matches and mismatches between two samples (Wang et al., 2010). This matrix was then be used for hypothesis testing using PERMANOVA (Anderson and Walsh, 2013). Split network was chosen for cluster analysis. It uses neighbor-net algorithm to create clusters of Goodall distances between samples (Bryant and Moulton, 2004). PERMANOVA design was created based on the current study with land-use type and pre/post rain as two independent fixed factors and locations and rain-events as random factors. While, pre/post rain and rain-events were orthogonal to all other factors, factor, rain-events, was nested within land-use types. All factors had two levels. Land-use type had, residential and industrial, pre/post rain had,

pre-rain and post-rain locations had, location 1&2 and rain-event had event1&2. PERMANOVA was performed in commercially available software PRIMER6 (version 6.1.13) with PERMANOVA+ add on (version 1.0.3) from PRIMER-E Ltd (USA) and Split clusters were created using MEGAN 5 (Huson et al., 2011)

Results

Differences in microbial community composition

Whole genome sequence abundance based annotation indicated that microbial community structure was different in the two land-use sediment-types, residential and industrial. Figure 5.3 shows the split network of Goodall distances between sediment microbiomes of samples from different land-use types collected before and after rain. Microbial communities from industrial samples showed higher spread than industrial samples. While residential land-use sediment-type microbial communities at genus level, showed significant differences between pre and post rain, differences in microbial communities from industrial land-use sediment-types were less conspicuous (Table A5.5B).

Abundance of different phylum in sediment microbiome showed noticeable differences between land-use types as well as pre and post rain-event. A total of 75 phyla were detected with top 21 representing more than 85% of abundance. *Proteobacteria* was the most abundant phyla, followed by Cyanobacteria, Bacteroidetes, Verrucomicrobia, Actinobacteria, Firmicutes, Planctomycetes, Acidobacteria and Chloroflexi. Whereas, Cyanobacteria, Verrucomicrobia, Firmicutes, Bacillariophyta, Spirochaete, Chlorobi and Chlamydiae were also found to be higher in industrial sediment-types, Actinobacteria, Planctomycetes, Acidobacteria, Chloroflexi and Deinococcus-Thermus were higher in residential sediment-types. Proteobacteria was indifferent before and after rain in either

residential or industrial sediment microbiome. Whereas, Cyanobacteria, Actinobacteria, Planctomycetes, Acidobacteria, Nitrospirae and Deinococcus-Thermus showed to be significantly higher after rain in microbial communities of both sediment-types, Bacteroidetes and Firmicutes appeared to reduce in abundance in industrial sediment-type (Fig. 5.4) (Student t-test: $p<0.05$).

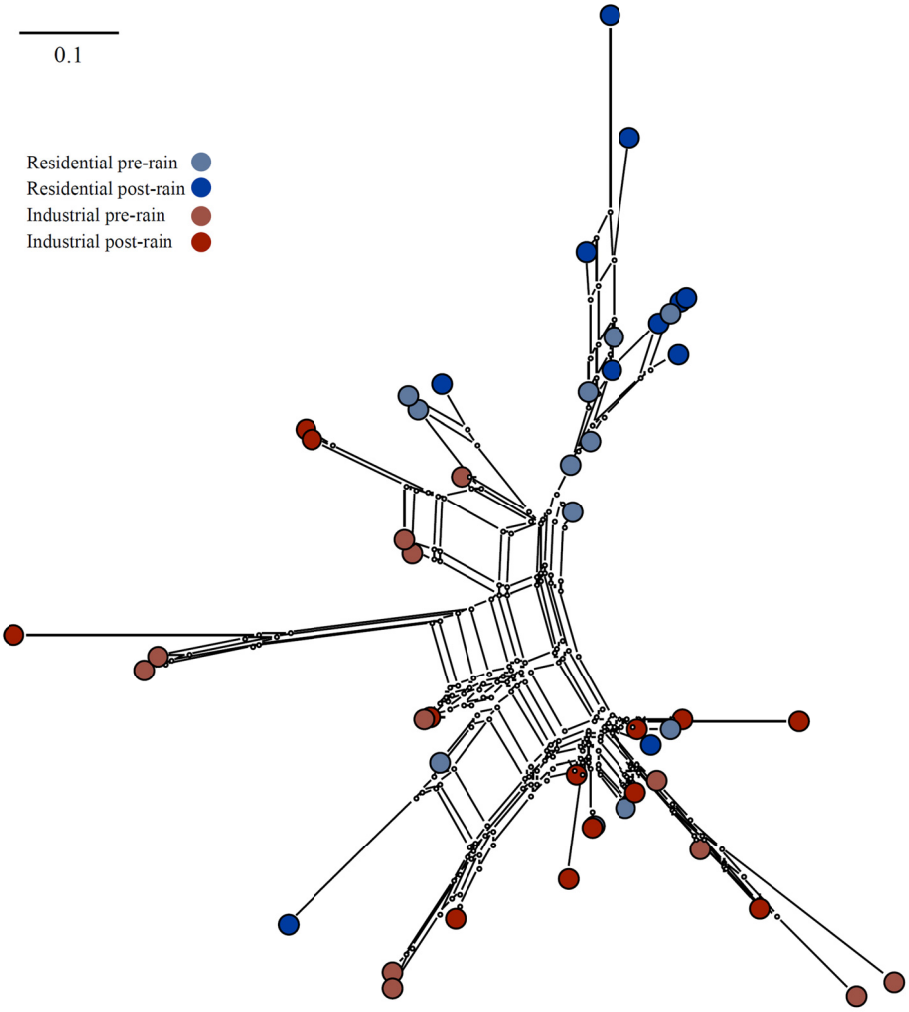

Figure 5.3. Split-clusters visualization of Goodall distance matrix calculated for profiles of microbial communities using neighbor-net method. Each point represents composition of microbial community taxa groups obtained from sequence abundances of taxa groups annotated using NCBI database search and edges denote the distance between samples.

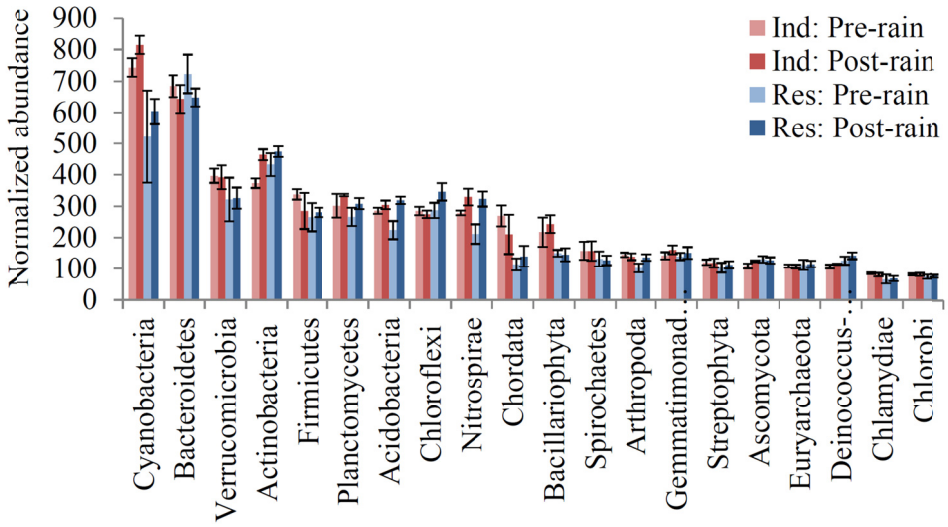

Figure 5.4. Normalized abundance (sequence counts) of top 21 phyla (except Protobacteria) contributing to more than 85% of microbial community taxa abundance from Pre and Post rain at residential and industrial land-use sediment-type microbiomes. Random factors, such as, locations and rain-events were pooled, resulting in n=12 for each data point. Error bars represent standard error.

Differences in functional potential of microbial communities

Figure 5.5 shows the split network of Goodall distances between functional potential of sediment microbial communities from different land-use types collected before and after rain. Functional potential of microbial communities showed noticeable differences between residential and industrial sediment-types but the spread of residential microbial functions was greater than microbial communities from industrial sediment-type. Functional potential of microbial communities form both residential and industrial sediment-type showed significant differences before and after rain which was more prominent on rain event 1 than rain event 2 (Tables A5.8-A5.12).

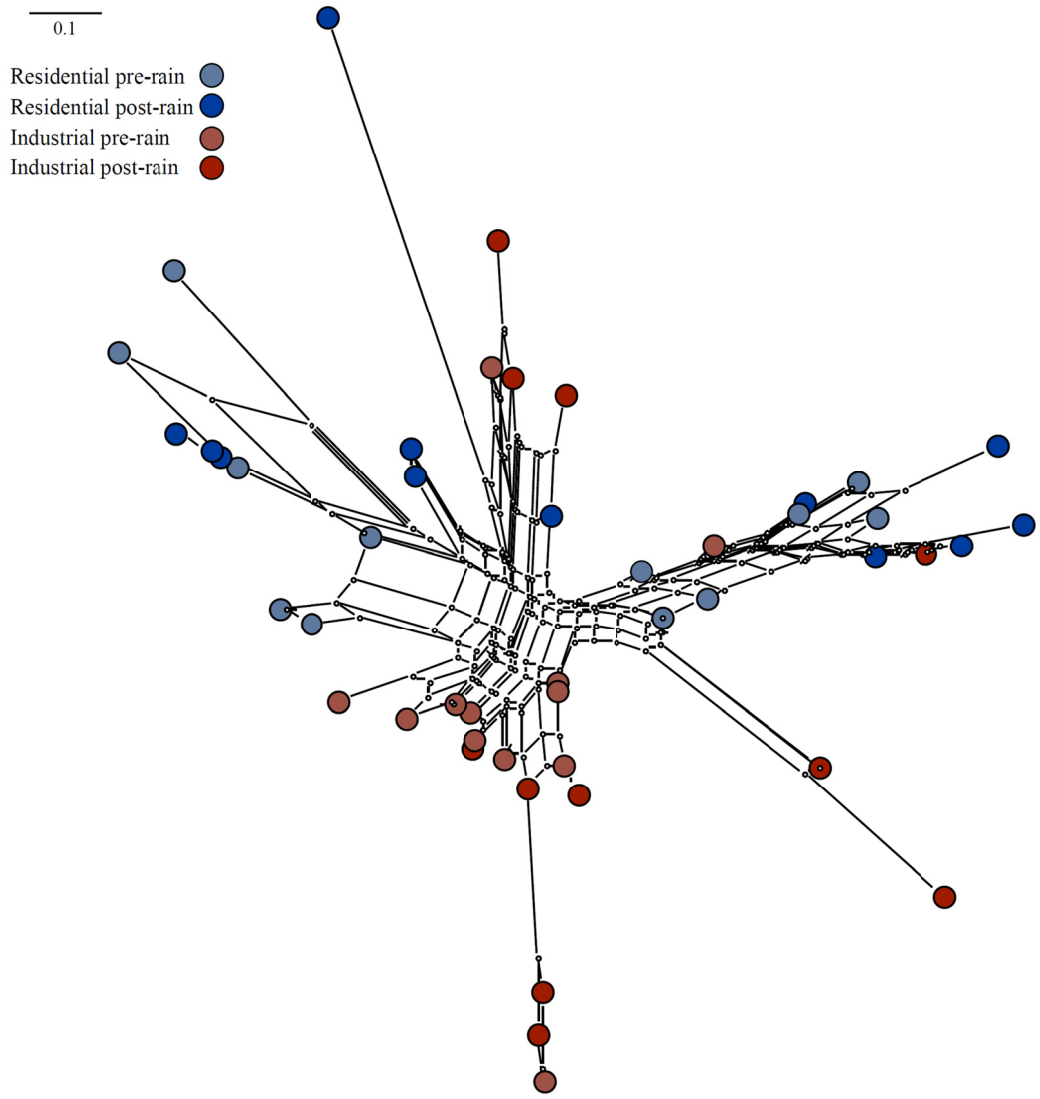

Figure 5.5. Split-clusters visualization of Goodall distance matrix calculated for profiles of microbial functional genes using neighbor-net method. Each point represents microbial community functional potential obtained from sequence abundances of functional groups annotated using NCBI database search and edges denote the distance between samples.

All the functional level, genes were binned into 27 broad pathways carbohydrates, virulence, amino acids and protein metabolism, DNA metabolism, respiration, cofactors and vitamins metabolism as top >40% abundant processes (Fig 5.6). No noticeable difference of functional gene abundance between land-use types or before/after rain was detected (Student t-test: $p>0.05$). Pathways essential for biomass growth such as protein and amino acid, nucleic acid, respiration, cofactors and vitamins and cell-wall synthesis

were highly dominant over secondary metabolism pathways such as stress response and metabolism of aromatic compounds which accounted for less than 6% of total abundance of all functional pathways. Fatty acids and isoprinoid metabolic pathways which are used by microorganisms in many organic compound degradation process was also detected in mid-range abundance. Nitrogen and sulfur metabolism pathways were also detected in abundance more than 5% of total abundance. Interestingly, whereas, virulence related genes formed the second highest functionally abundant gene category with more than 6.8% of total abundance, phages related genes were least abundant.

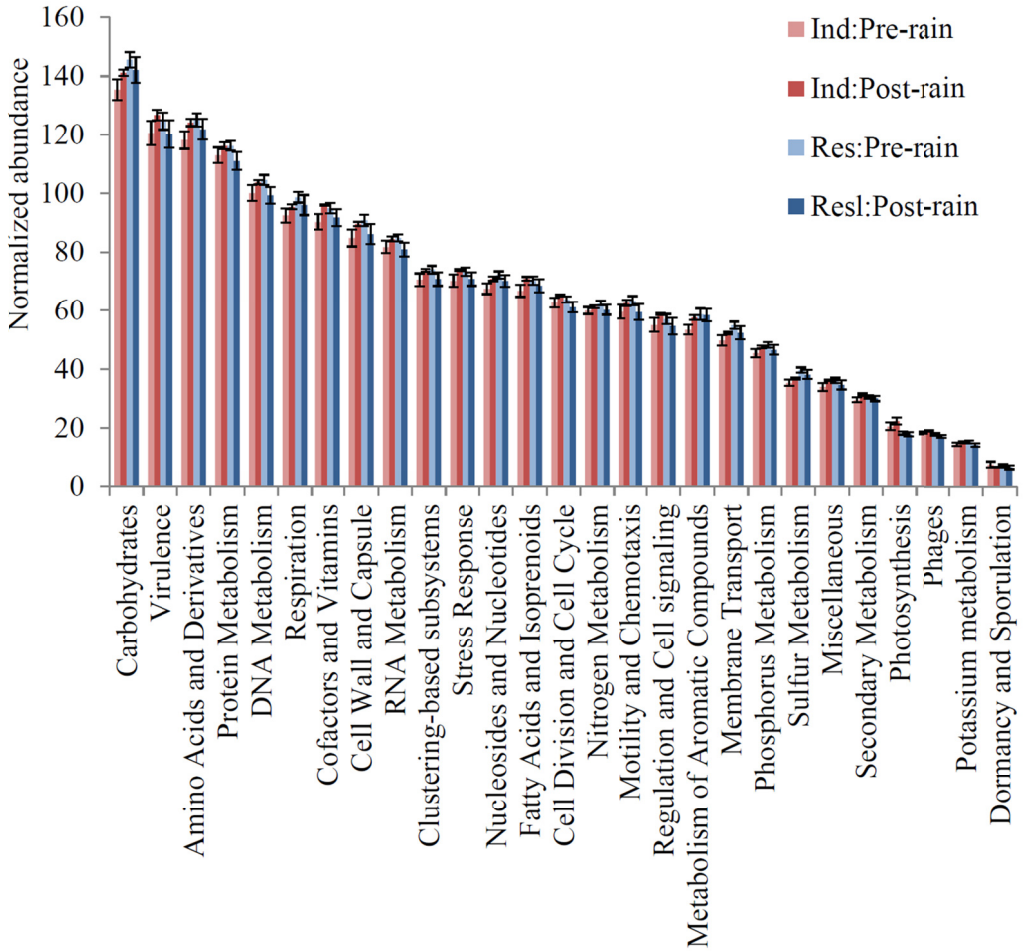

Figure 5.6. Normalized abundance (sequence counts) of functional gene categories from Pre and Post rain at residential and industrial land-use types. Random factor, such as, locations and rain-events were pooled, resulting in n=12 for each data point. Error bars represent standard error.

PERMANOVA results

Microbial community taxa variations at different taxonomic levels

The structure of microbial assemblages for all taxa groups at species level, differed between before and after rain, but this was dependent on the rain-event and the location (PERMANOVA pseudo-$F_{2,32} = 4.6$, $p < 0.001$; Table A5.3). During the first rain-event at both industrial locations and at one residential location, microbial assemblages differed between before and after rain. There were, however, no differences during the second rain-event at any of the sampled locations (Table A5.3). No differences were found between land-use types. There was significant variability across rain-events and locations (Table A5.3). Presence/Absence of microbial assemblages also showed no difference across land-use types or between before and after rain-events. Rather, there was significant variation across rain-events and locations (Table A5.4). In terms of dispersion, the structure of microbial assemblages in the residential land-use type had a greater dispersion than those in industrial land-use type (PERMDISP $F_{1,46} = 5.17$, $p < 0.04$). There were no differences in dispersion between before and after rain (PERMDISP $F_{1,46} = 0.96$, $p = 0.42$). No differences in dispersion between land-use types or before and after rain were found for composition (PERMDISP $F_{1,46} = 0.17$, $p = 0.73$, $F_{1,46} = 0.05$, $p = 0.84$).

Similarly, microbial assemblages for all taxa at Genus level differed between before and after rain, but this was dependent on the rain-event and the location (PERMANOVA pseudo-$F_{2,32} = 5.35$, $p < 0.001$; Table A5.5). During the first rain-event at both industrial locations and at one residential location, microbial assemblages differed between before and after rain. During the second rain-event, differences were only found on one residential location (Table A5.5). No differences were found between land-use types. There was significant variability across rain-events and locations (Table A5.5).

No differences were detected in microbial assemblage (presence/absence) across land-use types nor between before and after rain-events. Rather, there was significant variation across rain-events and locations (Table A5.6). Additionally, the structure of microbial assemblages in the residential land-use type had a greater dispersion than those in industrial land-use type (PERMDISP $F_{1,46} = 7.57$, $p < 0.01$). There were no differences in dispersion between before and after rain (PERMDISP $F_{1,46} = 0.97$, $p = 0.40$). No differences in dispersion between land-use types or before and after rain were found for composition (PERMDISP $F_{1,46} = 0.49$, $p = 0.56$, $F_{1,46} = 0.13$, $p = 0.76$).

For *Bacteria* and *Archaea* taxa groups at Genus level, the structure of microbial assemblages differed between before and after rain at all locations and rain-events, with the exception of one industrial and one residential location during the second rain-event (pseudo-$F_{2,32} = 8.81$, $p < 0.001$; Table A5.1). No differences were found between land-use types (Table A5.1). There was significant variability across rain-events and locations. There were no differences in composition between land-use types nor before and after rain (Table A5.2). In terms of dispersion, the structure of microbial assemblages in the residential land-use type had a greater dispersion than those in industrial land-use type (PERMDISP $F_{1,46} = 10.82$, $p < 0.002$). There were no differences in dispersion between before and after rain (PERMDISP $F_{1,46} = 2.06$, $p = 0.18$). No differences in dispersion between land-use types or before and after rain were found for composition (PERMDISP $F_{1,46} = 0.92$, $p = 0.42$, $F_{1,46} = 3.00$, $p = 0.12$).

Microbial community functional potential variations at different levels

At level 2 of functional genes annotated through KEGG database, there were no differences in the structure of functional genes between land-use types or before and after rain (Table A5.7). There was significant variability across rain-events and locations (Table A5.7). However, at level 3, the structure of functional genes differed between

before and after rain, but this was dependent on the rain-event and the location (PERMANOVA pseudo-$F_{2,32}$ = 2.42, p < 0.04; Table A5.8). During both rain-events at one industrial location and at one residential location, function differed between before and after rain (Table A5.8). No differences were found between land-use types. There was significant variability across rain-events and locations (Table A5.8). At the last level (individual enzymes), the structure of functional genes differed between before and after rain, but this was again dependent on the rain-event and the location (PERMANOVA pseudo-$F_{2,32}$ = 3.19, p < 0.001; Table A5.9). Function differed between before and after rain at one industrial location during the first rain-event and at one industrial and one residential location during the second rain-event (Table A5.9). During the first rain-event, however, there was a trend for differences at both industrial locations. No differences were found between land-use types. There was significant variability across rain-events and locations (Table A5.9).

At level 2 of functional genes annotated through SEED database, the structure of functional genes differed between before and after rain, but this was dependent on the rain-event and the location (PERMANOVA pseudo-$F_{2,32}$ = 3.85, p < 0.004; Table A5.10). Function differed between before and after rain at one industrial and one residential location during the first rain-event and at one industrial location during the second rain-event (Table A5.10). No differences were found between land-use types. There was significant variability across rain-events and locations (Table A5.10). At level 3, the structure of functional genes differed between before and after rain, but this was dependent on the rain-event and the location (PERMANOVA pseudo-$F_{2,32}$ = 3.92, p < 0.001; Table A5.11). During both rain-events at one industrial location and at one residential location, function differed between before and after rain (Table A5.11). No differences were found between land-use types. There was significant variability across rain-events and locations (Table A5.11). At the last level (individual level), the structure

of functional genes differed between before and after rain, but this was dependent on the rain-event and the location (PERMANOVA pseudo-$F_{2,32} = 3.69$, $p < 0.001$; Table A5.12). During both rain-events at one industrial location and at one residential location, function differed between before and after rain (Table A5.12). No differences were found between land-use types. There was significant variability across rain-events and locations (Table A5.12).

Discussion

The previous field study (Chapter 4) found the evidences for differentiation of microbial community structure and function due to inputs from land-use types. However, the previous study was conducted after a rain event, because of, which, the influence of rain was not studied. Therefore, in this study, the aim was to understand the influence of rain perturbation on structure and functional potential of sediment-associated microbial communities from residential and industrial land-use types.

Overall, the study found that though profiles of microbial communities of sediment samples clustered between residential and industrial sediment-types, the influence of rain was land-use specific. Although, overall differences were not detected in main PERMANOVA test, pair-wise test revealed that the differences were rain-event specific. The finding that the differences were detected mostly during rain-event 1 and few on rain-event 2, explains that a longer dry periods before rain allow structure of microbial communities to differ significantly from the fresh sediment community after rain (please see "study site description and sample collection section" in "materials and methods" of this chapter for details on rain events). However, grouping of some samples in clusters of other factors is explained by the high variability detected among the random factors such as rain-events and locations. This variability could be attributed to multiple

factors, such as sediment heterogeneity in the catchment, variations during sample processing and sequencing.

Among different Phyla detected, presence of Proteobatcteria as most dominant phyla was expected for it is among the major group of bacteria and has been widely studied (Gupta, 2000). But its abundance was not significantly different between microbial communities of the sediments from residential and industrial land-use types indicating that the members of this phylum continue to dominate the microbial communities, irrespective of pressures from land-use or rain disturbances. Dominance of Cyanobacteria as a major phylum indicates that primary productivity is intact in sediments of urban waterways and that the urban waterways could be seeded by Cyanobacteria from the catchment explains the increase in its abundance after rain in both the sediment types. Similarly, shifts in phylum such as Bacteroidetes, Verrucomicrobia, Actinobacteria, Firmicutes, Planctomycetes, Acidobacteria, Chloroflexi and Nitrospirae are important because these phylum are involved in diverse functions making microbial communities more stable from functional perspective (El-Sheekh and Hamouda, 2013; Kirchman et al., 2004; Ledin, 2000; Radwan et al., 2002; Zanaroli et al., 2012b; Zhang et al., 2003). For example, phylum Acidobacteria has been reported to utilize diverse carbon sources from simple sugars to complex substrates such as hemicellulose, cellulose, and chitin. In addition they are also known to reduce nitrates and nitrites without producing nitrogen (Ward et al., 2009)

Functional potential of microbial communities was also found be grouping according to the land-use types. However, similar trends were not observed for rain-perturbation. Additionally, the intermodal distances between samples were smaller than what was detected in microbial community taxa profiles, indicating that the functional potential is less affected than microbial community structure either by land-use or rain

disturbances. Presence of primary processes, such as carbohydrates, protein metabolism, DNA metabolism and respiration in high abundance along with secondary ones such as virulence, stress response and metabolism of aromatic compounds indicates evenness among different processes, which also explains the stability of microbial functional potential in microbial communities of sediment form urban waterways.

Conclusions

This study concludes that despite high variability associated with field environmental samples, trends can be observed. In this study, structure and functional potential of sediment microbial communities in urban waterways was found to be influenced more by rain in location and rain-event specific manner. The functional potential of microbial communities was found to be more stable, compared to microbial community structure, and had less impact due to rain.

Chapter 6: Succession of sediment microbial communities

Background and aim of the study

Tropical regions are characterized by frequent cycles of storm events and dry periods. The physicochemical perturbations induced by these cycles can have profound effects on the microbial community in the catchments and canals. The canal ecological system which includes sediment and associated microbial communities has to cope and settle to these perturbation cycles and reach equilibrium. In order to study 1) how the sediment-associated microbial communities adapt and reach equilibrium after a rain perturbation and 2) how the responses differ in microbial communities from different land-use, this study was conducted in a partially controlled environment with sediments from residential, industrial and mixed (sediments from residential and industrial mixed in equal proportion). Mixed sediment type was created to understand the interactions of two microbial communities of different origin. Both land-use types were expected to contain different chemical and physiological environmental parameters which are washed with water after the rain-event and are channeled through a dense network of drains and concrete channels to bigger canal, thus, making the sediment system in canals representative of local catchment environment.

Materials and methods

Experimental design

In expectation to cover the full successional cycle, a 30 day experiment was designed for this study with ten sampling time-points. The experiment design was PERMANOVA based with three factors (Fig. 6.1). Sediment type and time were fixed factors and reactor number was random factor and nested in sediment type. Three sediment types, residential, industrial and mixed were studied during the experiment. Each sediment type was run in three parallel replicated experiments and each experimental replicate was sampled three times as technical replicates. Therefore, 270 (3×3×3×10) samples were collected for each time-series measurement. The experiment was randomized at each level (unless otherwise stated) and conducted in a semi-open environment with protection from rain.

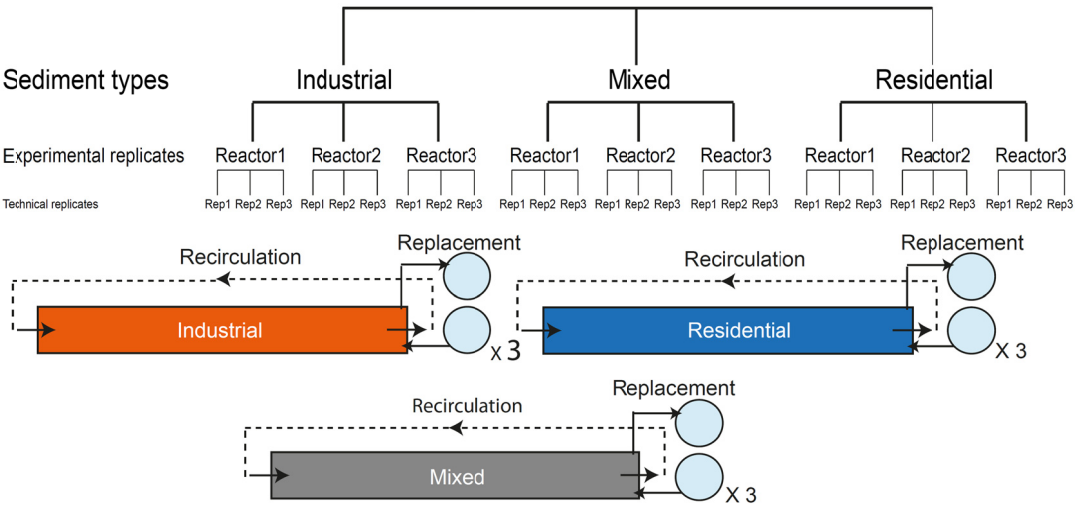

Figure 6.1. The experiment design to study succession of microbial communities. Three reactors each were used for each of sediment type and were placed randomly. Each reactor was attached to separate recirculation and replacement circuit.

Mesocosm reactor design

Mesocosm reactors were fabricated using 1.8 cm thick acrylic glass sheets (Fig. 6.2). Each reactor was 235.1cm long (internal length: 231.5cm), 18.6cm wide (internal width:

15cm) and 16.8cm high (internal height: 15cm). Space along the length, for sediment bed to be paved, was provided in the middle of the reactors. 10cm of reactor space along the length on the extreme ends of the reactors was isolated from rest of the reactor using 0.5cm thick partitions with 5mm holes on the top (10cm) and 2mm holes at the bottom (5cm), to smoothen the flow of recirculating water, entering from the inlet and to keep the sediment bed packed and from being washed away with the water flow. Each reactor was fitted with its own recirculation and replacement circuit. The recirculation circuit included water outflow, sink, connecting polyvinyl chloride (PVC) pipes (32mm), centrifugal pump (Eheim 5000, 41.5-83.3 $Lmin^{-1}$) and gate valves. Centrifugal pumps were run at full workload and excess water on the pressure side was bypassed to the sink to avoid any resistance buildup on the pump. Only required amount of water was allowed to flow towards the reactor inlet. The replacement circuit included replacement water tanks (PVC150L), silicon tubes (5mm), peristaltic pump (MasterFlex L/S® Easy-Load® II), connector PVC piping and two-stop pump tubing (silicone platinum-cured) tubes: MasterFlex L/S® 16). To keep the same flow, single peristaltic pump was used for incoming as well as outgoing water. Fresh water was stored in separate tanks for each reactor. Fresh water was filtered through a mesh (≈1mm) to strain the debris from entering the reactor system. The whole set-up was kept on the elevated platform which was shared by two reactors. PVC sheets were raised between the reactors to prevent cross contamination. Reactors were covered with aluminum foil to reduce the light penetration and discourage algal growth.

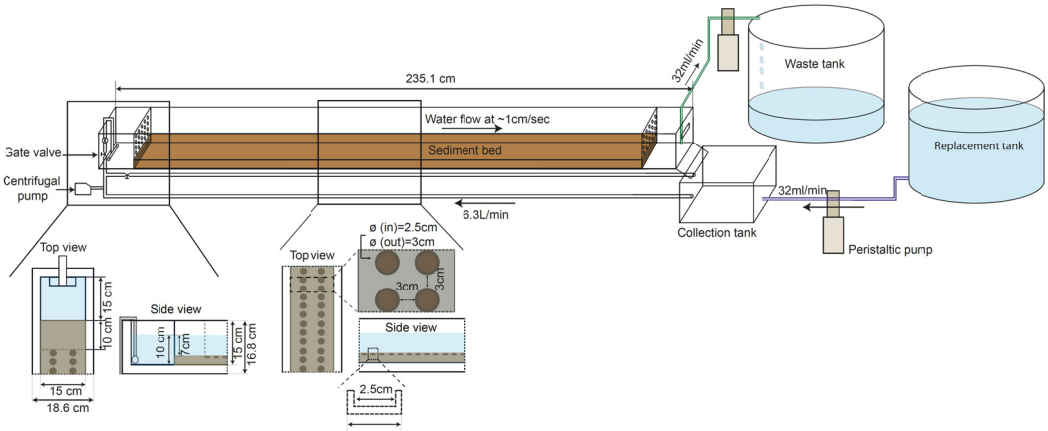

Figure 6.2. Schematic of mesocosm reactor design. A 235.1 cm (external dimensions) acrylic glass (1.8cm thick) laminar flow mesocosm reactor was designed with recirculation and replacement circuit. A single mesocosm reactor set-up is shown. 15cm space on both sides of the reactor was left for entry and exit of water from the system (left and right respectively). Sediment bed is spread across the length of the reactor (200.5×3cm). The height of the sediment bed can be adjusted according the requirement of the experiment. The collection tank on the right side of the reactor collects water from the recirculation circuit. Replacement circuit included replacement tank to store fresh canal water, waste tank, peristaltic pump and connecting pipes.

Hydrodynamic settings

The reactors were operated at continuous recirculation and replacement of water with constant flow. The recirculation flow was kept laminar and maintained at ≈6.3Lmin^{-1} (±5%) to get the mean bulk velocity of water above the sediments ≈1cm s^{-1} (±5%) at all times during the experiment. In the present study, to calculate Reynolds number for rectangular open flow channel, hydraulic radius (Y) was first calculated as:

$$Y = \frac{WD}{W + 2D}$$

Where W is width of reactor and D is water head over sediments. The Reynolds number was then calculated using following formula:

$$N_R = V \frac{Y}{v}$$

Where V is the bulk velocity of water and v is kinematic viscosity. The outflow was kept at 10cm from the bottom (inner surface) of the reactor in order to maintain a constant the water head of 7cm above the sediment bed. Outflowing water was captured in the sink

and was pumped back to the upstream of the reactors for recirculation. Flow of fresh water was adjusted to replace the full reactor volume (≈23L) every 12 hours. Fresh water was continuously injected from replacement tank to the reactors from sink while at the same time it was taken out from the downstream end of the reactors at a constant rate of 32ml/min. Fresh water was brought from the same locations and replacement tank was replenished every 48 hours.

Seeding of reactors and daily maintenance

Sediments and water were collected from two sites which are representative of residential and industrial land use types in Ulu Pandan catchment of Singapore. The industrial site is located at Jurong east area (1.332133, 103.749433) (Industrial location 2 in previous study; Fig. 5.2B) whereas the residential site is located at Clementi area (1.318195, 103.771985) (Residential location 1 in previous study; Fig. 5.2B). The third sediment type, mixed, was prepared by mixing the above two sediment types in equal proportions. Sediment and water was collected from both sites on the morning of 23rd November 2012 after rain event. The duration between rain event and sediment/water collection was between 6 to 8 hours. Freshly settled top layer of sediments was carefully collected and transferred into the clean buckets. Water was collected from the same site in pre-cleaned 25L cowboys and immediately transferred to the experimental site. The sediments were homogenized and cleared of coarse wood and leaf debris before spreading into the reactors to the height of 3cm. Ceramic cups, made of natural clay were equilibrated with canal water for 15 minutes before they were buried in the top 1cm layer of sediments. Water from respective source was filled in the reactors to start the recirculation circuit. Replacement tanks were also filled with same water and replacement circuit was also switched-on. The reactors were monitored on daily basis to check the water flow, water quality (reactors and fresh water), and sediment dissolved oxygen and ORP. The

replacement tanks were filled with fresh water from respective locations every alternate day.

Figure 6.3. Flow of events in setting-up the mesocosm experiment. The top lane shows the initial preparations of the reactors before seeding the reactors. All the nine reactors were cleaned, disinfected, dried and covered with aluminum foil. All the connections were made and reactors were kept operationally ready for seeding. Second lane shows the events during the seeding of reactors on day0 of experiment. The sediments were collected in the morning after 6-8hrs of rain event (during night). The sediments were homogenized and spread in the reactors. Ceramics cups were buried and water was filled in the reactors. Recirculation and replacement circuits were switched-on and reactors were covered with aluminum foil to start the experiment.

Sampling design and daily monitoring of environmental parameters

The sampling was divided into two parts: sampling on time points and daily monitoring (Fig. 6.4). Sediment samples were collected on the time-points for meta-omics and meta-environment parameters measurements. The omics analysis included DNA figureprinting for microbial community profiling (T-RFLP) and metatranscriptomics whereas meta-environment parameters included metals, nutrients (ammonium, nitrates, nitrites, sulfates and phosphates) and biomass (cell-counts). Ceramic cups with internal diameter 2.5cm and 0.5cm deep were buried 1cm in the sediment bed placed in the reactors for sediment sampling. The spacing between the ceramic cups was about 3cm from each other and from the side walls (Fig. 6.2). Samples were collected in triplicates from random location within the reactor to reduce any linear trend, if any, due to linear water flow. In order to

avoid sample artifacts at the extreme ends, 10cm length of sediment bed on both ends was kept free of sampling. Water samples were also analyzed for metals and nutrients during the time-points. For the daily monitoring, water samples were tested for physicochemical parameters such as temperature, pH, conductivity, salinity, dissolved oxygen, oxidation-reduction potential (ORP) using 556 multi-probe system and 650MDS data recorder from YSI. Sediments were tested for partial pressure of oxygen (pO_2) and oxidation-reduction potential using Clark Type Needle Sensor (for pO_2) and Redox Needle Electrode (ORP) from Unisense A/S.

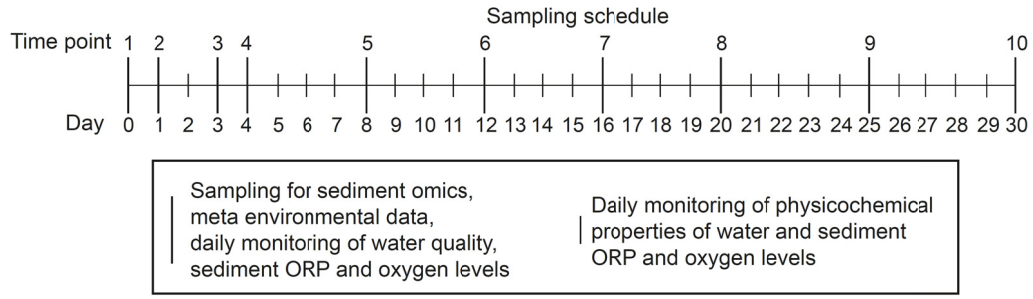

Figure 6.4. Time-line for the sampling schedule is shown on central horizontal line. The longer vertical lines represent time-points spread over time-line. Samples on these time-points were collected for meta-omics (sediments), meta-environment measurements (sediment and water) with regular daily monitoring of sediment and water parameters. Small vertical lines represent sampling for regular daily monitoring of reactor (recirculation circuit) and fresh water (replacement circuit). Please see below table for the list of measured parameters.

Table 6.1. Summary of approaches used in the experiment. NA: not applicable

Name of the parameter	Source		Frequency		Sample processing		Reference		Platform	
	Sediment	Water	Sediment	Water	Sediment	Water	Sediment	Water	Sediment	Water
Nitrates	✓	✓	Time-points	Time-points	Shaking overnight with MiliQ water	0.2 µm filtration			Ion-Exchange	Ion-Exchange
Nitrites	✓	✓	Time-points	Time-points	Shaking overnight with MiliQ water	0.2 µm filtration	(Irshad et al., 2013)	NA	Ion-Exchange	Ion-Exchange
Ammonium	✓	✓	Time-points	Time-points	Shaking overnight with MiliQ water	0.2 µm filtration	(Irshad et al., 2013)	NA	Ion-Exchange	Ion-Exchange
Sulfates	✓	✓	Time-points	Time-points	Shaking overnight with MiliQ water	0.2 µm filtration	(Irshad et al., 2013)	NA	Ion-Exchange	Ion-Exchange
Metals (12)	✓	✓	Time-points	Time-points	Shaking overnight with MiliQ water	Filtration and acidification	(Meers et al., 2006)	NA	ICP-MS	ICP-MS
Physicochemical parameters (5)		✓	Daily	Daily	NA	*In situ* measurement	(Richardson et al., 2011)		NA	YSI 556 System
Dissolved oxygen	✓		Daily	NA	NA	*In situ* measurement	(Peter Revsbech, 2005)		Clark Type Needle Sensor	NA
Oxidation-reduction potential	✓		Daily	NA	NA	*In situ* measurement	(Peter Revsbech, 2005)		Redox Needle Electrode	NA
Cell counts	✓		Time-points	NA	Sonication-syber green	NA	(Amalfitano and Fazi, 2008; Duhamel and Jacquet, 2006)		Flow-cytometry	NA
T-RFLP	✓		Time-points	NA	Freeze-thaw & chemical lysis	NA	(Schütte et al., 2008)		Applied Biosystems 3730xl	NA
Meta-transcriptomics	✓		Time-points	NA	MO BIO RNA Isolation Kit	NA	(McGrath et al., 2008)		Illumina HiSeq	NA

Sample transportation and storage

Water samples were collected in clean 15mL BD Falcon™ tubes and kept on dry-ice during transportation. For sediment sampling, buried ceramic cups were carefully taken out without disturbing the nearby sediments and the contents were immediately transferred to clean 50mL BD Falcon™ tubes filled pre-chilled buffers and stored on dry-ice. The samples were transported immediately to the labs for further processing. Water samples were stored in freezer (-20^{0}C) till analysis. Sediment samples were processed on the same day from DNA extraction and stored in -80^{0}C till processing for RNA extraction.

Nutrients, metals and cell counting sample preparation

Metals and nutrients loosely attached to sediments and soluble in pore water and bioavailable to the microorganisms were measured. The protocol to extract the water extractable fraction of metals and nutrients was adapted from previous reported methods (Irshad et al., 2013; Meers et al., 2006) with slight modifications. Extractions of 1g of sediment samples were performed with 20mL of mili-Q water (18.2 MΩ·cm) was added to the samples. The samples were shacked at 200 rpm for 16hrs at room temperature to detach the sediment surface-associated inorganic compounds. Extracted Inorganic compounds in the supernatants were filtered using 0.2um filter. The filters were flushed first with acidified with mili-Q water (pH 3) and then with neutral pH water prior to sample filtration. Nutrient ions were tested from 10mL of supernatant using Prominence HIC-SP IC dual system for anion and cation simultaneous analysis system from Shimadzu. Remaining 10mL of water was acidified (500µL of analytical grade nitric acid) for metals analysis using ICP-MS (Agilent 7700).

For cell-counting (done with Mr. Toh Jun Wei, RA, SCELSE), The protocols were adapted from previously reported studies (Amalfitano and Fazi, 2008; Duhamel and Jacquet, 2006) sediment samples were dewatered and weighed to 0.2g and placed in 2mL eppendorf tubes. 1.5mL of 10% methanol (90% filtered PBS, pH 7.4) was added to the samples and sonicated at 37khz, 320W for 15mins at 35^0C. Samples were placed on ice for 5mins. Sonication and cooling on ice was repeated. The samples were then centrifuged at 200g for 2mins to remove unwanted sediment particles. Equal volume of supernatant with dislodged cells was transferred into 2 separate eppendorf tubes (0.75mL each). The supernatant was centrifuged at 8000g for 5min to obtain cell pellet. The supernatant was discarded and 0.2mL of 4% paraformaldehyde into one of the eppendorf tube for fixing gram-negative bacteria. In the other tube 0.2mL of 100% Ethanol was added to fix gram-positive bacteria. Samples were incubated overnight at 4^0C. Cell pellet was obtained by centrifuging samples at 8000g for 5mins. Pallet was washed twice with 0.2mL of filter sterilized PBS and re-suspended in 0.5mL of equal volumes of 100% ethanol and PBS. 0.1mL of the sample was mixed with 0.5ul SYBR Green 100X working solution. Samples were incubated in dark for 30mins and centrifuged at 8000g for 5mins.Samples were washed and re-suspended in 0.5mL PBS. Samples were then transferred flow cytometry tubes, for cell counting.

Nucleic acids extraction

Genomic DNA was extracted from the samples immediately after sampling. Sediments were dewatered and DNA was extracted by a combination of mechanical, chemical and thermal lysis and chloroform-isoamyl alcohol purification using protocol described in Zhou et al (1996) (Zhou et al., 1996b). Briefly, 5 gm of dewatered sediments were mixed with DNA stabilization buffer. Mixture was transferred to pestle and mortar; pre-chilled

liquid-nitrogen. The samples were grinded and freeze-thawed thrice flooded with liquid-nitrogen. The contents were then transferred to lysis buffer and heated to 65^0C for 3 minutes. Proteinase K was added to the mixture and contents were heated again for 2hrs with mixing the samples every 20mins. Samples were removed from the heating oven and centrifuged at 10,000g for 20 min. Supernatant was collected in a clean tube without disturbing the layer between liquid and sediment phase. The step was repeated to remove further impurities. The contents were added with equal volume of 1:24 isoamyl-alcohol:chloroform and gently shacked for 5 min. The contents were centrifuged at 14,000g and supernatant was collected without disturbing the impurities settled at the phase boundary. The step was repeated twice. The supernatant was then mixed with 0.6 volume of absolute iso-propanol and incubated overnight in -80^0C. The samples were taken out of the incubation, thawed at room temperature and centrifuged at maximum speed for 20min. The DNA pallet was recovered and re-suspended in nuclease free water. Removal of co-precipitated humic substances was achieved by OneStep™ PCR Inhibitor Removal Kit from Zymo Research Corporation (USA) following manufacturer's protocol. DNA was suspended in nuclease free water and quantified using nano-drop and pico green.

Total RNA extraction was carried out (with Mr. Woo Yissue, Research helper and RA, SCELSE) using RNA PowerSoil® Total RNA kit (MOBIO, USA) using 2g of sediments. Extracts were quantified using Qubit®2.0 fluorometer (Life Technologies, USA). DNA contamination was removed using RTS DNAse Kit (MOBIO, USA) to the RNA quality was checked using Agilent 2100 Bioanalyzer (Agilent, USA).

Nutrients analysis

The samples were submitted to SCELSE technologist Ms. Kar Ling and data was obtained. Commercially available certified solutions from Merck, Darmstadt, Germany were used to prepare standard curves for measuring nutrients. Samples were diluted 10x and transferred to clean IC vials. 1mL of sample aliquot was analyzed using Shimadzu Prominence Ion Chromatography dual system (Shimadzu, Japan). 500µl sample were injected into the ion chromatography machine through auto-sampler (Shimadzu, Japan). Anions were analyzed using column shim-pack IC-SA2 and cations with shim-pack IC-C3. 12mM sodium bicarbonate and 0.6mM sodium bicarbonate in water (MERCK, Germany) was used as solvent for anions solvent and injected at a flow-rate of 1mL/min. For cation, solvent used was 2.5mM oxalic acid in water (Sigma Aldrich, USA) which was injected at a flow-rate of 0.95mL/min. Areas of detected peak were integrated with the retention time (RT) of ions of interest using Shimadzu lab solution software V5.51. Concentrations of ions of interest were calculated from the standard curve within its linearity range.

Metals analysis

Samples were acidified and diluted 10x before transferring into clean 5mL ICM-MS vials. The introduction of samples to ICM-MS was automated via auto-sampler attached to the machine. ICM-MS was tuned for Helium in spectrum mode to detect multiple elements in single run. Desired metals with their respective mass were then selected from the periodic table and a method indicating the samples and their corresponding vial numbers was created. Sample uptake time was set to 20 sec while stabilization time was set at 30 sec. Washout procedures were included after the standards and at an interval of 10 samples. The procedure included two washes of 40 sec with ultraclean MiliQ water

separated by 2% HNO_3 wash for 30 sec. Randomly picked standard and blanks were tested After every 15 samples and 20 samples, respectively, for quality control. Standard curves were prepared from using ICP-MS complete standard - IV-ICM-MS-71A in HNO_3 and Mercury for ICP-MS in HCl from Inorganic Ventures Virginia USA and run for each set of samples.

T-RFLP analysis

Sample preparation

PCR amplification of the purified genomic DNA was performed to amplify the fragment covering variable region 4 to 9 of small sub unit of bacteria 16s rDNA. Primers, BSF517 (5'-GCCAGCAGCCGCGGTAA-3') and BSR1541 (5'-AAGGAGGTGATCCAGCCGCA-3') (Cai et al., 2003) were tagged with fluorescent dye FAM and PET respectively. One microliter of genomic DNA (~25ng) was transferred to 96 well plate, containing mastermix solution of 12.5 µl of 1X Immomix Mastermix buffer (Bioline, Australia), 0.5uL of forward and reverse primers (Applied Biosystems, USA), and 10.5 uL of nuclease-free water. The reaction mixture was then run in a ThermocyclerR pro (Eppendorf, USA) with an initial denaturation at 97^0C (10 min), followed by 30 cycles of amplification (denaturation at 97^0C, 1min; annealing at 55^0C, 30s; extension at 72^0C, 1 min) and final extension at 72^0C, 7 min. PCR product were purified using QIAquick PCR purification kit (Qiagen, USA) as per instructions from manufacturer. The amplified product size and concentration were checked by agarose (1% (w/v)) gel electrophoresis stained with SYBR Green I (Life Technologies, USA) and viewed with a Gel DocTM XR+ system (Biorad, USA) and nanodrop readings. The tagged PCR product was then digested with two set of restriction enzymes, i.e. AluI and

BsuRI (Fermantas, Canada) following manufacturer's instructions to generate fluorescently-labeled terminal restriction fragments for T-RFLP analysis. Briefly 1 unit of AluI and 1 unit of BsuRI were used to digest 1uL PCR product separately at 370C for 13 hrs, followed by thermal inactivation at 80^0C for 20 min.

Sample analysis

2µl of fluorescence labeled terminal restriction fragments were added to 18.5µl HiDi formamide and 0.5µl size standard of 50bp – 600bp (Applied Biosystems, USA). The fragments were resolved by capillary electrophoresis using ABI 3730XL automatic DNA sequencing machine (Applied Biosystems, USA).

Data collection and organization

Four different profiles were generated from one PCR sample for two restriction enzyme and two fluorescent dyes labeling for forward and reverse primers (AluI_FAM, AluI_PET, BsuRI_FAM and BsuRI _PET). Data from the sequencer was imported to GeneMapper where actual size of T-RFs was calculated by interpolation using local southern algorithm. Fluorescent intensity was used to estimate peak abundance and represented as peak height and peak area. Fragments were aligned by nearest integer rounding method and binned according the fragment size. Data was exported in three formats, first, full dataset without removing noise, peak area/height after removing peaks <100 fluorescent units (FU) and presence absence with the same threshold. Data was then exported which included the peak area/height and presence/absence of fragments binned according to fragment size, calculated from size standards. The datasets were organized into an abundance/PA matrix of sample by fragment size. Five datasets were created for statistical analysis. Four separate datasets were created with four profiles of each sample

and in fifth dataset all the four profiles for each sample were appended in the order AluI_FAM, AluI_PET, BsuRI_FAM and BsuRI _PET. Samples, for which the terminal fragment peaks were not detected (even for a single restriction enzyme_dye combination), were excluded from the analysis.

Cell counting sample analysis

Separate gating boundaries for PFA and ethanol fixation conditions were determined with different stain concentrations (0-5µl of 100x working solution of syber-green), with and without (negative control) sediments. Day 30 samples were used to confirm the gating boundaries. Threshold was set at 800 on PF-1 (Green fluorescent) under both fixation conditions. Done with Mr. Toh Jun Wei (RA, SCELSE)

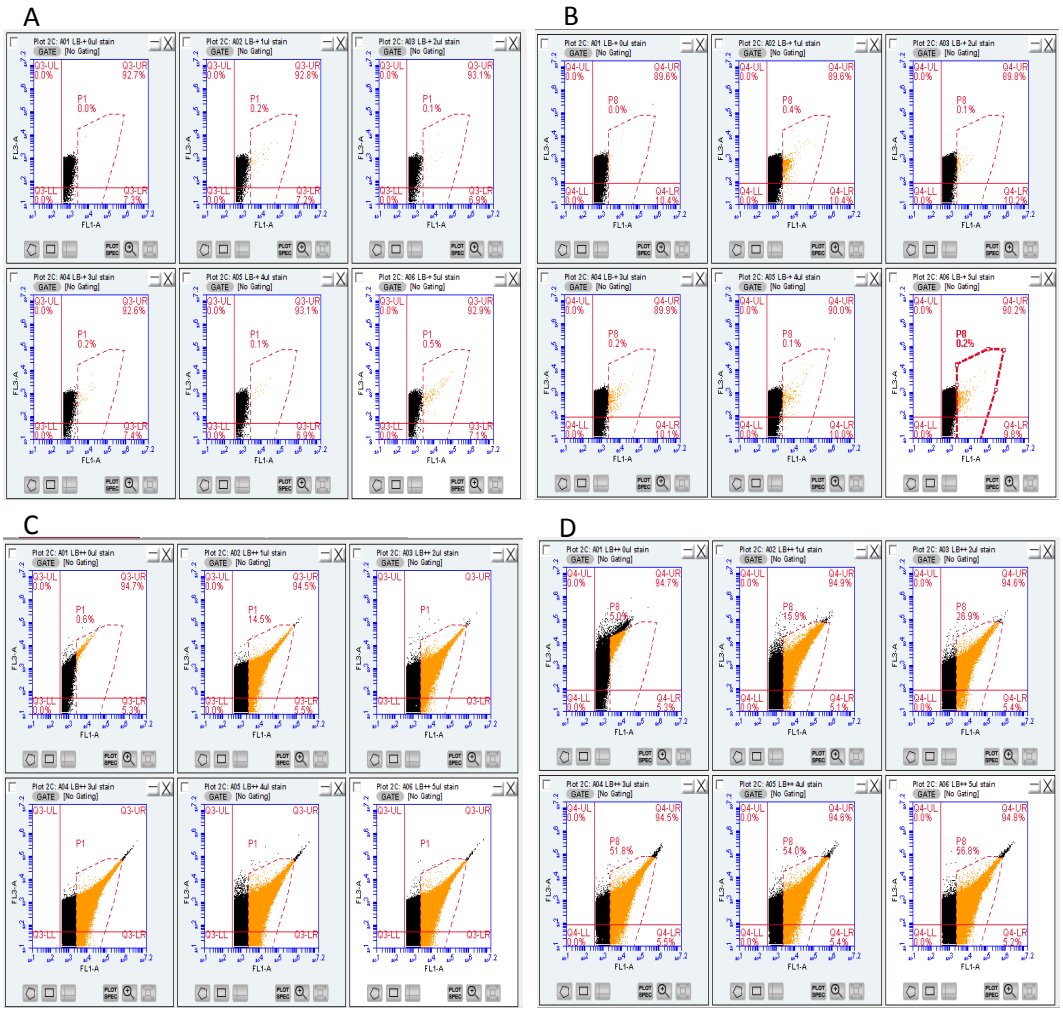

Figure 6.5. Establishment of gating boundaries for cell counting for sediment samples. Gating boundaries were established using negative controls and day30 sediment samples at 6 stain dilutions (0-5µl of 100x working solution of syber-green). (A) Ethanol fixation without sediment samples (B) PFA fixation without sediment samples (C) Ethanol fixation with sediment samples (D) PFA fixation with sediment samples (Done with Mr. Toh Jun Wei, RA (SCELSE))

Total RNA sequencing

Day0, 1, 4, 8, 12 and 30 total-RNA of sediments from one sample per reactor of residential and industrial sediment type were submitted for next generation MiSeq and HiSeq meta-transcriptomics sequencing at SCELSE (in collaboration with Dr. Stefan Schuster and Dr Daniela Drautz). This resulted in Miseq RNA sequencing data from 9 samples (3 time-points × 3 sediment type) and HiSeq RNA sequencing data from 36 samples (2 sediment type × 3 samples per sediment type × 6 time-points). Sequencing data was run through standard bioinformatics pipeline for RNA sequencing data. Active functional transcript (mRNA) sequences were pulled out and annotated with KEGG ontology groups (in collaboration with Dr. Rohan Williams) to understand the functional changes in microbial community whereas v5 region of 16s rRNA transcripts were screened and annotated using NCBI database search for understanding changes in active microbial community (in collaboration with Dr Xie Chao).

Statistical analysis

Grouping of samples were visualized by Non-metric Multidimensional Scaling (NMDS) plots and Hierarchical clustering (Kruskal, 1964; Murtagh, 1983). Data was first standardized across samples and transformed. Three types of transformations were tested based on the type of analysis required. Log_{10} transformation brings down the influence of highly abundant taxa and shows the variation due to less abundant ones; square root transformation retains the effect of both whereas presence/absence identifies the variation due to community structure only (Kruskal, 1964). Followed by standardization and transformation, dissimilarity matrix based on either Bary-Curtis or Jaccard distance was created. Bray-Curtis dissimilarity was used with abundance data to calculate compositional dissimilarity whereas Jaccard distance was used to calculate structural

dissimilarity of the microbial community by counting matches and mismatches between two samples (Wang et al., 2010). This matrix was then be used for multidimensional ordination plots such as NMDS, cluster analysis and hypothesis testing such as PERMANOVA and ANOSIM (Anderson and Walsh, 2013). NMDS is a rank based ordination method used to visualize samples characterized by multivariate data in two or three dimensional space. The samples grouping closer are similar than those placed far away. The method attempts to place the samples in such a way that their ranked distances remain preserved. Non-parametric methods such as NMDS, PERMANOVA and ANOSIM perform better than other parametric methods, such as PCoA and ANOVA, because the non-parametric analyses use ranked distances into account rather than the absolute distances (Anderson and Walsh, 2013; Kruskal, 1964). NMDS analysis used Kruskal stress to determine minimum stress and 50 restarts were allowed to reach the solution. Shepard plots of observed verses obtained ranked distances were created to test the quality of result. A good linear fit between observed and obtained ranked distances and small stress (<0.2) indicates minimal loss of information during reduction of dimension from multi-dimension (number of variables in samples) to 2 or 3 dimensions (Kruskal, 1964).

Hierarchical clustering was chosen for cluster analysis. Hierarchical clustering heat-map of variable abundance was plotted using Spearman rank correlation for creating distance matrix and average linkage method for generating clusters (Murtagh, 1983). The data was transformed, median centered and normalized across samples and variables. Heat-map of clusters was viewed in Treeview (http://rana.lbl.gov/EisenSoftware.htm).

PERMANOVA design was created based on the current study with sediment-type and time as two independent fixed factors and reactor number as random factor nested within land-use types. T-RFLP data, for, which samples from all sediment-types

and time-points were analyzed, represented the full sample-set for microbial community DNA finger-prints. Here, factor sediment type had three levels, residential, industrial and mixed, time-point had ten levels and reactor had nine levels. However, for mRNA transcripts data, sediment type had two levels, residential and industrial, time-points had 6 levels and reactor had 6 levels. PERMANOVA was performed with 9999 permutations of residuals under reduced model. Monte Carlo *p*values were estimated where number of permutations was lower than 10 in pairwise tests for fixed factors (Anderson and Walsh, 2013). Pairwise one-way ANOSIM was run on time-points and on sediment-type within time-points using Bary-Curtis distance matrix (Anderson and Walsh, 2013). *p*value was estimated based on 9999 permutations to test null hypothesis.

Parametric and non-parametric correlations were used to identify the associations between different variables. Pearson's coefficient was calculated for parametric correlation and Kendall tau's coefficient was used to calculate non-parametric correlations (Newson, 2002). The significance of correlation was tested by a two tailed ttest. Kruskal wallis non-parametric ANOVA were used to compare the means of two populations (Khan and Rayner, 2003).

In order to identify the associations between microbial community and environmental parameters, Canonical Correspondence Analysis (CCA) was performed (Cajo J. E ter and Piet E M, 1995). A subset of environmental parameters from sediment samples were tested for their associations with sediment-associated microbial communities from four time-points, day0, day 8, day 16 and day 30. The time-points were selected to cover the initial adaptive phase (one time-point), intermediate phase (one time-point) and final phase (two time-points). Based on their variations over time sediment samples 3 nutrient ions, oxygen levels, oxidation-reduction potential and 7 metals from sediment samples were tested for associations. CCA attempts to explain

microbial community data by environmental data (Cajo J. E ter and Piet E M, 1995), therefore, environmental data was used to extract pattern from explained variation using direct gradient analysis. Monte Carlo permutations were used to test the significance of first ordination axis and all axes together with 999 permutations. A bipot of microbial community ordination and environmental variables Eigen vectors was plotted to show the relationships of environmental parameters with microbial community shifts.

PERMANOVA and ANOSIM were performed in commercially available software PRIMER6 (version 6.1.13) with PERMANOVA+ add on (version 1.0.3) from PRIMER-E Ltd (USA). Cluster analysis was performed in CLUSTER 3.0 from Stanford University and University of Tokyo and viewed using TreeView 1.16r4 (http://rana.lbl.gov/EisenSoftware.htm). Correlations were calculated using software PAST 2.17c from University of Oslo. CCA was performed using Canoco4.5 and Canodraw4.14 from Wageningen UR.

Results

Dynamics of environmental parameters in sediments

Trends of nutrient Ions:

Nutrient ions such as ammonium, nitrites, nitrates and sulfates in sediment samples showed similar patterns in the three sediment types. The ions were largely within the within the parameters prescribed for healthy aquatic systems (Environmental Health Ready Reference, 1983). Ammonium was below the limit of 75µg/gram with some variation between land-use types during the initial phase but increased to >100µg/gram for a short period (day8) before coming back to original levels in the late phase of the experiment (Fig. 6.6A). Nitrite followed the trend with a spike on day8. Similar to

ammonium, nitrite levels were also detected lower than original levels after the spike on day8 (Fig. 6.6B). Nitrates, on the other hand, showed inverse trend. It showed high variations between the three sediment-types, highest in industrial and lowest in residential and midway in mixed sediment-type. Nitrate levels were detected below 1µg/gram on day8 (Fig. 6.6C). However, similar to ammonium and nitrites, its levels remained below the original levels during recovery after the dip on day8. Sulfates, however, showed totally different trend. It remained below 50µg/gram till day8 but start to build-up after that (Fig. 6.6D).

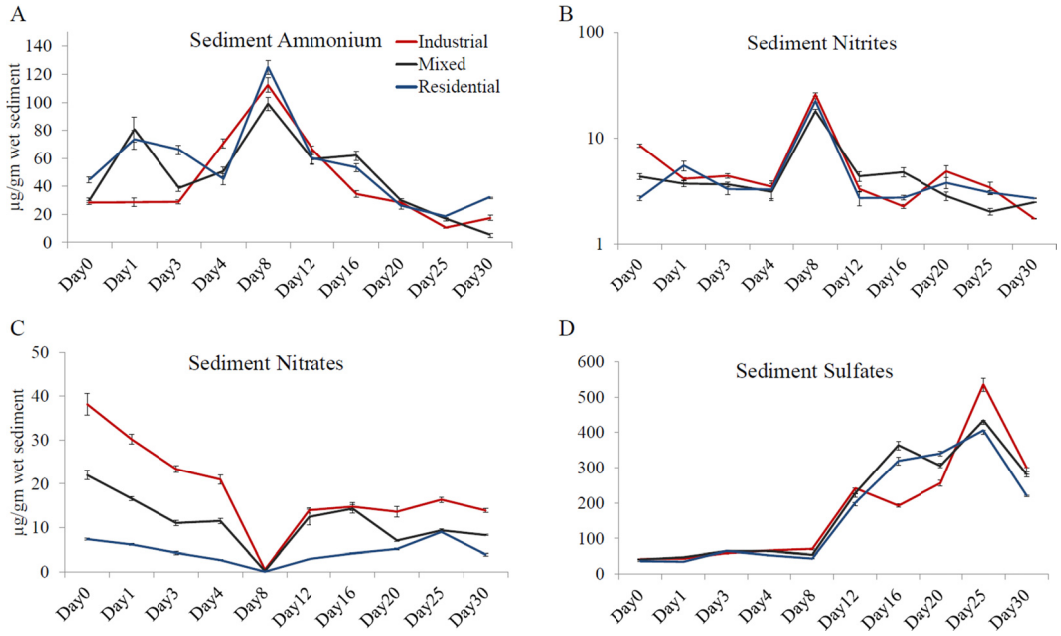

Figure 6.6. Trends of nutrient ions levels in sediments of three land-use types over 30 days. Each data point shows the average of 9 data-points from 3 biological replicates and 3 technical replicates. Error bars show the standard error (A) Sediment ammonium (B) Sediment nitrites (C) Sediment nitrates and (D) Sediment sulfates

Biomass levels:

Cell count levels followed a mixed trend. The counts were detected in the order of 6.5 on day0 but increased by half-an-order on day1. Biomass came down to 6 on day4 before building-up again after that and reached a peak of ≈7 till day20 before starting to come

down in the late phase of the experiment. All the three sediment types followed similar trend. Number of bacteria from sediment-associated microbial community of mixed sediment type remained between that from industrial and residential sediment-associated microbial community cell counts during growth phase from day4 to day16 (Fig. 6.7).

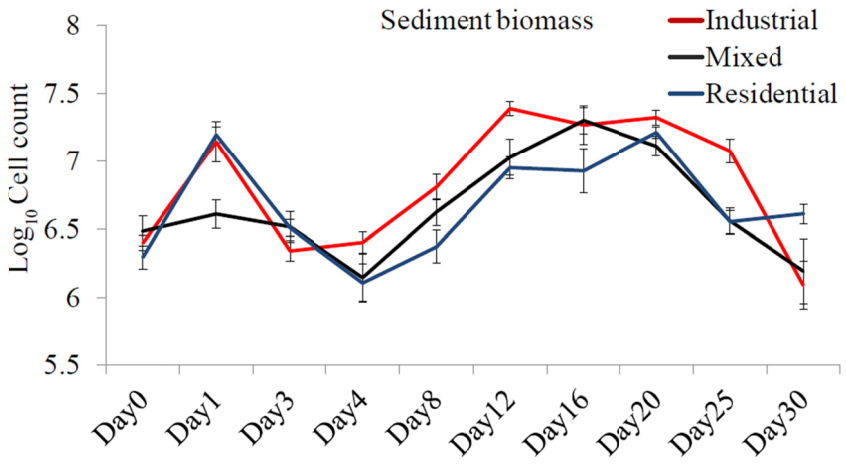

Figure 6.7. Trends of cell counts (biomass) in sediments of three land-use types over 30 days. Each data point shows the average of 9 data-points from 3 biological replicates and 3 technical replicates. Error bars show the standard error

Oxygen and ORP levels:

Sediment oxygen levels showed high variations in industrial sediment types during the initial phase of the experiment. The partial pressure of oxygen was found to be in the range of 3-8mmHg during the initial phase. It came down to around 2mmHg on day7-8. The low oxygen phase lasted till day12 when it starts to increase again. After day 16 it again started to taper down and reached the levels of 3mmHg on day28. An increase in oxygen partial pressure on day 30 was, however, detected in all the three sediment types (Fig. 6.8A).

The Oxidation-reduction potential (OPR) of sediment was largely in negative range, indicating a reducing environment. All the three sediment types showed similar

trends. ORP showed trends similar to oxygen partial pressure. It was in the range of -200 to -100mV till day 5 and came down to -300 to -150mV range on day8-10 after a spike on day7. The ORP recovered to -200mV to -100mV range on day11-15 and came down to -300 to -200mV range during the last phase of the experiment. Similar to oxygen, ORP also showed a spike during the last two days of the experiment (Fig. 6.8B).

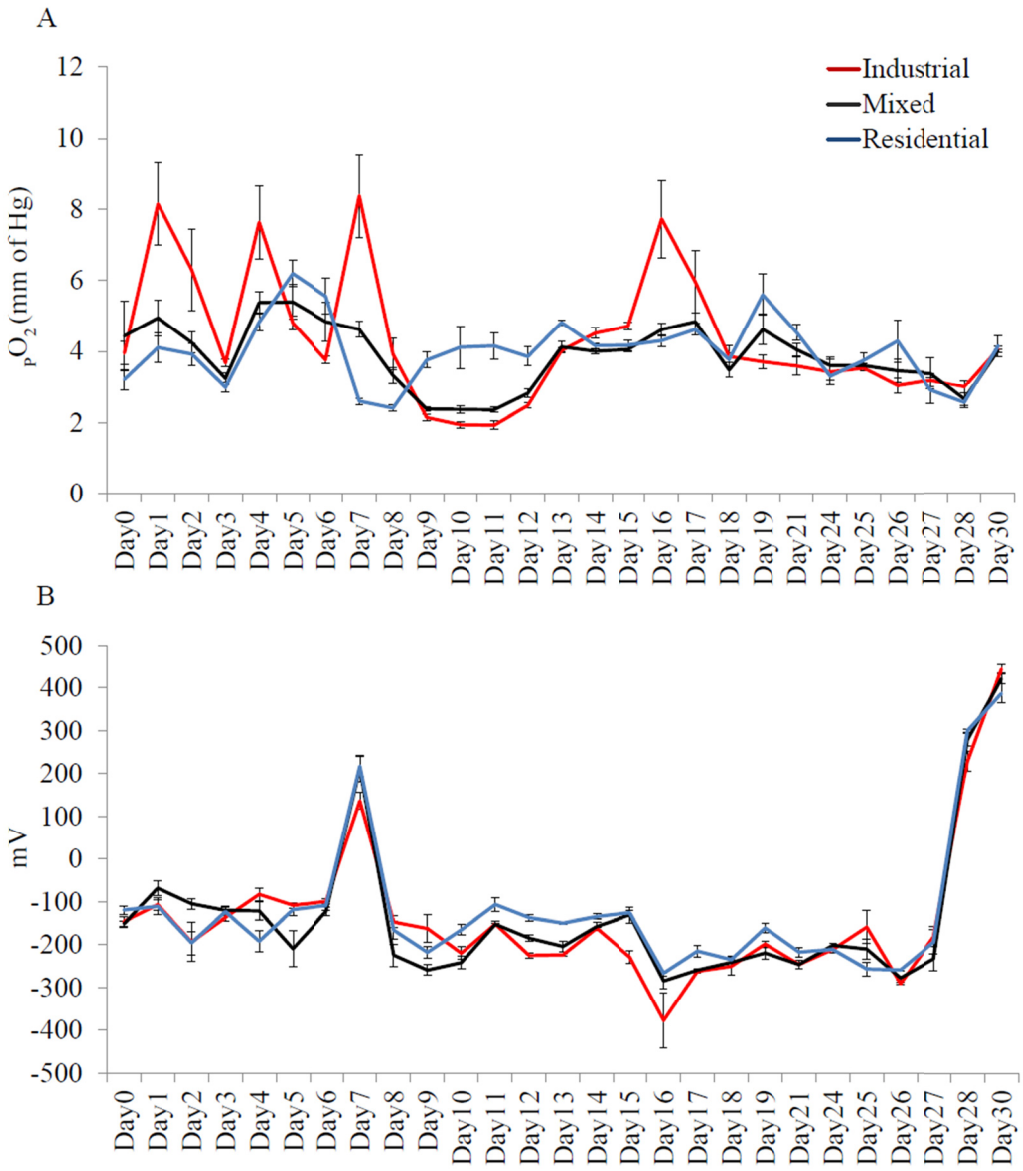

Figure 6.8. Trends of oxygen partial-pressure and oxidation-reduction potential in sediments of three land-use types during succession. Each data point shows the average of 9 data-points from 3 biological replicates and 3 technical replicates. Error bars show

the standard error. (A) Sediment oxygen partial pressure (B) Sediment oxidation-reduction potential (ORP)

Dynamics of metal levels:

Metal levels showed three broad patterns in sediment samples over time during the 30 day experiment which are a 1) decreasing trend 2) first decreasing and the increasing and 3) first increasing and then decreasing trend (Fig. 6.9). The trends observed were largely similar in all the three land-use types tested with metal levels in mixed sediment falling in between residential and industrial in most cases. Magnesium (Mg), iron (Fe), copper (Cu) and zinc (Zn) started with relatively high levels but showed decreasing trends as experiment progressed. Mg showed spike on day 3 but gradually decreased after that. Aluminum (Al) was initially in the range of 100-200 ng/gram but it came down to 50-100 ng/gram range before going up again during the late phase of the experiment. Iron (Fe) too started with high levels in sediments but it quickly came down to 20-60 ng/gram range on day 4 and its levels remained constant thereafter. Zn also showed gradual decrease with a dip on day1. Whereas, Al, Zn, Cu and As showed a sudden increase, Mg, Fe and Hg showed mild increase in their levels on day 30. Lead (Pb) was highly variable between three sediment types during first three days. It increased slowly after coming down drastically on day 4. Arsenic (As) and mercury (Hg) both showed first increasing and then decreasing trend. While, rise and fall of As was slow, Hg increased and decreased sharply, with highest levels recorded on day 8. Whereas, nickel (Ni) was highly variable and undetected in most samples, chromium (Cr) followed decreasing and then increasing trend. Cobalt (Co) followed trend similar to As and Hg. Cadmium (Cd) followed zigzag trend. It is interesting to note that many metals such as As, Hg, Both, Co and Cd were recorded in high levels on day 8.

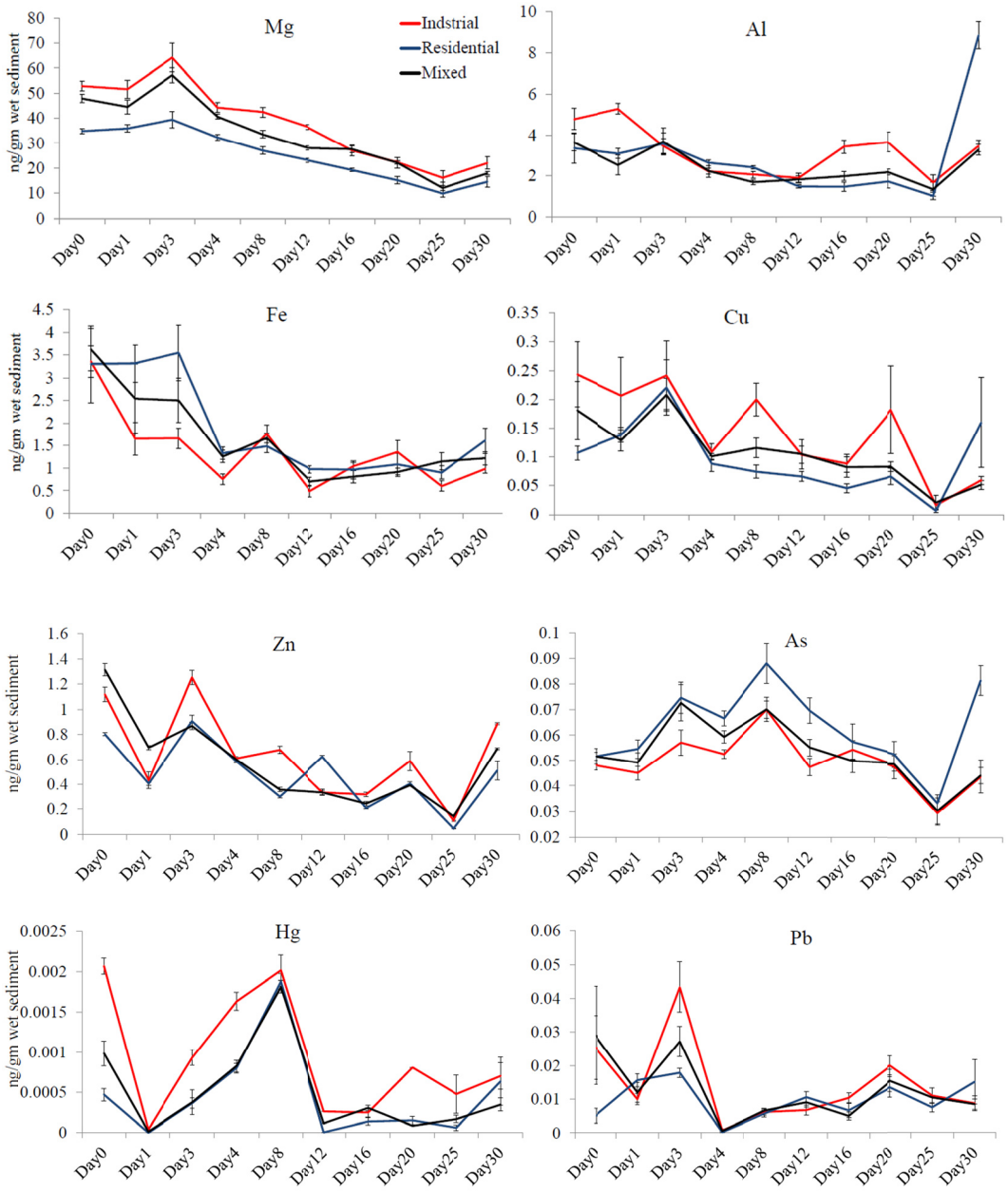
Mg
Indstrial
Residential
Mixed
Al
Fe
Cu
Zn
As
Hg
Pb
ng/gm wet sediment
Day0
Day1
Day3
Day4
Day8
Day12
Day16
Day20
Day25
Day30

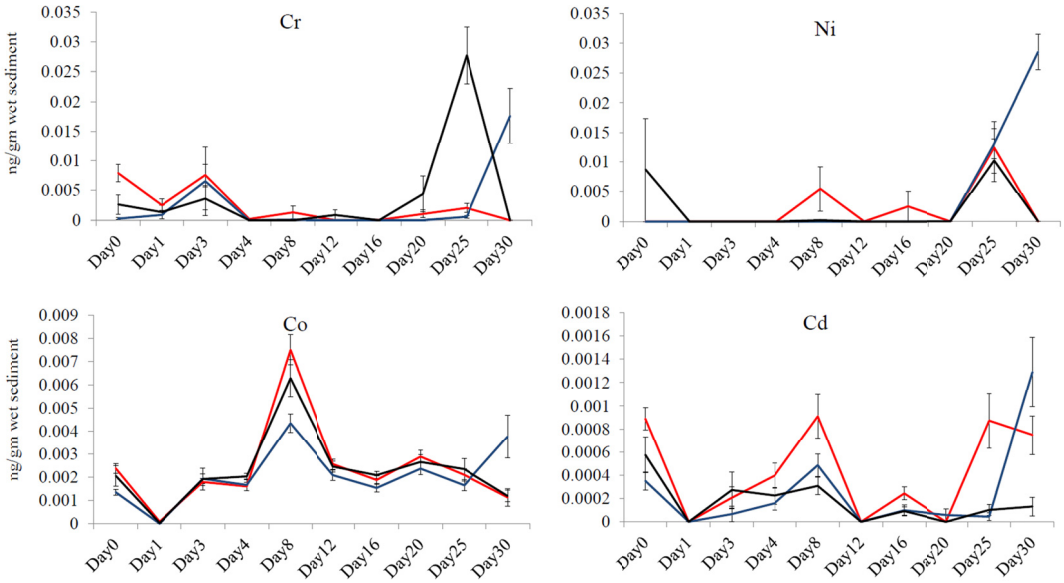

Figure 6.9. Trends of 12 metals levels in sediments of three land-use types during succession. Each data point shows the average of 9 data-points from 3 biological replicates and 3 technical replicates. Error bars show the standard error. Full name of metals symbols are available in abbreviation list.

Dynamics of environmental parameters in water

Trends of nutrient Ions:

Water nutrient ions such as ammonium, nitrites, nitrates and sulfates, though showed similar patterns, they were more variable in the three land-use types (Fig. 6.10). Ammonium was below detection on first two days. It started to appear in water on the fourth day of experiment (day3) and remained high till day8 and reached the original near zero on day 12, 16 and 20 for residential, mixed and industrial land-use types respectively (Fig. 6.10A). Nitrite (Fig. 6.10B) was within detection limits from day0 but started to accumulate from day4 onwards. After reaching its peak levels on day 12 and 16 for residential and industrial/mixed land-use types, respectively, it came down on day 20 and 25 before increasing again in industrial and mixed land-use types on day30. Nitrates levels gradually decreased and started to increase again from day8 (Fig. 6.10C). The

relative change of nitrates over time in water samples was less dramatic than sediment samples. Sulfates varied significantly between the three land-use types and similar to sediment samples, it showed an upward trend after day 8 for industrial and mixed land-use types and from day 4 for residential land-use type (Fig. 6.10D).

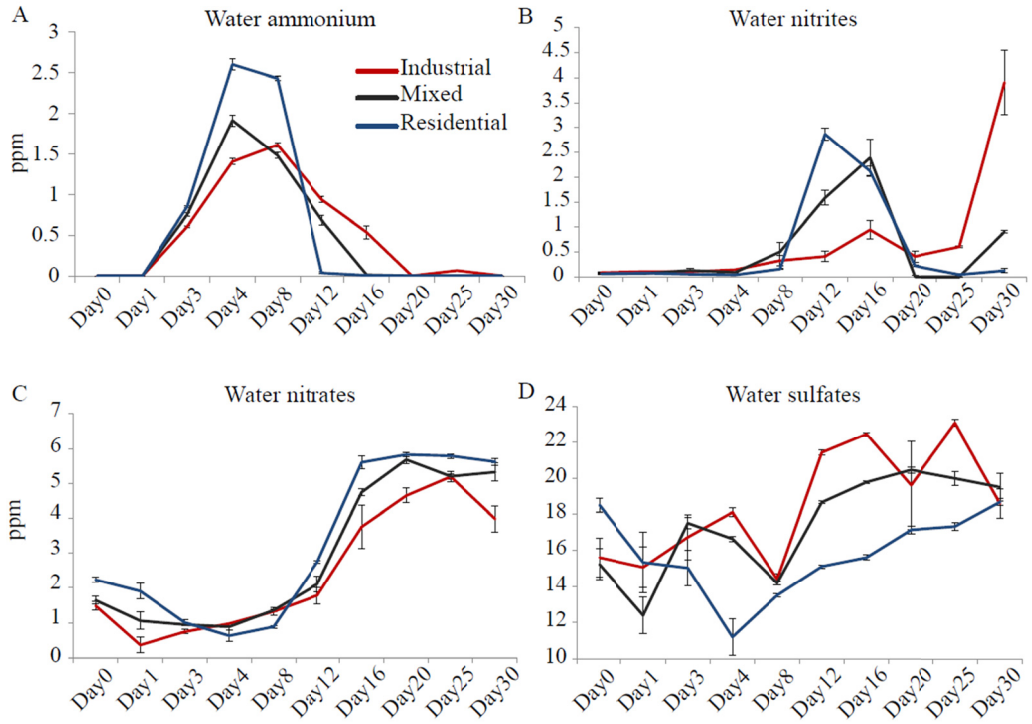

Figure 6.10. Trends of nutrient ions levels in water samples of three land-use types during succession. Each data point shows the average of 9 data-points from 3 biological replicates and 3 technical replicates. Error bars show the standard error (A) Water ammonium (B) Water nitrites (C) Water nitrates and (D) Water sulfates

Dynamics of metal levels:

Similar to sediments, metals levels in water also showed three broad patterns over time during the 30 day experiment which are 1) decreasing trend 2) first decreasing and the increasing and 3) first increasing and then decreasing trend (Fig. 6.11). In addition, similar to sediment samples, the trends of metals in water were largely similar in all the

three land-use types tested with metal levels in mixed type falling in between residential and industrial in most cases. Magnesium (Mg) levels dipped on day1 but increased to maximum levels on day 4. The levels gradually came down after day 4 till the end of the experiment. Aluminum (Al) levels were highest during initial days, day 0 and 1, but they came down to their lowest on day 3. After day 3, the levels increased gradually and were recorded relatively higher levels on day 20 and 30. Iron (Fe), Arsenic (As), mercury (Hg) and cobalt (Co) and zinc (Zn) showed first increasing and then decreasing trend. While, rise and fall of Fe, As and Co was slow, Hg increased and decreased sharply, with highest levels recorded on day 4. Whereas, copper (Cu) showed a clear gradual decreasing trend, lead (Pb) showed an increasing trend with high variation between land-use types during the end phase of the experiment. Zinc (Zn) was highly variable between land-use types and over time. Similar to sediment samples, nickel (Ni) was largely undetected and only appeared in the end phase of the experiment. Chromium (Cr) and Cadmium (Cd) trends were also similar to sediment samples. Cr followed decreasing then increasing trend and Cd followed zigzag trend over time. Interestingly, whereas, Zn As Hg and Co showed peaks on day 4, Fe and Cd were high on both days, day 4 on day 8.

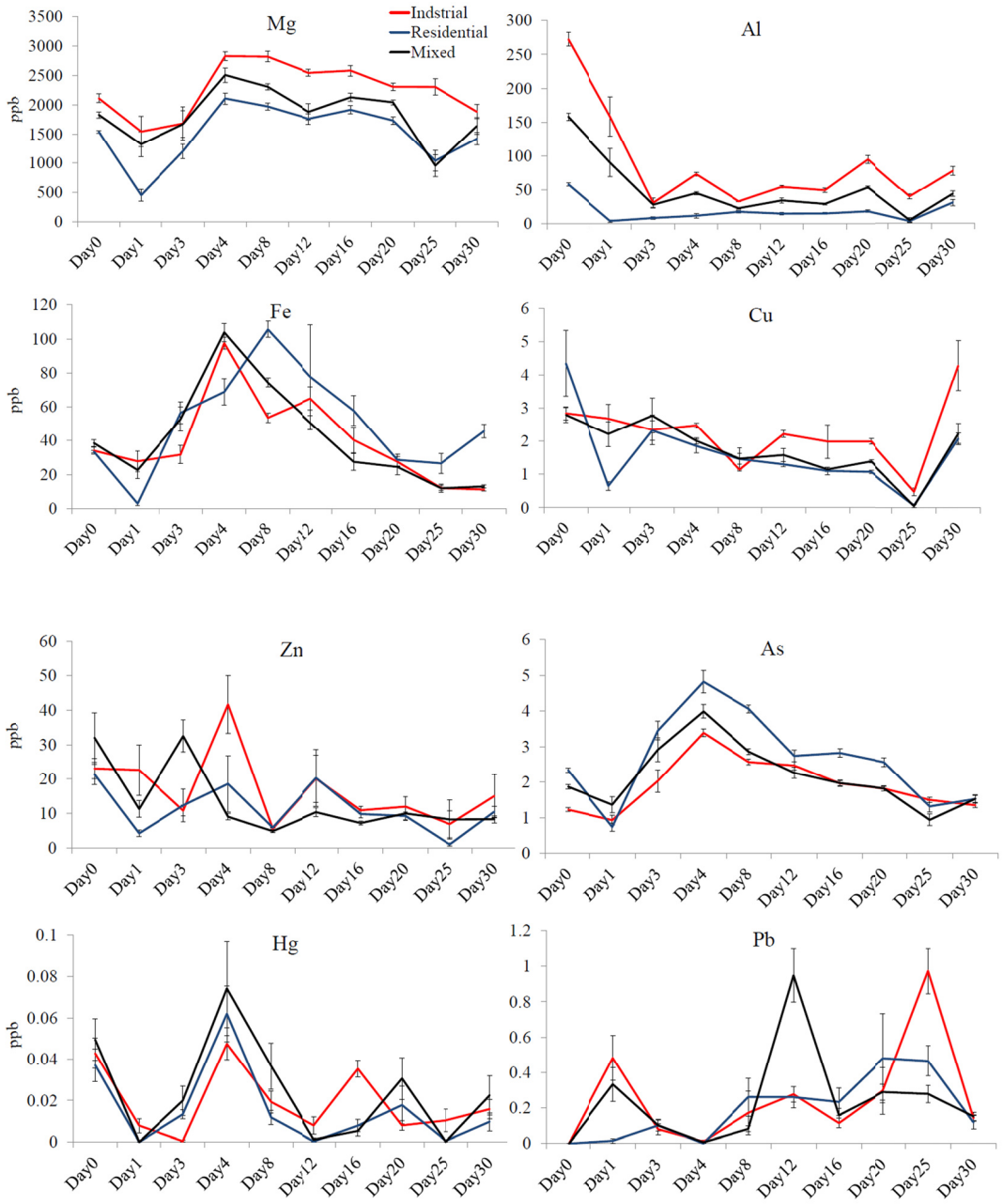
Mg
Indstrial
Residential
Mixed
ppb
Al
Fe
Cu
Zn
As
Hg
Pb
Day0
Day1
Day3
Day4
Day8
Day12
Day16
Day20
Day25
Day30

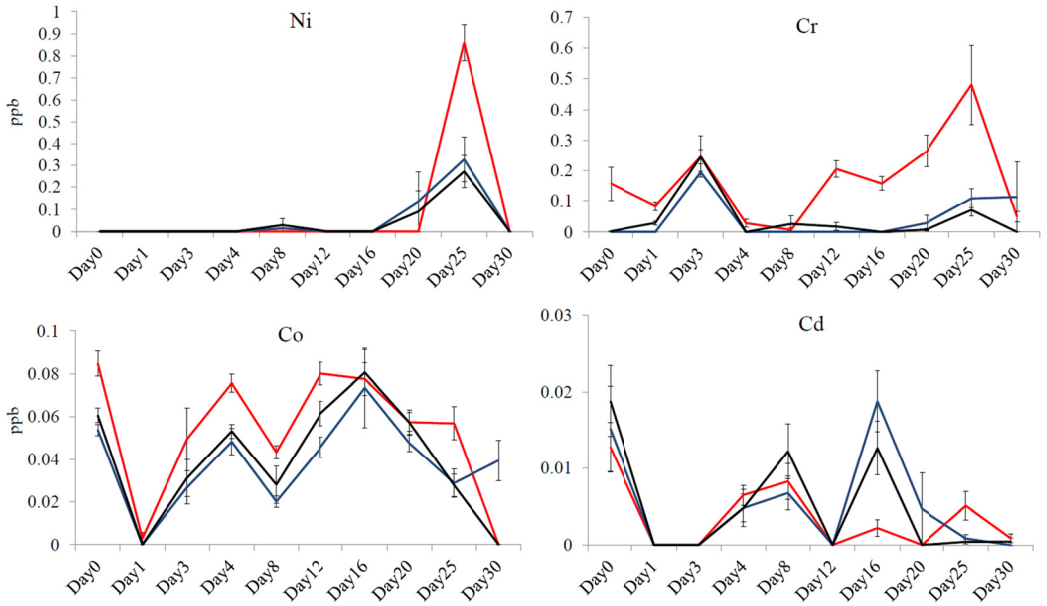

Figure 6.11. Trends of 12 metals levels in water of three land-use types during succession. Each data point shows the average of 9 data-points from 3 biological replicates and 3 technical replicates. Error bars show the standard error. Full name of metals symbols are available in abbreviation list.

Succession of microbial communities

Sediment depth profile (from side of the reactor) showed distinct black layer of anoxic zone below the top sediment layer from day 8 onwards, which reduced towards the end (Fig. 6.12). Sediment texture and sediment-associated microbial communities showed three distinct phases, an initial phase, an intermediate phase and the late phase. Sediment texture and color appeared brown during the initial phase of the experiment.

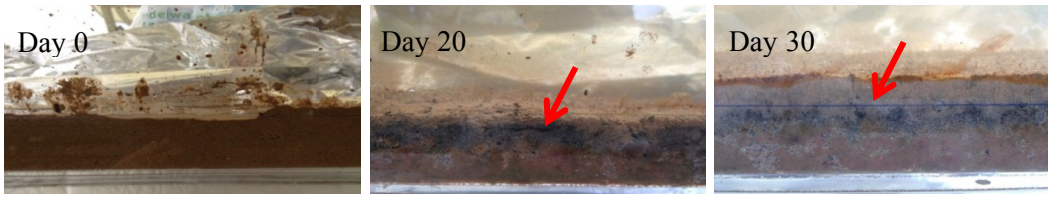

Figure 6.12. Changes in vertical profiles of sediment texture. Distinct black layer of sediments below top layer indication anoxic zone

It turned black with patches of brown spots during intermediate phase on day 8. The texture was similar in all the three sediment types (Fig. 6.13A). Interestingly, the brown patches were seen in close contact with a white mat like structure. The initiation of the mat was in black zone where sulfides are reported to be present (13). The initiation of the white mat structure was followed by beginning of brown patches consisting mainly of oxy-hydroxides (13). As the brown patch grew, the white mat moved sideways growing the brown patch in size (See zoomed box in Fig. 6.13A). After the intermediate phase, the sediments were covered by top layer of brown sediments. As shown in Fig. 6.12, the brown layer increased in depth as time progressed. Small and big worms were detected moving in this zone which could be helping in oxygen transfer to top sediment layers.

Concordant with the sediment color and texture, TRF profiles of microbial communities in the three land-use types also showed three distinct phases. The initial adaptive phase which lasted till day 4 showed high variation between days (Fig. 6.13 B and C). Microbial communities' profiles on day 1 were very different from day 0. They seemed to return to original community structure on day 3 and on day 4, the profiles were closest to day 0 microbial communities. As seen in the sediment texture, day 8 microbial communities TRF profiles changed completely from day 4 community. After day 8, microbial community profiles followed zigzag successions moving away and close to day 8 microbial communities. Day 12 microbial communities showed highest variation after day 8. While, microbial communities on day 12, 20 and 25 were closer to each other and formed a group away from initial and intermediate phase, day 8, 16 and 30 microbial communities formed another group close to intermediate phase. It was interesting to note that microbial communities from different land-use moved in similar direction on all days during the experiment. Microbial community profiles from mixed sediment-type

remained in between the microbial community profiles from industrial and residential sediment types on most days.

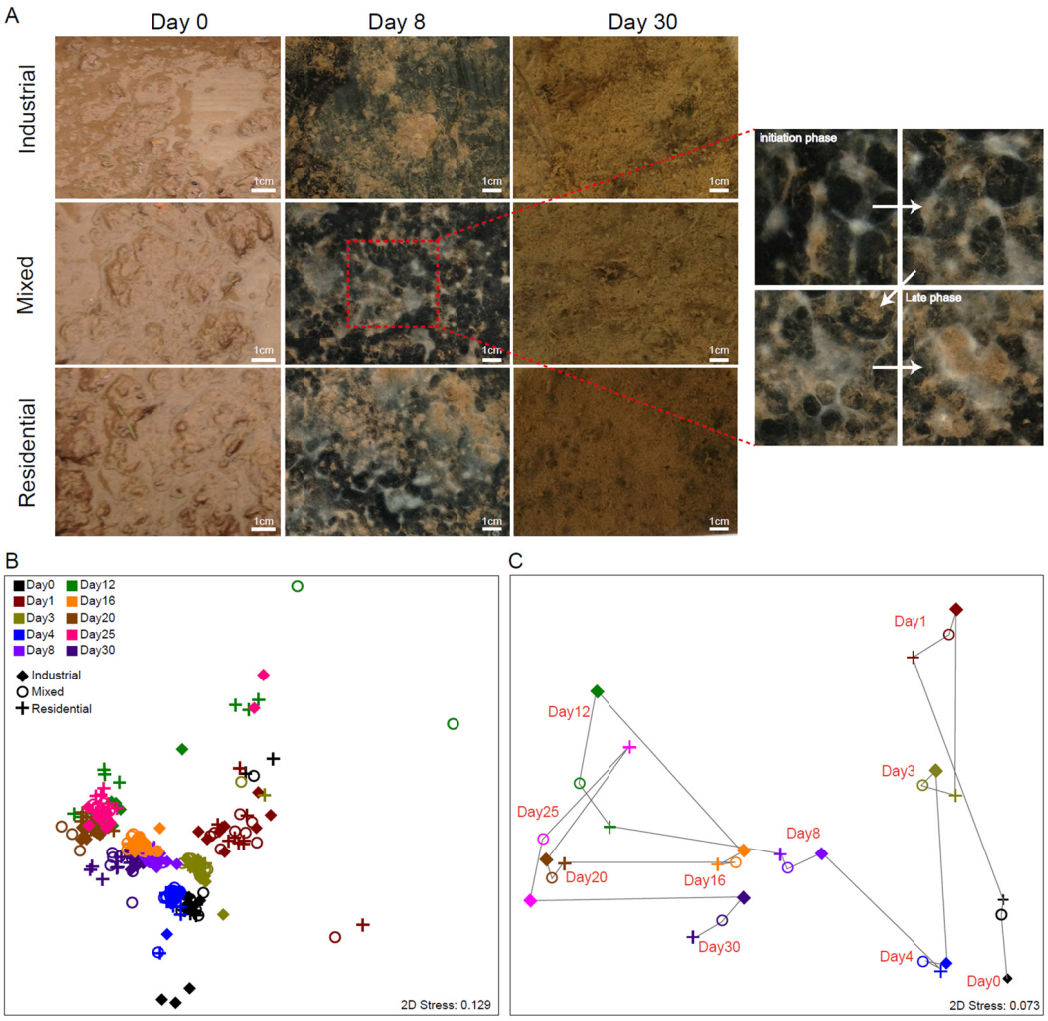

Figure 6.13. Changes in the profiles of microbial communities in sediments during succession. (A) Photographs of sediment surface, taken on day0, 8 and 30 for the three sediment types. White bar in the bottom right of each panel represent approximate 1cm distance. Red box shows different stages of white colonies on black sediments (B) NMDS plot of 16s rDNA TRF profiles (peak height data) from all 270 samples (3 sediment-types × 3 reactors/sediment-type × 3 samples/reactor × 10 time-points) collected during the experiment. Each data-point represents TRF profile of one sample. (C) NMDS conducted on centroids calculated for samples from one sediment-type on each time-point. Each data-point represents centroid of 9 samples from one sediment-type at each time-point. Days are differentiated by colors and sediment-types by symbols.

An assessment of microbial community profiles on each day revealed that the microbial communities from residential and industrial sediment-type were very different on most days (Fig 14). Whereas, microbial communities from residential and industrial sediment-types formed separate tight clusters, microbial communities from mixed sediment-type were found to be dispersed between the two. On day 0 microbial communities from mixed sediments were spotted in the middle of residential and industrial sediment types but day 1 and 3 mixed sediments microbial communities were relatively more dispersed than day 0. Unlike day 0, day 4 and day 12 where microbial communities profiles in mixed sediments were in between microbial communities profiles from residential and industrial sediment types, microbial communities from mixed sediment types on day 8, 20 and 25 formed separate group away from the other two sediment types. Day 16 and day 30 microbial community profiles from mixed sediment type were highly dispersed. PERMANOVA results (Table A6.1) showed that the structure of microbial assemblages significantly differed between all time-points (PERMANOVA pseudo-$F_{10,268}$ = 17.366, p < 0.001). Significant interactions were, however, detected between reactors (Reactor (sediment type) x Day) indicating variation between the reactors. Pairwise test for term "Reactor (sediment type) x Day" for pairs of levels of factor 'Day' revealed that except few, all pairs showed significant difference between days for all the sediment types (Monte Carlo p >0.05, 9999 permutations) (see Table A6.2). Differences between microbial communities from different sediment types were also detected (PERMANOVA pseudo-$F_{3,268}$ = 1.7496, p = 0.0503). Pairwise test for term "sediment type x day" for pairs of levels of factor "sediment type", showed significant differences between industrial and residential sediment type. One way ANOSIM on microbial community profiles also revealed similar results (Table A6.3). Pairwise tests showed highly significant difference between days (p<0.01, r>0.5, permutations: 9999). Test on factor

sediment types within time-points showed no difference between mixed sediments microbial communities and residential or industrial sediment types for day0 and day1. From day 3 onwards the differences were significant (Table A6.4).

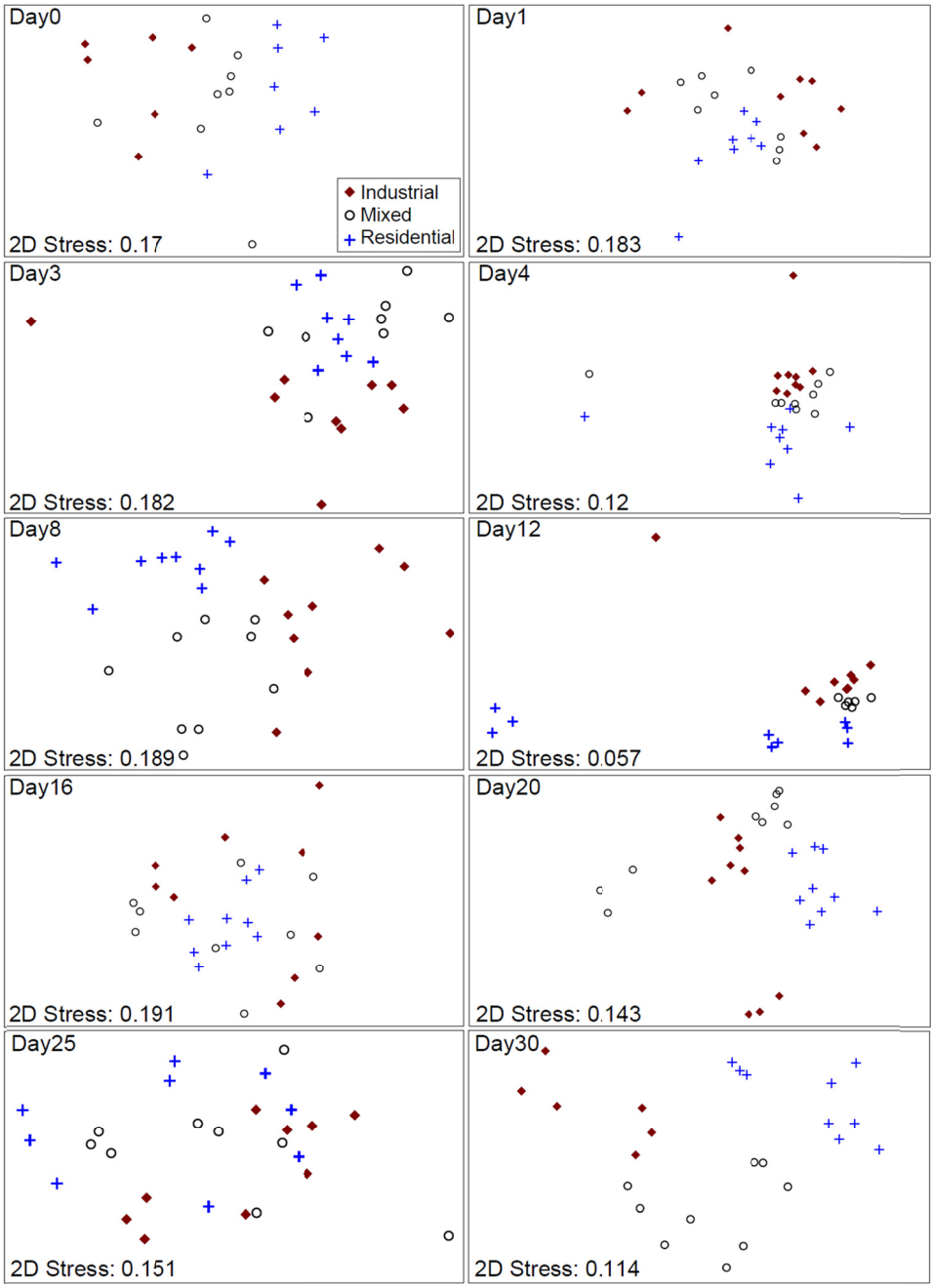

Figure 6.14. Differences in the profiles of microbial communities between sediment-types during succession. Each data-point represents 16s rDNA TRF profile (peak height data) of a sample. The sediment-types are shown as inset with different color and

symbols for day 0 plot. Samples, for which the terminal fragment peaks were not detected (even for a single restriction enzyme_dye combination), were excluded from the analysis (Please see data collection and organization section in materials and methods)

Microbial community composition

Overall active microbial community structure on day 0, day 8 and day 30 calculated by averaging taxa abundance of microbial communities from three land-use types using 16s rRNA sequences revealed that Microbial community composition varied considerably over a period of time. The sequences which could not be assigned to any taxa group were found to be in the range of 45-65% in all 9 samples. Among the assigned taxa groups, Cyanobacteria, Proteobacteria, Bacteroidetes, Acidobacteria, Firmicute, Spirochaetes and Chloroflexi were the top most abundant phyla comprising >90% of all assigned bacteria in the sediment microbial communities.

Cyanobacteria which were present in high abundance in all the sediment types on day 0, reduced in abundance in all the three sediment types on day 8. It continued to reduce in abundance in industrial sediments but remained constant in residential and mixed sediment types on day 30. Proteobacteria, on the other hand, changed marginally for residential and mixed sediment type microbial community. Industrial sediment type microbial community showed sharp increase in the abundance of Proteobacteria on day 30. Interestingly, all the rare phyla including Bacteroidetes, Acidobacteria, Firmicutes, Spirochaetes and Chloroflexi showed sharp relative increase in abundance on day 8 compared to day 0 but except Chloroflexi, all of them showed a decline on day 30 in both residential and industrial sediment types. Except Firmicutes, all the rare phyla showed upward trajectory from day 0 till day 30 with sharp increase on day 8. Whereas, Chloroflexi continued the increasing trend in all the three sediment types, Acidobacteria showed relative increase only in mixed sediment types.

Sequences which could not be assigned to any taxonomic groups group (Unknown) showed an overall decreasing trend over time. Similar to Cyanobacteria their proportion to rest of the microbial community decreased for industrial sediment type. However, mixed sediment type showed a moderate increase of unclassified taxonomic groups on day 8 and a sharp increase on day 30. In residential sediment type microbial community, unknown fraction showed opposite trend in mixed sediment community. Their abundance showed slight relative decline on day 8 with respect to day 0 and sharp decline on day 30 (Fig 15).

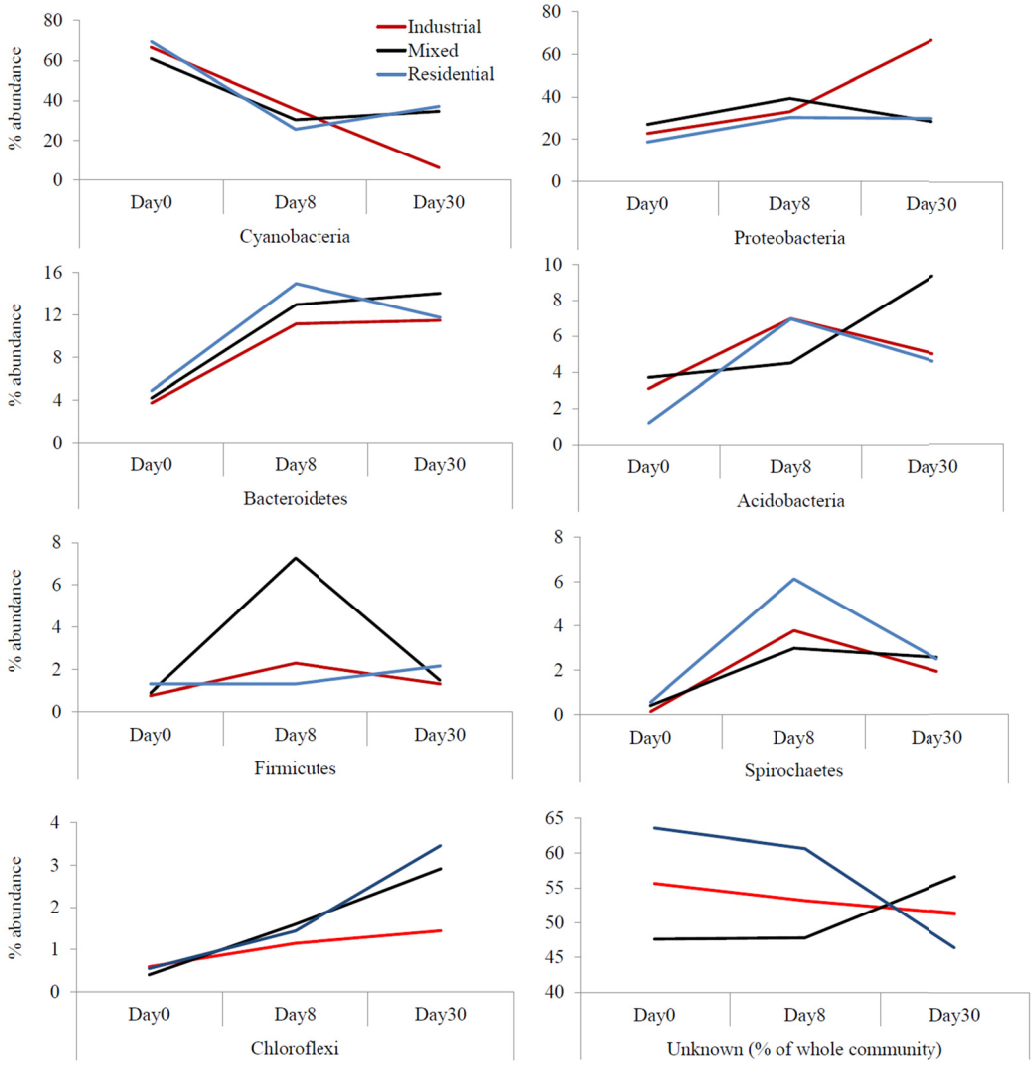

Figure 6.15. Trends of top 7 phyla abundance as a percentage of all assigned microbial taxa groups in the three sediment-types during succession. For unassigned (unknown) taxa groups, % abundance was calculated with respect to abundance of whole community.

Differences due to land-use types in microbial communities on day 0

The composition of active microbial community on day 0 showed high abundance of Cyanobacteria phyla, with abundance of >60% of total assigned taxa groups. Proteobacteria formed the second most abundant group with >18% of all the known taxa group abundance. Followed by the less abundant taxa groups, such as Bacteroidetes, Acidobacteria, Firmicutes, Spirochaetes and Chloroflexi which constituted <10% of total abundance (Fig. 6.16A). Together, these less abundant phyla constituted 8.3%, 9.6% and 8.5% of the total known taxa abundance in industrial, mixed and residential sediment types, respectively.

Microbial community composition showed remarkable differences between the three sediment-types. Whereas, Cyanobacteria were high in abundance in both residential and industrial than mixed sediments, Proteobacteria and Acidobacteria were high in mixed than either residential or industrial sediments. Both the phyla were higher in industrial sediments when compared to residential ones. Bacteroidetes, Firmicutes and Spirochaetes showed similar trends, low abundance in industrial sediments, medium in mixed and high abundance in residential sediments. Chloroflexi, from less abundant phyla, however, showed similar pattern to Cyanobacteria. Its abundance was less in mixed sediment type and higher in both residential and industrial sediment-type. Acidobacteria and Spirochaetes abundances showed high differences between different sediment types. Whereas, Acidobacteria was detected in very low abundance compared to industrial and mixed sediment type, Spirochaetes abundance was very low in industrial sediment type compared to residential and mixed sediments (Fig. 6.16B and C). Classes within more abundant phylum, such as Cyanobacteria and Proteobacteria, showed considerable compositional differences between different sediment-types but less abundant phyla did not show huge the same differences (Fig. 6.16B).

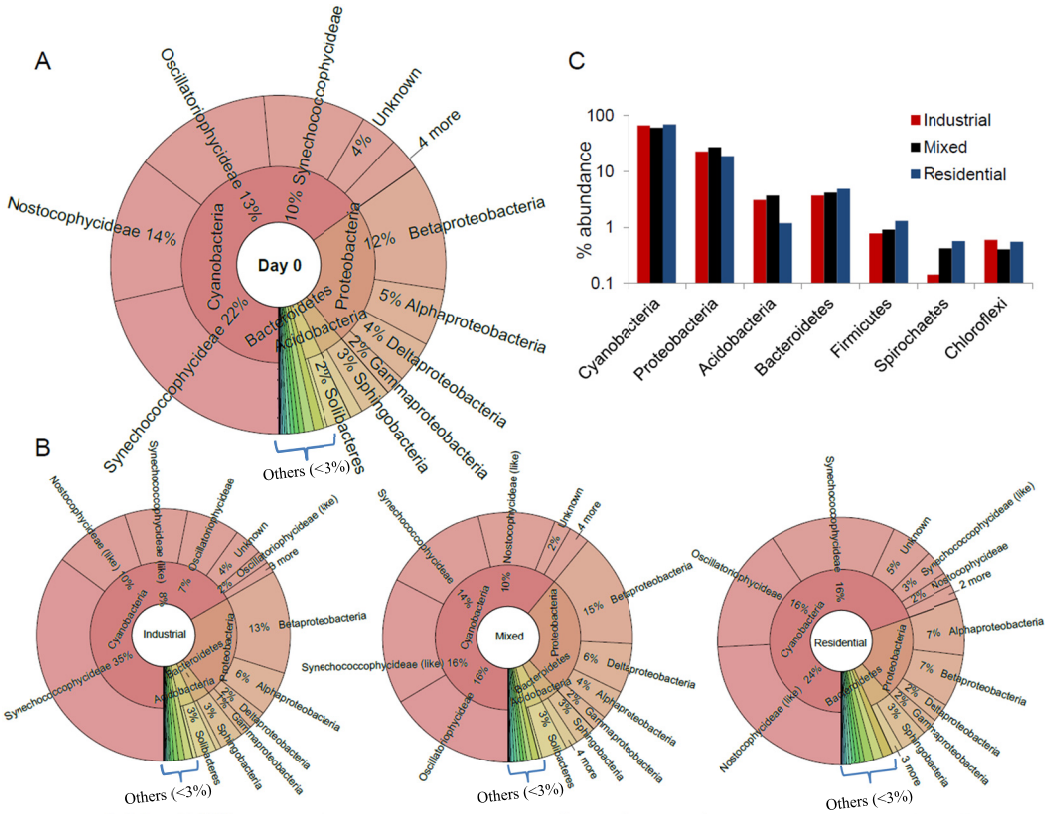

Figure 6.16. Difference in the structure of active microbial community between sediment-types on day 0. Percent abundance of each taxa-group based on number of hits was plotted. (A) Overall structure (average abundance of taxa-group from the three sediment-types) of active microbial community on day 0. (B) Comparison of active microbial community structure of three sediment-types. (C) Differences in the % abundance of top four taxa-groups in the three sediment-types.

Differences due to land-use types in microbial communities on day 8

Day 8 overall active microbial community composition was considerably different from day 0. Cyanobacteria and Proteobacteria which remained the top two most abundant phyla, were present in equal abundance. Together, they constituted >55% of all assigned taxa groups. Other less abundant taxa groups, such as Bacteroidetes, Acidobacteria, Firmicutes, Spirochaetes and Chloroflexi together constituted >29% of total abundance with ≈26% in industrial sediment type, 24.3% in mixed sediment type and 36.7% in residential sediment type. Overall microbial community seemed to be uniformly

distributed among Cyanobacteria, Proteobacteria and less abundant phyla taken together (Fig. 6.17A).

Between the three sediment types, microbial community composition showed detectable differences with relatively higher differences in less abundant phyla compared to more dominant ones. Cyanobacteria were high in abundance in industrial and least in residential with intermediate abundance in mixed sediments, Proteobacteria were high in mixed than either residential or industrial sediments. Bacteroidetes were the third top phyla with 13% of total abundance. Their abundance between three sediment type showed trend opposite to Cyanobacteria with industrial having the least abundance and residential sediments having the most. Firmicutes and Spirochaetes showed similar trends with low abundance in mixed sediments, medium in industrial and high abundance in residential sediments. Acidobacteria, Firmicutes, Spirochaetes and Chloroflexi belonging to less abundant phyla, showed considerable relative differences between three sediment types. Whereas, Acidobacteria was found to be low in abundance in mixed sediments than residential and industrial sediment type, Chloroflexi showed opposite trend (Fig. 6.17B and C). Cyanobacteria and Proteobacteria classes showed considerable compositional differences between different sediment-types but not in other less abundant phyla (Fig. 6.17B).

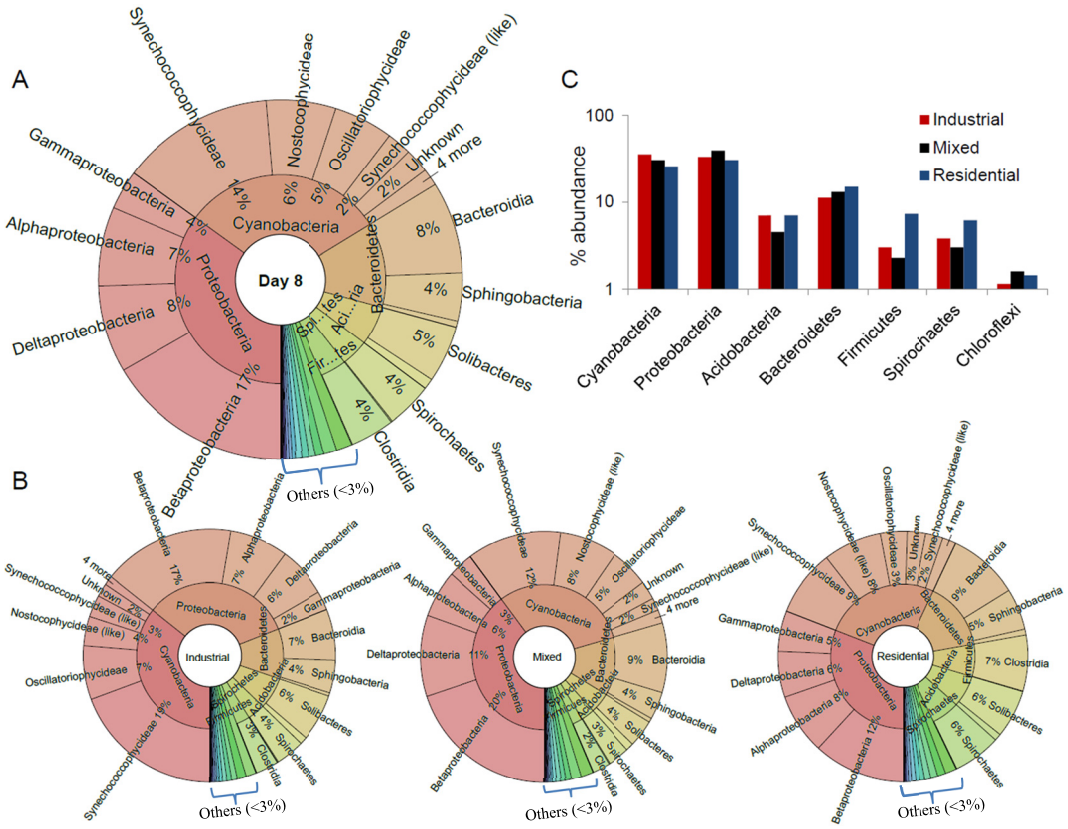

Figure 6.17. Difference in the structure of active microbial community between sediment-types on day 8. Percent abundance of each taxa-group based on number of hits was plotted. (A) Overall structure (average abundance of taxa-group from the three sediment-types) of active microbial community on day 8. (B) Comparison of active microbial community structure of three sediment-types. (C) Differences in the % abundance of top four taxa-groups in the three sediment-types.

Differences due to land-use types in microbial communities on day 30

Average of active microbial community composition of day 30 does not represent the microbial community composition from industrial sediment type. Even so, Cyanobacteria and Proteobacteria, remained the top two most abundant phyla with >63% of all assigned taxa groups. Other less abundant taxa groups, such as Bacteroidetes, Acidobacteria, Firmicutes, Spirochaetes and Chloroflexi together constituted >25% of total abundance with ≈21.2% in industrial sediment type, 30.3% in mixed sediment type and 24.5% in residential sediment type. Except industrial sediment-associated microbial community

which was heavily overtaken by Proteobacteria, overall it seemed to be uniformly distributed among Cyanobacteria, Proteobacteria and less abundant phyla taken together (Fig. 6.18A).

Between the three sediment types, microbial community composition showed large differences between industrial sediment-associated microbial communities and residential or mixed sediment-associated microbial communities. It was interesting to note that day 30 microbial community composition of mixed sediment type was closer to residential sediment-associated microbial community than that of industrial. Cyanobacteria were detected in lowest abundance in industrial sediment type but were detected in high abundance in residential and mixed sediment type with equal proportions in both the sediments from two land-uses. Proteobacteria were detected in very high abundance in industrial sediment but lower abundance in residential and mixed sediment type with equal proportions in both the sediments from two land-uses. Bacteroidetes, Acidobacteria and Spirochaetes were high in abundance in mixed sediment types compared to the other two. Firmicutes and Chloroflexi were detected in high abundance in residential sediment type, flowed by mixed and industrial sediment types (Fig. 6.18 B and C).

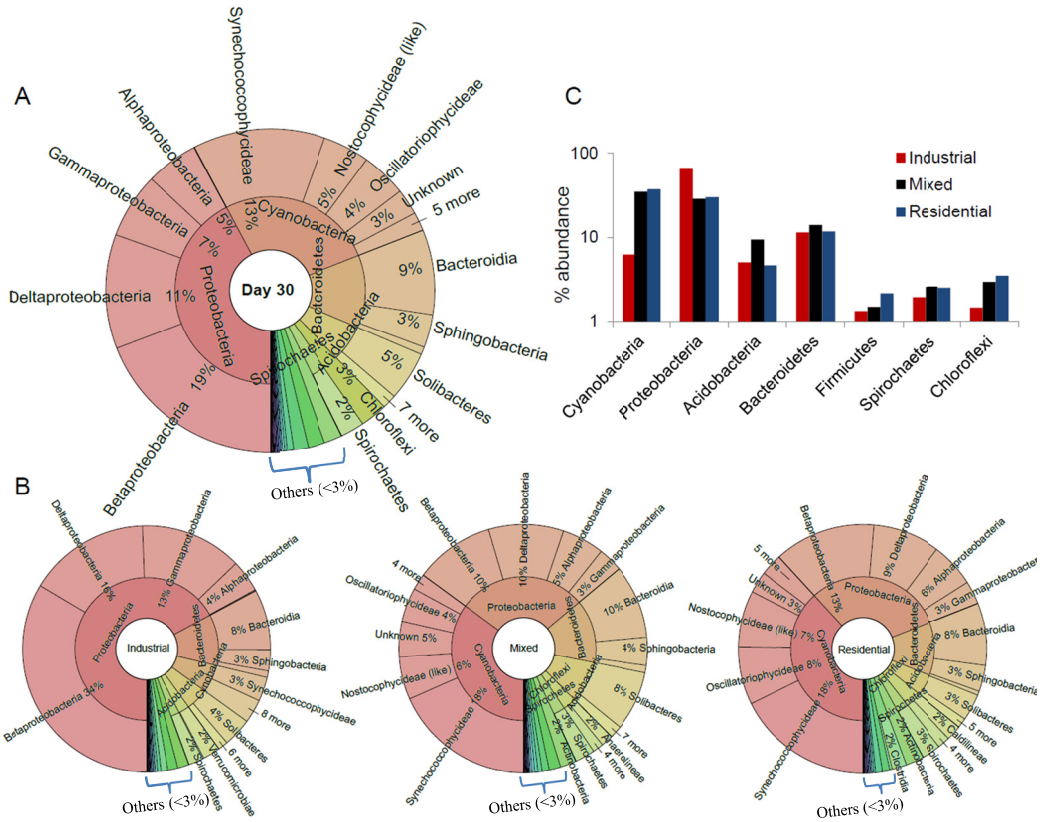

Figure 6.18. Difference in the structure of active microbial community between sediment-types on day 30. Percent abundance of each taxa-group based on number of hits was plotted. (A) Overall structure (average abundance of taxa-group from the three sediment-types) of active microbial community on day 30. (B) Comparison of active microbial community structure of three sediment-types. (C) Differences in the % abundance of top four taxa-groups in the three sediment-types.

Associations of microbial communities with environmental parameters

Microbial community profiles from four time-points showed clear separation between themselves. Associations of nutrient ions were equally spread between three phases, initial (day 0), intermediate (day 8) and late phase (day 16 and 30). Whereas, nitrates vector pointed between day 0 and day 30 microbial communities with an inclination towards day 0, ammonium was found to be highly associated with microbial communities on day 8. Sulfates on the other hand showed high association with microbial communities from late phase microbial comminutes which were from day 16 and day 30. Oxygen levels in sediment samples were also associated with microbial communities from day 16 and day 30. ORP showed opposite trend with associating equally with microbial communities from day 0 and day 8.

Metals also showed wider spread in their associations with microbial community profiles. Aluminum was found to be closely associated with taxa groups from initial (day 0) and late phase (day 30) microbial communities, with high inclination towards day 30. Iron, copper and zinc showed associations with microbial communities from day 0. Mercury was equally associated with day 0 and day 8 microbial community profiles. Arsenic was associated with day 8 and day 16 (more towards day 8) and cobalt with day 8 (Fig. 6.19). In order to identify the associations of functions with metals, Pearson's correlation coefficient of mRNA abundance with metals in 36 sediment samples which included 3 samples each from residential and industrial sediment types on 6 time-points (transcriptomics data), was calculated (Table A6.4). Results show significant correlations.

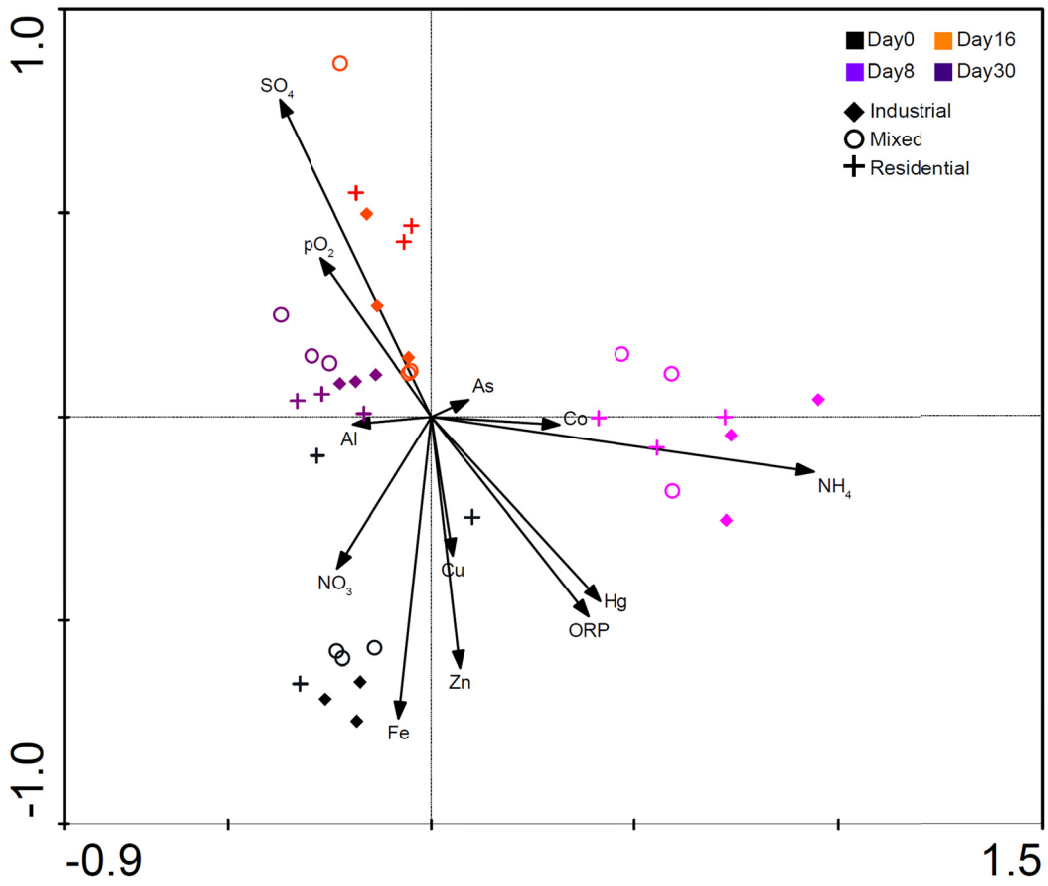

Figure 6.19. Canonical correspondence analysis of sediment microbial community structure and environmental variables. Variables, such as, 3 nutrient-ions, 6 metals, oxygen and ORP levels were chosen from sediment samples. Data-points represent the 16s rDNA TRF profile (peak height data) of a sample. Arrows represent Eigen-vectors of environmental parameters.

Succession in functions of sediment microbial communities

Active transcripts of functional genes of residential and industrial sediment types from 6 time-points, day 0, 1, 4, 8, 12 and 30 also showed three major phases which were early, intermediate and later phase in the end of the experiment. Genes associated with nitrogen and sulfur cycling also showed trends following the above three phases.

Hierarchical clustering of relative abundance of active functional genes (mRNA transcripts) showed three broad clusters of sediment samples. The first cluster (Fig. 6.20, yellow box) was dominated with sediment samples from day 0 and day 1. Within this

cluster, separation between residential and industrial sediment type was also seen. Industrial samples from day 0 and residential samples on day 1 formed tight clusters and grouped separately. Day 0 residential and day 1 industrial samples showed higher variation than day 0 industrial and day 1 residential samples. The second cluster (Fig. 6.20, green box), referred to as intermediate showed predominance of samples from day 4, day 8 and day 12 and was therefore, quite heterogeneous in terms of mid phase time points. Though, residential and industrial sediment types showed separate groupings, the differences between time-points were minimal. Residential samples showed higher variations than industrial samples during intermediate phase. Last phase cluster cluster (Fig. 6.20, violet box) which predominantly included day 30 samples showed grouping based on sediment-type.

Clustering of functional genes also showed two major clusters. The top small cluster (Fig. 6.20, black box) which showed patterns of high abundance during initial phase, low abundance during intermediate phase and high abundance in the end phase comprised 2,058 functional genes. The genes in this cluster mostly belonged to biosynthesis of secondary metabolites (146 genes), microbial metabolism in diverse environments (125 genes), two-component system (82 genes), ABC transporters (70 genes), oxidative phosphorylation (64 genes) and carbon metabolism (47 genes) among other. Nitrogen cycling genes detected in this cluster included nasB (assimilatory nitrate reductase electron transfer subunit), nirA (ferredoxin-nitrite reductase), narB (ferredoxin-nitrate reductase), nirK (nitrite reductase (NO-forming)), narH (nitrate reductase beta subunit), narJ (nitrate reductase delta subunit), narI (nitrate reductase gamma subunit), nitronate monooxygenase, pmoB-amoB (methane/ammonia monooxygenase subunit B). The sulfur cycling genes included cysH (phosphoadenosine phosphosulfate reductase) sir (sulfite reductase (ferredoxin)) cysW (sulfate transport system permease protein) glpE

(thiosulfate sulfurtransferase), sulfite dehydrogenase and metZ (O-succinylhomoserine sulfhydrylase).

Second cluster contained 7,192 genes (Fig. 6.20, light-blue box) which included microbial metabolism in diverse environments (452 genes), biosynthesis of secondary metabolites (397 genes), ABC transporters (212 genes), two-component system (197genes), carbon metabolism (187 genes) and oxidative phosphorylation (127 genes) and among other. Nitrogen cycling genes detected in this cluster included nirB (nitrite reductase (NAD(P)H) large subunit) nirD (nitrite reductase (NAD(P)H) small subunit) nasA (assimilatory nitrate reductase catalytic subunit), nosZ (nitrous-oxide reductase). The sulfur cycling genes included cysJ (sulfite reductase (NADPH) flavoprotein alpha-component), cysI (sulfite reductase (NADPH) hemoprotein beta-component) asrC (anaerobic sulfite reductase subunit C) SUOX (sulfite oxidase) aprA (adenylylsulfate reductase, subunit A), aprB (adenylylsulfate reductase, subunit B), cysA (sulfate transport system ATP-binding protein), cysU (sulfate transport system permease protein), cysP (sulfate transport system substrate-binding protein), APR (adenylyl-sulfate reductase (glutathione)), dmsA (anaerobic dimethyl sulfoxide reductase subunit A), dmsB (anaerobic dimethyl sulfoxide reductase subunit B (DMSO reductase iron- sulfur subunit)), dmsC (anaerobic dimethyl sulfoxide reductase subunit C (DMSO reductase anchor subunit)), phsA (thiosulfate reductase / polysulfide reductase chain A), phsB (thiosulfate reductase electron transport protein), phsC (thiosulfate reductase cytochrome b subunit), dsrA (sulfite reductase alpha) and dsrB (sulfite reductase beta subunit).

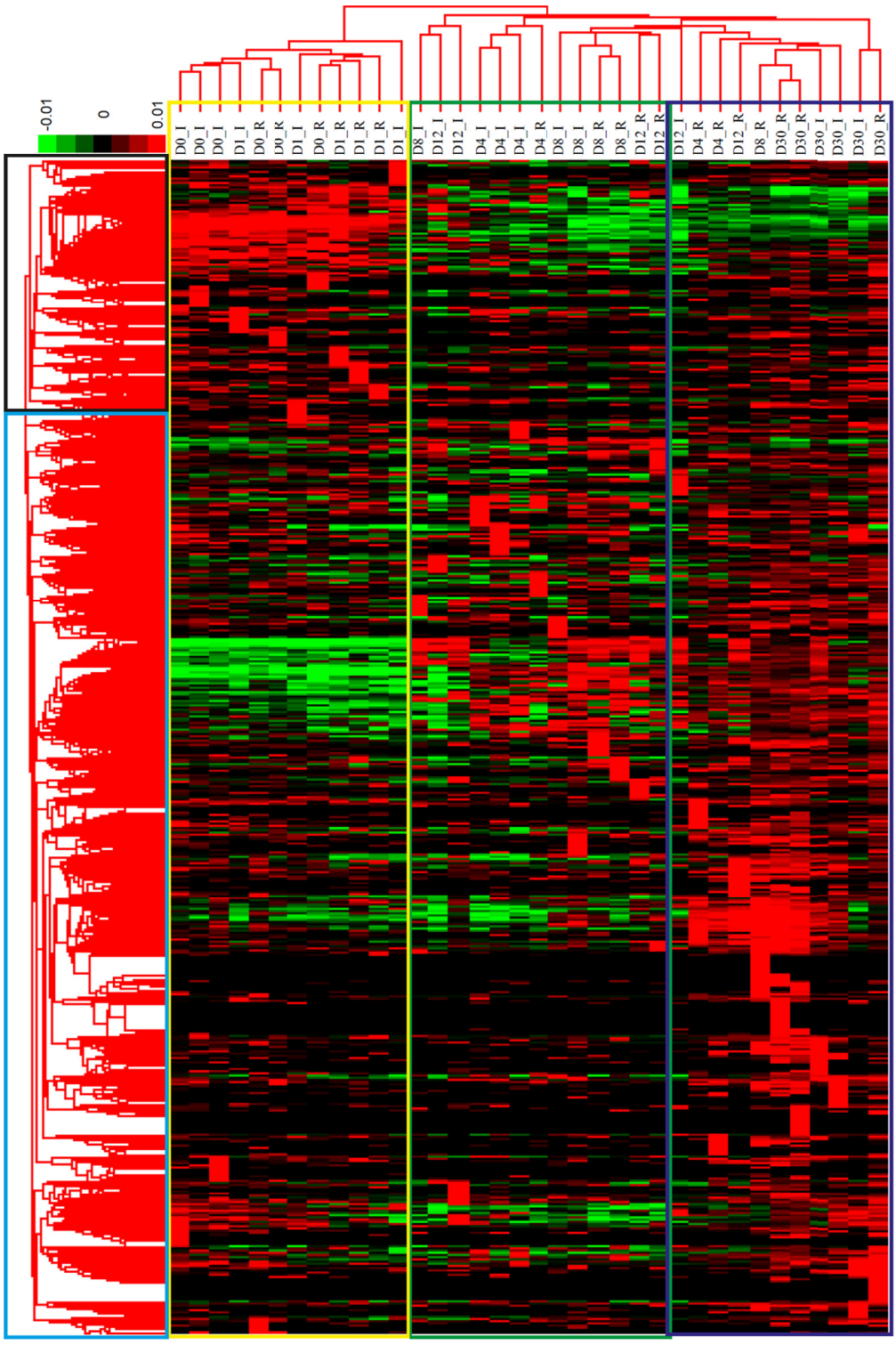

Figure 6.20. Hierarchical clustering of mRNA transcripts abundance, estimated from number of hits for each annotated functional gene using KEGG database. Heat-map of relative abundances was plotted as cluster of samples. Clustering was performed on Bray-Curtis distance matrix of samples using average-linkage method.

Nitrogen-sulfur redox reactions as energy pathways

Nitrogen cycling genes: Four different profiles of genes associated with nitrogen cycling were observed. Respiratory nitrate, nitrite reductase, ammonium transport and ammonium resistance showed decreasing trend between initial and intermediate phase of successions but their abundance increased at day 30 during the end phase (Fig. 6.21A). Peripalsmic and assimilatory nitrate reductases showed a gradual increase during different succession phases. Genes involved in nitrate and nitrite sensing also showed gradual increase (Fig. 6.21B). While, ferredoxin nitrate and nitrite reductases showed sharp reduction in their abundance during the experiment, transport systems and binding genes required for nitrates and nitrites increased their expressions sharply as experiment progressed.

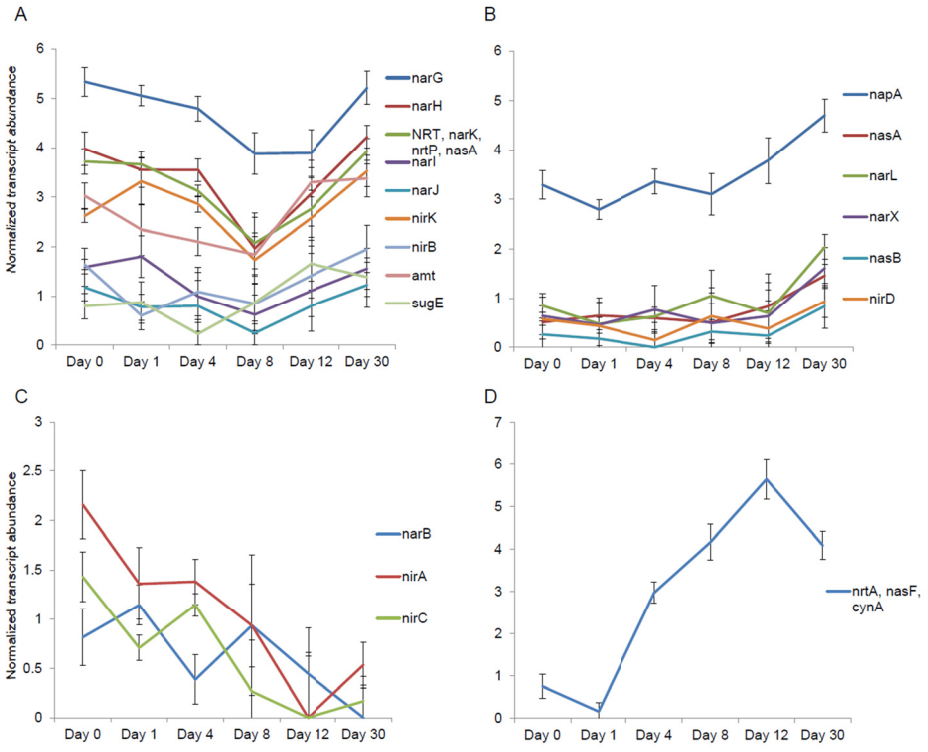

narG	Nitrate reductase alpha subunit
narH	Nitrate reductase beta subunit
NRT, narK, nrtP, nasA	Nitrate/nitrite transporter
narI	Nitrate reductase gamma subunit
narJ	Nitrate reductase delta subunit
nirK	Nitrite reductase
nirB	Nitrite reductase
amt	Ammonium transporter
sugE	Quaternary ammonium compound-resistance

napA	Periplasmic nitrate reductase
nasA	Assimilatory nitrate reductase
narL	Nitrate/nitrite response regulator
narX	Nitrate/nitrite sensor histidine kinase
nasB	Assimilatory nitrate reductase electron transfer
nirD	Nitrite reductase

narB	Ferredoxin-nitrate reductase
nirA	Ferredoxin-nitrite reductase
nirC	Nitrite transporter

nrtA, nasF, cynA	Nitrate/nitrite transport system

Figure 6.21. Trends of genes associated with nitrogen cycling. (A) First panel show trend of genes expression coming down and then increase, second (B) shows increasing trend, third (C) shown genes expression coming down and last (D) shows genes increasing their expression much higher than others.

Sulfur cycling genes: Two broad profiles of sulfur cycling genes were detected which were increasing trend (Fig. 6.22A) and decreasing and increasing trend (Fig. 6.22B). Most of the sufite reductases and thiosulphate reductases showed an upward trend but expression of sulfite oxidase started with low relative abundance, came down further on day 8 but increased sharply on day 12 and day 30.

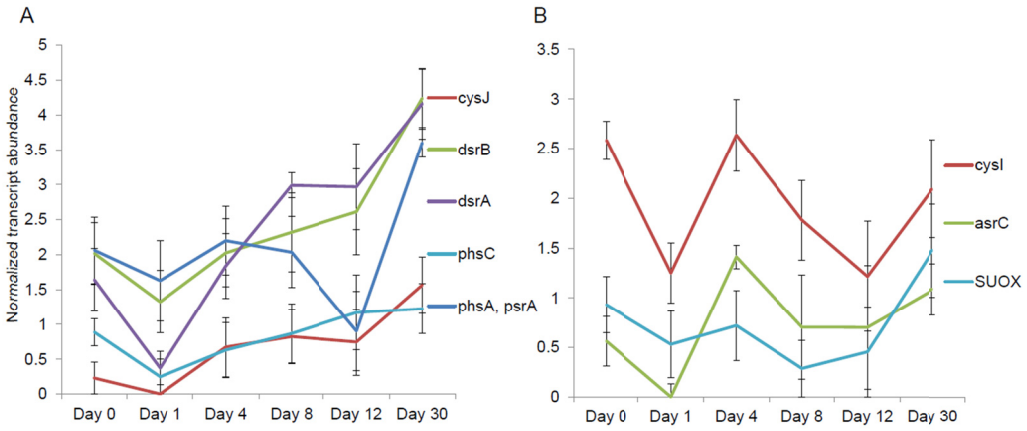

cysJ	Sulfite reductase
dsrB	Sulfite reductase beta subunit
dsrA	Sulfite reductase alpha subunit
phsC	Thiosulfate reductase
phsA, psrA	Thiosulfate reductase

cysI	Sulfite reductase
asrC	Anaerobic sulfite reductase
SUOX	Sulfite oxidase

Figure 6.22. Trends of genes associated with sulfur cycling. First panel (A) show increasing trend of genes expression and second (B) shows genes with relatively constant expression.

Discussion

The present study was conducted to understand the response of sediment-associated microbial communities in urban water ways system. Two broad questions were asked. Firstly, what is the fate of microbial communities upon entering storm water canal network? and secondly, do microbial communities of different land-use origin behave differentially or similarly, over time? Short recovery time to regain (near) pre-disturbed state after pulse physical disturbance is essential for the stability of sediment microbial ecosystem (Shade et al., 2012). In the current study profiles sediment-associated microbial communities appeared to stabilize during the first 4 days after initial disturbance on day 1 and 2. This period is referred to as initial adaptive phase. Large differences in profiles microbial communities on day 1 from day 0, characterized by low number of T-RFLP peaks compared to other days can be explained as the initial response

to pulse disturbance due to rain and habitat relocation of test-sediments from canals to mesocosm reactors. The T-RFLP profile of day 1 might represent resilient taxonomic groups dominating the microbial community on day 1. The return of microbial communities close to the initial state on day 4 implies the short duration required by urban canals sediment-associated microbial community in response to physical perturbations such as storm-event, when compared to other perturbations such as chemical or heat pressure (Peng et al., 2013; Xiang et al., 2014). Such short durations are especially important in tropical areas where frequency of storm events are predicted to be influenced by climate change in coming future (Emanuel, 2005; Goswami et al., 2006; Immerzeel et al., 2010).

After, the initial adaptive response, microbial communities entered the anaerobic phase characterized by reduction in sediment oxygen levels, ORP, turning of sediment color from brown to black and significant reduction in primary producers. The reduction in biomass levels at this stage could also be attributed to the reduction in primary producers. Interestingly, white mat like structures were spotted on the top of day 8 sediment surface. The appearance of these colonies in black zone rich in metal sulfides and emergence of brown patches rich in oxy-hydroxides below their surface indicates the process of sulfide reduction to sulfates. This coincided with the appearance of sulfates, both, in sediments (Fig. 6.6D) and water (Fig. 6.10D) on day 8. Although, the identification of species in the white mats could not be done, their morphology and ability to oxidize sulfides indicates the possibility of *Beggiatoa* or *Acidobacteria*.

Profiles of microbial communities on day 8, which predominantly represents the anaerobic phase, marked the beginning of succession in sediment microbial communities between the two broad groups. Microbial communities move towards and away from the microbial community profiles on day 8 on days 16/30 and 12/20/25, respectively. Such a

pattern in sediment-associated microbial communities indicates the continuous successional cycles, interrupted by occasional rain perturbations.

Interestingly, although, the microbial communities from the three sediment types were different at all time-points, their relative shifts in the sediment microbial communities profiles for the three sediment types remained same (Fig. 6.14 and Table A6.4). This indicates the conserved trends of microbial communities' successions in an urban catchment, irrespective of the pressures from land-use types.

The composition of microbial community revealed that primary producers, such as, Cynobacteria, appears as a dominant phylum in the canals sediments after rain perturbations. Its abundance, however, reduces significantly as the microbial community settles after rain with secondary producers, such as Proteobacteria Bacteroidetes, and Acidobacteria replacing it. Emergence of taxa groups that were less dominant on day 0 at the cost of more dominant ones during intermediate and later stages, emphasize the resilience of microbial community in urban waterways sediment system. Phyla such as Acidobacteria and Chloroflexi are considered rare and widely reported in soil and sediments (Quaiser et al., 2003; Ward et al., 2009; Zanaroli et al., 2012b). The members of these phyla are known to be involved in diverse pathways, such as, utilization of wide range of complex sugars, reduction of nitrates and nitrites without denitrification, dehalogenation and degradation of halogenated organic compounds which makes them best suited to low nutrient conditions such as urban waterways (Ward et al., 2009). Emergence of the above taxa in sediments shows the functional diversity microbial community that can utilize diverse organic compounds and recruit alternate redox reactions as carbon source and energy harvesting strategies, respectively.

Dissimilatory nitrate reduction to ammonium (DNRA) is reportedly preferred under strong reducing environments over denitrification because of the availability of

more electrons in DNRA (+5 → -3) than denitrification (+5 →0) (Strohm et al., 2007). Decrease in nitrates levels in sediments on day 8 with an increase in ammonium levels in sediment and water on the same day indicated the possibility of DNRA as a process to harvest energy in an anaerobic environment. An accumulation of sulfates after day 8 implied that the process could be sulfide-induced where sulfides are utilized as electron donors. This has been reported in many studies done in fresh water sediments where anaerobic conditions are developed (An and Gardner, 2002; Brunet and Garcia-Gil, 1996; Laverman et al., 2007; Yang et al., 2012). However, the sharp changes in the levels of nitrates, ammonium, oxygen levels and ORP were detected during intermediate phase (day 8). Therefore, the possibility of DNRA process to be functional is more during the intermediate phase than initial or late phase. The continuous accumulation of sulfates after the intermediate phase, however, indicates continuous oxidation of sulfur species. Therefore, nitrates appeared to be driving the energy capturing strategies of microbial communities till the intermediate phase of limiting oxygen levels were over.

Apart from redox reactions, microbial communities were also seemed to be affected by metals. Similar inferences could be made from the correlations of relative gene transcript abundance and metals levels in sediments over time (Table A6.5). The spread of their associations across all stages of successions points out the selective influence of metals on microbial communities from different phases. Aluminum and copper which associated with initial (Al and Cu) and late phase (Al) microbial communities, could be influencing the more aerobic microbial functioning. Cobalt could be participating as cofactor in anaerobic processes during intermediate phase.

Successions of microbial communities were not limited to the taxa assemblage only; rather they were extended to functions of microbial communities. However, functional successions were slower than taxa. Even though, microbial community

structure of day 0 and day 1 were very different, their functions grouped together. Similarly, global pattern of day 4 active genes grouped with day 8 and 12, indicating that even though, microbial community at the end of initial adaptive phase was functionally active to enter intermediate phase (Fig. 6.20). Similar results were reported for algal associated microbial communities where assemblage of microbial communities was found to be based more on functional genes than taxa groups (Burke et al., 2011).

The microbial community functions appeared to cover diverse functions as time progressed. A closer look at the nitrogen and sulfur cycling gene expression revealed that most respiratory nitrate reductase genes were active during the initial phase but their expression declined during intermediate phase. This trend is opposite to the nitrate levels detected in sediment and water phase. The explanation to such a phenomenon could be the time lag between gene expression, translation and appearance of reaction byproducts in the environment. Nitrate transporters, however, follow the trend of nitrate availability. Nitrate sensors and periplasmic/assimilatory nitrate reductases however showed trend in accordance with the nitrate levels in sediments and water which strengthens the possibility of DNRA during the intermediate phase.

Sulfite oxidation gene cluster *SUOX* which showed decreasing and increasing trend was in accordance with sulfate levels in sediment and water. However, other sulfite reductase detected which showed increasing trend during experiment did not relate to the increasing sulfate levels. Because sulfides were not tested, the increasing trend of sulfite reductase could not be explained. There seems to be a possibility of reverse functioning of sulfite reductase as previous reported (Loy et al., 2009). Therefore, with the observed trends of sulfates, there is a possibility of reverse dissimilatory sulfite reductase activity in the urban waterways sediment system.

Lastly, even though microbial communities recover the change brought by pulse physical perturbation such as rain in a relatively shorter period, the influence of factors due to land-use differences remains visible in both microbial community and functioning at each succession level.

Conclusions

The present study concludes that pulse disturbances such as rain perturbations could initiate successional response in sediment-associated waterways microbial communities but the shorter recovery time ensures the stability of microbial community in these systems. Such successional changes are, however, more pronounced in taxa assemblage than functions of the community. Although, the successional changes show conserved patterns among microbial communities from different land-use types, inputs from different land-use types seem to have permanent shifts between microbial community structure and functions form these land-use types. Lastly, DNRA pathway seems to be potentially recruited by microbial communities for energy requirements during intermediate phase of successions.

Chapter 7: Overall conclusions and future perspectives

Major conclusions from this study point that well-managed stormwater systems could keep the contaminant levels below the allowable limits, especially in highly urbanized environments. However, the environmental pressures from land-use, even at levels lower than the allowable limits, could still influence the structure and functions of resident microbial communities. This study shows that in a highly urbanized waterways system influence of organic contaminants can be minimal while soft metals can be the major drivers of microbial communities that provide ecosystem services to keep such canal networks clean in low energy regime.

This study further concludes that physical disturbances such as rain can influence the structure and functional potential of sediment microbial communities in urban waterways by initiating successional response, both in structure and functions of microbial communities. However, gradual shifts in microbial functions compared to the community structure points towards more stable functional potential and that the sediment-associated microbiome could be functioning as a unit by recruiting diverse pathways to sustain in nutrient limited urban waterways.

By understanding the spatial distribution and functioning of microbial communities of urban stormwater systems, it is possible to identify few key environmental variables that can be incorporated in the current management practices. If such well-managed systems can be scalable, different land-use types in a city plan can potentially support somewhat uniformly structured microbial communities, thus allowing development of common management practices on large scales.

The current study used a sub-network of a small catchment in Singapore. Further studies are needed at larger scale so that ecological principles learned can be used at wider scale. In addition, new studies can now focus on the underlying mechanisms of microbial community interaction with the soft metals. For example, having no reported biological role, mechanism of aluminum in shaping the microbiome functions is still not explained. Therefore, new studies can elucidate the interactions of aluminum in environmental microbial communities.

In addition, impact of coupled redox reactions involving nitrogen and sulfur species in energy harvesting strategies on dynamics of microbial communities and resulting elemental flux need to be understood in urban waterways context. Progression of research in this direction will help us further our understanding about ecological principles driving the microbial ecology which can later be used to device strategies to enhance ecological services, provides by the microbial communities in freshwater systems.

Bibliography

Amalfitano, S., Fazi, S., 2008. Recovery and quantification of bacterial cells associated with streambed sediments. J. Microbiol. Methods 75, 237–243. doi:10.1016/j.mimet.2008.06.004

An, S., Gardner, W.S., 2002. Dissimilatory nitrate reduction to ammonium (DNRA) as a nitrogen link, versus denitrification as a sink in a shallow estuary (Laguna Madre/Baffin Bay, Texas). Mar. Ecol. Prog. Ser. 237, 41–50. doi:10.3354/meps237041

Anderson, M.J., Walsh, D.C., 2013. PERMANOVA, ANOSIM, and the Mantel test in the face of heterogeneous dispersions: What null hypothesis are you testing? Ecol. Monogr. 83, 557–574.

Anoop, V.M., 2003. Modulation of Citrate Metabolism Alters Aluminum Tolerance in Yeast and Transgenic Canola Overexpressing a Mitochondrial Citrate Synthase. PLANT Physiol. 132, 2205–2217. doi:10.1104/pp.103.023903

Arnell, N.W., Reynard, N.S., 1996. The effects of climate change due to global warming on river flows in Great Britain. J. Hydrol. 183, 397–424. doi:10.1016/0022-1694(95)02950-8

Arnfield, A.J., 2003. Two decades of urban climate research: a review of turbulence, exchanges of energy and water, and the urban heat island. Int. J. Climatol. 23, 1–26. doi:10.1002/joc.859

Arnold CL, Gibbons CJ. 1996. Impervious surface coverage: the emergence of a key environmental indicator. Am. Planners Assoc. J. 62:243–58, n.d.

Ask, J., Karlsson, J., Persson, L., Ask, P., Byström, P., Jansson, M., 2009. Whole-lake estimates of carbon flux through algae and bacteria in benthic and pelagic habitats of clear-water lakes. Ecology 90, 1923–1932. doi:10.1890/07-1855.1

Badin, A.-L., Faure, P., Bedell, J.-P., Delolme, C., 2008. Distribution of organic pollutants and natural organic matter in urban storm water sediments as a function of grain size. Sci. Total Environ. 403, 178–187. doi:10.1016/j.scitotenv.2008.05.022

Bender, M.A., Knutson, T.R., Tuleya, R.E., Sirutis, J.J., Vecchi, G.A., Garner, S.T., Held, I.M., 2010. Modeled Impact of Anthropogenic Warming on the Frequency of Intense Atlantic Hurricanes. Science 327, 454–458. doi:10.1126/science.1180568

Besemer, K., Singer, G., Quince, C., Bertuzzo, E., Sloan, W., Battin, T.J., 2013. Headwaters are critical reservoirs of microbial diversity for fluvial networks. Proc. R. Soc. B Biol. Sci. 280, 20131760. doi:10.1098/rspb.2013.1760

Brezonik, P.L., Stadelmann, T.H., 2002. Analysis and predictive models of stormwater runoff volumes, loads, and pollutant concentrations from watersheds in the Twin Cities metropolitan area, Minnesota, USA. Water Res. 36, 1743–1757. doi:10.1016/S0043-1354(01)00375-X

Brodie, E.L., DeSantis, T.Z., Joyner, D.C., Baek, S.M., Larsen, J.T., Andersen, G.L., Hazen, T.C., Richardson, P.M., Herman, D.J., Tokunaga, T.K., Wan, J.M., Firestone, M.K., 2006. Application of a High-Density Oligonucleotide Microarray Approach To Study Bacterial Population Dynamics during Uranium Reduction and Reoxidation. Appl. Environ. Microbiol. 72, 6288–6298. doi:10.1128/AEM.00246-06

Brodie, E.L., DeSantis, T.Z., Parker, J.P.M., Zubietta, I.X., Piceno, Y.M., Andersen, G.L., 2007. Urban aerosols harbor diverse and dynamic bacterial populations. Proc. Natl. Acad. Sci. 104, 299–304. doi:10.1073/pnas.0608255104

Brunet, R. c., Garcia-Gil, L. j., 1996. Sulfide-induced dissimilatory nitrate reduction to ammonia in anaerobic freshwater sediments. FEMS Microbiol. Ecol. 21, 131–138. doi:10.1111/j.1574-6941.1996.tb00340.x

Bryant, D., Moulton, V., 2004. Neighbor-Net: An Agglomerative Method for the Construction of Phylogenetic Networks. Mol. Biol. Evol. 21, 255–265. doi:10.1093/molbev/msh018

Burke, C., Steinberg, P., Rusch, D., Kjelleberg, S., Thomas, T., 2011. Bacterial community assembly based on functional genes rather than species. Proc. Natl. Acad. Sci. 108, 14288–14293. doi:10.1073/pnas.1101591108

Buytaert, W., De Bièvre, B., 2012. Water for cities: The impact of climate change and demographic growth in the tropical Andes. Water Resour. Res. 48, n/a–n/a. doi:10.1029/2011WR011755

Cai, H., Archambault, M., Prescott, J.F., 2003. 16S Ribosomal RNA Sequence—Based Identification of Veterinary Clinical Bacteria. J. Vet. Diagn. Invest. 15, 465–469. doi:10.1177/104063870301500511

Cai, X., Rosegrant, M.W., 2002. Global Water Demand and Supply Projections: Part 1. Water Int. 27, 159–169. doi:10.1080/02508060208686989

Cajo J. E ter, B., Piet E M, V., 1995. Canonical correspondence analysis and related multivariate methods in aquatic ecology. Aquat. Sci. 57, 255 – 289.

Canfield, D.E., Stewart, F.J., Thamdrup, B., Brabandere, L.D., Dalsgaard, T., Delong, E.F., Revsbech, N.P., Ulloa, O., 2010. A Cryptic Sulfur Cycle in Oxygen-Minimum–Zone Waters off the Chilean Coast. Science 330, 1375–1378. doi:10.1126/science.1196889

Canstein, H. von, Li, Y., Leonhäuser, J., Haase, E., Felske, A., Deckwer, W.-D., Wagner-Döbler, I., 2002. Spatially Oscillating Activity and Microbial Succession of

Mercury-Reducing Biofilms in a Technical-Scale Bioremediation System. Appl. Environ. Microbiol. 68, 1938–1946. doi:10.1128/AEM.68.4.1938-1946.2002

Chan, Y., Van Nostrand, J.D., Zhou, J., Pointing, S.B., Farrell, R.L., 2013. Functional ecology of an Antarctic Dry Valley. Proc. Natl. Acad. Sci. 110, 8990–8995.

Characklis, G.W., Wiesner, M.R., 1997. Particles, metals, and water quality in runoff from large urban watershed. J. Environ. Eng. 123, 753–759.

Chen, J., 2007. Rapid urbanization in China: A real challenge to soil protection and food security. CATENA 69, 1–15. doi:10.1016/j.catena.2006.04.019

Cotner, J.B., Biddanda, B.A., 2002. Small Players, Large Role: Microbial Influence on Biogeochemical Processes in Pelagic Aquatic Ecosystems. Ecosystems 5, 105–121. doi:10.1007/s10021-001-0059-3

Cregger, M.A., Schadt, C.W., McDowell, N.G., Pockman, W.T., Classen, A.T., 2012. Response of the Soil Microbial Community to Changes in Precipitation in a Semiarid Ecosystem. Appl. Environ. Microbiol. 78, 8587–8594. doi:10.1128/AEM.02050-12

Cruz-Martínez, K., Rosling, A., Zhang, Y., Song, M., Andersen, G.L., Banfield, J.F., 2012. Effect of Rainfall-Induced Soil Geochemistry Dynamics on Grassland Soil Microbial Communities. Appl. Environ. Microbiol. 78, 7587–7595. doi:10.1128/AEM.00203-12

Da Cruz, F.J.R., da Silva Lobato, A.K., da Costa, R.C.L., dos Santos Lopes, M.J., Neves, H.K.B., de Oliveira Neto, C.F., da Silva, M.H.L., dos Santos Filho, B.G., de Lima Junior, J.A., Okumura, R.S., 2011. Aluminum negative impact on nitrate reductase activity, nitrogen compounds and morphological parameters in sorghum plants. Aust. J. Crop Sci. 5, 641.

Debroas, D., Humbert, J.-F., Enault, F., Bronner, G., Faubladier, M., Cornillot, E., 2009. Metagenomic approach studying the taxonomic and functional diversity of the bacterial community in a mesotrophic lake (Lac du Bourget – France). Environ. Microbiol. 11, 2412–2424. doi:10.1111/j.1462-2920.2009.01969.x

DeBruyn, J.M., Nixon, L.T., Fawaz, M.N., Johnson, A.M., Radosevich, M., 2011. Global Biogeography and Quantitative Seasonal Dynamics of Gemmatimonadetes in Soil. Appl. Environ. Microbiol. 77, 6295–6300. doi:10.1128/AEM.05005-11

DeFries, R., Pandey, D., 2010. Urbanization, the energy ladder and forest transitions in India's emerging economy. Land Use Policy 27, 130–138. doi:10.1016/j.landusepol.2009.07.003

Drummond, R.D., Guimarães, C.T., Felix, J., Ninamango-Cárdenas, F.E., Carneiro, N.P., Paiva, E., Menossi, M., 2001. Prospecting sugarcane genes involved in aluminum tolerance. Genet. Mol. Biol. 24, 221–230.

Ducklow, H., 2008. Microbial services: challenges for microbial ecologists in a changing world. Aquat. Microb. Ecol. 53, 13–19. doi:10.3354/ame01220

Duhamel, S., Jacquet, S., 2006. Flow cytometric analysis of bacteria- and virus-like particles in lake sediments. J. Microbiol. Methods 64, 316–332. doi:10.1016/j.mimet.2005.05.008

Easterling, D.R., Meehl, G.A., Parmesan, C., Changnon, S.A., Karl, T.R., Mearns, L.O., 2000. Climate Extremes: Observations, Modeling, and Impacts. Science 289, 2068–2074. doi:10.1126/science.289.5487.2068

El-Sheekh, M.M., Hamouda, R.A., 2013. Biodegradation of crude oil by some cyanobacteria under heterotrophic conditions. Desalination Water Treat. 1–7. doi:10.1080/19443994.2013.794008

Elsner, M.M., Cuo, L., Voisin, N., Deems, J.S., Hamlet, A.F., Vano, J.A., Mickelson, K.E.B., Lee, S.-Y., Lettenmaier, D.P., 2010. Implications of 21st century climate change for the hydrology of Washington State. Clim. Change 102, 225–260. doi:10.1007/s10584-010-9855-0

Emanuel, K., 2005. Increasing destructiveness of tropical cyclones over the past 30 years. Nature 436, 686–688. doi:10.1038/nature03906

Environmental Health Ready Reference, 1983. . Michigan Environmental Health Association.

Fera, N.C., Feona, I., Lee, K.H., Kawi, B., 2013. Water quality status of Liwagu River, Tambunan, Sabah, Malaysia. J. Trop. Biol. Conserv. 10, 67–73.

Francis, R.A., Chadwick, M.A., 2013. The Ecology of Urban Environments. Routledge.

Freudenberg, N., Galea, S., 2008. Cities of Consumption: The Impact of Corporate Practices on the Health of Urban Populations. J. Urban Health Bull. N. Y. Acad. Med. 85, 462–471. doi:10.1007/s11524-008-9278-7

Ganguli, A., Tripathi, A., 2002. Bioremediation of toxic chromium from electroplating effluent by chromate-reducing Pseudomonas aeruginosa A2Chr in two bioreactors. Appl. Microbiol. Biotechnol. 58, 416–420. doi:10.1007/s00253-001-0871-x

Gibb, H., Hochuli, D.F., 2002. Habitat fragmentation in an urban environment: large and small fragments support different arthropod assemblages. Biol. Conserv. 106, 91–100. doi:10.1016/S0006-3207(01)00232-4

Goddard, M.A., Dougill, A.J., Benton, T.G., 2010. Scaling up from gardens: biodiversity conservation in urban environments. Trends Ecol. Evol. 25, 90–98. doi:10.1016/j.tree.2009.07.016

Goswami, B.N., Venugopal, V., Sengupta, D., Madhusoodanan, M.S., Xavier, P.K., 2006. Increasing Trend of Extreme Rain Events Over India in a Warming Environment. Science 314, 1442–1445. doi:10.1126/science.1132027

Greger, J.L., 1993. Aluminum metabolism. Annu. Rev. Nutr. 13, 43–63.

Grimm, N.B., Faeth, S.H., Golubiewski, N.E., Redman, C.L., Wu, J., Bai, X., Briggs, J.M., 2008. Global Change and the Ecology of Cities. Science 319, 756–760. doi:10.1126/science.1150195

Gupta, R.S., 2000. The phylogeny of proteobacteria: relationships to other eubacterial phyla and eukaryotes. FEMS Microbiol. Rev. 24, 367–402.

He, Z., Deng, Y., Van Nostrand, J.D., Tu, Q., Xu, M., Hemme, C.L., Li, X., Wu, L., Gentry, T.J., Yin, Y., Liebich, J., Hazen, T.C., Zhou, J., 2010a. GeoChip 3.0 as a high-throughput tool for analyzing microbial community composition, structure and functional activity. ISME J. 4, 1167–1179. doi:10.1038/ismej.2010.46

He, Z., Deng, Y., Van Nostrand, J.D., Tu, Q., Xu, M., Hemme, C.L., Li, X., Wu, L., Gentry, T.J., Yin, Y., Liebich, J., Hazen, T.C., Zhou, J., 2010b. GeoChip 3.0 as a high-throughput tool for analyzing microbial community composition, structure and functional activity. ISME J. 4, 1167–1179. doi:10.1038/ismej.2010.46

He, Z., Deng, Y., Van Nostrand, J.D., Tu, Q., Xu, M., Hemme, C.L., Li, X., Wu, L., Gentry, T.J., Yin, Y., Liebich, J., Hazen, T.C., Zhou, J., 2010c. GeoChip 3.0 as a high-throughput tool for analyzing microbial community composition, structure and functional activity. ISME J. 4, 1167–1179. doi:10.1038/ismej.2010.46

He, Z., Gentry, T.J., Schadt, C.W., Wu, L., Liebich, J., Chong, S.C., Huang, Z., Wu, W., Gu, B., Jardine, P., Criddle, C., Zhou, J., 2007. GeoChip: a comprehensive microarray for investigating biogeochemical, ecological and environmental processes. ISME J. 1, 67–77. doi:10.1038/ismej.2007.2

He, Z., Wu, L., Li, X., Fields, M.W., Zhou, J., 2005. Empirical Establishment of Oligonucleotide Probe Design Criteria. Appl. Environ. Microbiol. 71, 3753–3760. doi:10.1128/AEM.71.7.3753-3760.2005

Heaney, J.P., Huber, W.C., 1984. Nationwide Assessment of Urban Runoff Impact on Receiving Water Quality1. JAWRA J. Am. Water Resour. Assoc. 20, 35–42. doi:10.1111/j.1752-1688.1984.tb04639.x

Henderson-Sellers, A., Zhang, H., Berz, G., Emanuel, K., Gray, W., Landsea, C., Holland, G., Lighthill, J., Shieh, S.-L., Webster, P., McGuffie, K., 1998. Tropical Cyclones and Global Climate Change: A Post-IPCC Assessment. Bull. Am. Meteorol. Soc. 79, 19–38. doi:10.1175/1520-0477(1998)079<0019:TCAGCC>2.0.CO;2

Huson, D.H., Auch, A.F., Qi, J., Schuster, S.C., 2007. MEGAN analysis of metagenomic data. Genome Res. 17, 377–386. doi:10.1101/gr.5969107

Huson, D.H., Mitra, S., Ruscheweyh, H.-J., Weber, N., Schuster, S.C., 2011. Integrative analysis of environmental sequences using MEGAN4. Genome Res. 21, 1552–1560. doi:10.1101/gr.120618.111

Immerzeel, W.W., Beek, L.P.H. van, Bierkens, M.F.P., 2010. Climate Change Will Affect the Asian Water Towers. Science 328, 1382–1385. doi:10.1126/science.1183188

Irshad, M., Eneji, A.E., Hussain, Z., Ashraf, M., 2013. Chemical characterization of fresh and composted livestock manures. J. Soil Sci. Plant Nutr. 13, 115–121.

Jackson, R.B., Carpenter, S.R., Dahm, C.N., McKnight, D.M., Naiman, R.J., Postel, S.L., Running, S.W., 2001. Water in a changing world. Ecol. Appl. 11, 1027–1045. doi:10.1890/1051-0761(2001)011[1027:WIACW]2.0.CO;2

Jiang, H., Dong, H., Zhang, G., Yu, B., Chapman, L.R., Fields, M.W., 2006. Microbial Diversity in Water and Sediment of Lake Chaka, an Athalassohaline Lake in Northwestern China. Appl. Environ. Microbiol. 72, 3832–3845. doi:10.1128/AEM.02869-05

Jones, A.C., Liao, T.S.V., Najar, F.Z., Roe, B.A., Hambright, K.D., Caron, D.A., 2013. Seasonality and disturbance: annual pattern and response of the bacterial and microbial eukaryotic assemblages in a freshwater ecosystem. Environ. Microbiol. n/a–n/a. doi:10.1111/1462-2920.12151

Jørgensen, S.E., Halling-Sørensen, B., 2000. Drugs in the environment. Chemosphere 40, 691–699. doi:10.1016/S0045-6535(99)00438-5

Khan, A., Rayner, G.D., 2003. Robustness to non-normality of common tests for the many-sample location problem. J. Appl. Math. Decis. Sci. 7, 187–206.

Kim, J.-S., Makama, M., Petito, J., Park, N.-H., Cohan, F.M., Dungan, R.S., 2012. Diversity of Bacteria and Archaea in hypersaline sediment from Death Valley National Park, California: Diversity of Bacteria and Archaea in Hypersaline Sediment. MicrobiologyOpen 1, 135–148. doi:10.1002/mbo3.20

Kirchman, D.L., Dittel, A.I., Findlay, S.E., Fischer, D., 2004. Changes in bacterial activity and community structure in response to dissolved organic matter in the Hudson River, New York. Aquat. Microb. Ecol. 35, 243–257.

Knutson, T.R., McBride, J.L., Chan, J., Emanuel, K., Holland, G., Landsea, C., Held, I., Kossin, J.P., Srivastava, A.K., Sugi, M., 2010. Tropical cyclones and climate change. Nat. Geosci. 3, 157–163. doi:10.1038/ngeo779

Krumins, J.A., Oevelen, D. van, Bezemer, T.M., Deyn, G.B.D., Hol, W.H.G., Donk, E. van, Boer, W. de, Ruiter, P.C. de, Middelburg, J.J., Monroy, F., Soetaert, K., Thébault, E., Koppel, J. van de, Veen, J.A. van, Viketoft, M., Putten, W.H. van der, 2013. Soil and Freshwater and Marine Sediment Food Webs: Their Structure and Function. BioScience 63, 35–42. doi:10.1525/bio.2013.63.1.8

Kruskal, J.B., 1964. Nonmetric multidimensional scaling: a numerical method. Psychometrika 29, 115–129.

Lao, W., Tsukada, D., Greenstein, D.J., Bay, S.M., Maruya, K.A., 2010. Analysis, occurrence, and toxic potential of pyrethroids, and fipronil in sediments from an urban estuary. Environ. Toxicol. Chem. 29, 843–851. doi:10.1002/etc.116

Laverman, A.M., Canavan, R.W., Slomp, C.P., Cappellen, P.V., 2007. Potential nitrate removal in a coastal freshwater sediment (Haringvliet Lake, The Netherlands) and response to salinization. Water Res. 41, 3061–3068. doi:10.1016/j.watres.2007.04.002

Ledin, M., 2000. Accumulation of metals by microorganisms — processes and importance for soil systems. Earth-Sci. Rev. 51, 1–31. doi:10.1016/S0012-8252(00)00008-8

Lee, K.W.K., Periasamy, S., Mukherjee, M., Xie, C., Kjelleberg, S., Rice, S.A., 2013. Biofilm development and enhanced stress resistance of a model, mixed-species community biofilm. ISME J. doi:10.1038/ismej.2013.194

Lehner, B., Verdin, K., Jarvis, A., 2008a. New Global Hydrography Derived From Spaceborne Elevation Data. Eos Trans. Am. Geophys. Union 89, 93. doi:10.1029/2008EO100001

Lehner, B., Verdin, K., Jarvis, A., 2008b. New Global Hydrography Derived From Spaceborne Elevation Data. Eos Trans. Am. Geophys. Union 89, 93. doi:10.1029/2008EO100001

Lehninger, A.L., 1950. Role of Metal Ions in Enzyme Systems. Physiol. Rev. 30, 393–429.

Leopold, L. B. 1968. Hydrology for urban land planning- a guidebook on the hydrologic effects of urban land use. Geological Survey Circular 554., n.d.

Liang, Y., Van Nostrand, J.D., Deng, Y., He, Z., Wu, L., Zhang, X., Li, G., Zhou, J., 2011. Functional gene diversity of soil microbial communities from five oil-contaminated fields in China. ISME J. 5, 403–413. doi:10.1038/ismej.2010.142

Lin, J., Mele, C., 2012. The Urban Sociology Reader. Routledge.

Linder, M.C., Hazegh-Azam, M., 1996. Copper biochemistry and molecular biology. Am. J. Clin. Nutr. 63, 797S–811S.

Loy, A., Duller, S., Baranyi, C., Mußmann, M., Ott, J., Sharon, I., Béjà, O., Le Paslier, D., Dahl, C., Wagner, M., 2009. Reverse dissimilatory sulfite reductase as phylogenetic marker for a subgroup of sulfur-oxidizing prokaryotes. Environ. Microbiol. 11, 289–299. doi:10.1111/j.1462-2920.2008.01760.x

MacPherson, I.S., Murphy, M.E.P., 2007. Type-2 copper-containing enzymes. Cell. Mol. Life Sci. 64, 2887–2899. doi:10.1007/s00018-007-7310-9

Mardis, E.R., 2008. Next-Generation DNA Sequencing Methods. Annu. Rev. Genomics Hum. Genet. 9, 387–402. doi:10.1146/annurev.genom.9.081307.164359

McDonald, R.I., Green, P., Balk, D., Fekete, B.M., Revenga, C., Todd, M., Montgomery, M., 2011. Urban growth, climate change, and freshwater availability. Proc. Natl. Acad. Sci. 108, 6312–6317. doi:10.1073/pnas.1011615108

McGrath, K.C., Thomas-Hall, S.R., Cheng, C.T., Leo, L., Alexa, A., Schmidt, S., Schenk, P.M., 2008. Isolation and analysis of mRNA from environmental microbial communities. J. Microbiol. Methods 75, 172–176. doi:10.1016/j.mimet.2008.05.019

Meers, E., Laing, G.D., Unamuno, V.G., Lesage, E., Tack, F.M.G., Verloo, M.G., 2006. Water Extractability of Trace Metals from Soils: Some Pitfalls. Water. Air. Soil Pollut. 176, 21–35. doi:10.1007/s11270-005-9070-1

Memarian, H., Balasundram, S.K., Talib, J.B., Sood, A.M., Abbaspour, K.C., 2012. Trend analysis of water discharge and sediment load during the past three decades of development in the Langat basin, Malaysia. Hydrol. Sci. J. 57, 1207–1222. doi:10.1080/02626667.2012.695073

Menon, R., Jackson, C.R., Holland, M.M., 2013. The Influence of Vegetation on Microbial Enzyme Activity and Bacterial Community Structure in Freshwater Constructed Wetland Sediments. Wetlands 33, 365–378. doi:10.1007/s13157-013-0394-0

MOEWR (2006) The Singapore Green Plan 2012, 2006 edition, (http://www.pub.gov.sg)., n.d.

Morrissey, E.M., Jenkins, A.S., Brown, B.L., Franklin, R.B., 2013. Resource Availability Effects on Nitrate-Reducing Microbial Communities in a Freshwater Wetland. Wetlands 33, 301–310. doi:10.1007/s13157-013-0384-2

Murtagh, F., 1983. A survey of recent advances in hierarchical clustering algorithms. Comput. J. 26, 354–359.

Mußmann, M., Ribot, M., von Schiller, D., Merbt, S.N., Augspurger, C., Karwautz, C., Winkel, M., Battin, T.J., Martí, E., Daims, H., 2013. Colonization of freshwater biofilms by nitrifying bacteria from activated sludge. FEMS Microbiol. Ecol. 85, 104–115. doi:10.1111/1574-6941.12103

Nasr, N., Carapetian, J., Heidari, R., Rezaei, S.A., Abbaspour, N., Darvishzadeh, R., Ghezelbash, F., 2011. The effect of aluminium on enzyme activities in two wheat cultivars. Afr. J. Biotechnol. 10, 3354–3364.

National University of Singapore, https://inetapps.nus.edu.sg/fas/geog/ajxdirList.aspx [WWW Document], 2013. URL https://inetapps.nus.edu.sg/fas/geog/ajxdirList.aspx (accessed 11.29.13).

Newell, S.Y., Moran, M.A., Wicks, R., Hodson, R.E., 1995. Productivities of microbial decomposers during early stages of decomposition of leaves of a freshwater sedge. Freshw. Biol. 34, 135–148. doi:10.1111/j.1365-2427.1995.tb00430.x

Newson, R., 2002. Parameters behind "nonparametric" statistics: Kendall's tau, Somers' D and median differences. Stata J. 2, 45–64.

Newton, R.J., Jones, S.E., Eiler, A., McMahon, K.D., Bertilsson, S., 2011. A Guide to the Natural History of Freshwater Lake Bacteria. Microbiol. Mol. Biol. Rev. 75, 14–49. doi:10.1128/MMBR.00028-10

Niemczynowicz, J., 1999. Urban hydrology and water management–present and future challenges. Urban Water 1, 1–14.

OKI, T., AGATA, Y., KANAE, S., SARUHASHI, T., YANG, D., MUSIAKE, K., 2001. Global assessment of current water resources using total runoff integrating pathways. Hydrol. Sci. J. 46, 983–995. doi:10.1080/02626660109492890

Oki, T., Kanae, S., 2006. Global Hydrological Cycles and World Water Resources. Science 313, 1068–1072. doi:10.1126/science.1128845

Orcutt, B.N., Sylvan, J.B., Knab, N.J., Edwards, K.J., 2011. Microbial Ecology of the Dark Ocean above, at, and below the Seafloor. Microbiol. Mol. Biol. Rev. 75, 361–422. doi:10.1128/MMBR.00039-10

Osborn, A.M., Moore, E.R., Timmis, K.N., 2000. An evaluation of terminal-restriction fragment length polymorphism (T-RFLP) analysis for the study of microbial community structure and dynamics. Environ. Microbiol. 2, 39–50.

Paul, M.J., Meyer, J.L., 2001. Streams in the urban landscape. Annu. Rev. Ecol. Syst. 333–365.

Peng, J., Li, H., Su, J., Zhang, Q., Rui, J., Cai, C., 2013. Response of bacterial communities to short-term pyrene exposure in red soil. Front. Environ. Sci. Eng. 7, 559–567. doi:10.1007/s11783-013-0501-8

Percival, S.L., Malic, S., Cruz, H., Williams, D.W., 2011. Introduction to Biofilms, in: Percival, S., Knottenbelt, D., Cochrane, C. (Eds.), Biofilms and Veterinary Medicine. Springer Berlin Heidelberg, Berlin, Heidelberg, pp. 41–68.

Peres-Neto, P.R., Legendre, P., Dray, S., Borcard, D., 2006. Variation Partitioning of Species Data Matrices: Estimation and Comparison of Fractions. Ecology 87, 2614–2625. doi:10.1890/0012-9658(2006)87[2614:VPOSDM]2.0.CO;2

Pernthaler, J., 2013. Freshwater Microbial Communities, in: Rosenberg, E., DeLong, E.F., Lory, S., Stackebrandt, E., Thompson, F. (Eds.), The Prokaryotes. Springer Berlin Heidelberg, Berlin, Heidelberg, pp. 97–112.

Peter Revsbech, N., 2005. Analysis of Microbial Communities with Electrochemical Microsensors and Microscale Biosensors, in: Jared R. Leadbetter (Ed.), Methods in Enzymology, Environmental Microbiology. Academic Press, pp. 147–166.

Petersen, D.G., Blazewicz, S.J., Firestone, M., Herman, D.J., Turetsky, M., Waldrop, M., 2012a. Abundance of microbial genes associated with nitrogen cycling as indices of biogeochemical process rates across a vegetation gradient in Alaska. Environ. Microbiol. 14, 993–1008. doi:10.1111/j.1462-2920.2011.02679.x

Petersen, D.G., Blazewicz, S.J., Firestone, M., Herman, D.J., Turetsky, M., Waldrop, M., 2012b. Abundance of microbial genes associated with nitrogen cycling as indices of biogeochemical process rates across a vegetation gradient in Alaska. Environ. Microbiol. 14, 993–1008. doi:10.1111/j.1462-2920.2011.02679.x

Piao, S., Ciais, P., Huang, Y., Shen, Z., Peng, S., Li, J., Zhou, L., Liu, H., Ma, Y., Ding, Y., Friedlingstein, P., Liu, C., Tan, K., Yu, Y., Zhang, T., Fang, J., 2010. The impacts of climate change on water resources and agriculture in China. Nature 467, 43–51. doi:10.1038/nature09364

Piña, R.G., Cervantes, C., 1996. Microbial interactions with aluminium. Biometals 9, 311–316.

Quaiser, A., Ochsenreiter, T., Lanz, C., Schuster, S.C., Treusch, A.H., Eck, J., Schleper, C., 2003. Acidobacteria form a coherent but highly diverse group within the bacterial domain: evidence from environmental genomics. Mol. Microbiol. 50, 563–575. doi:10.1046/j.1365-2958.2003.03707.x

Radwan, S.., Al-Hasan, R.., Salamah, S., Al-Dabbous, S., 2002. Bioremediation of oily sea water by bacteria immobilized in biofilms coating macroalgae. Int. Biodeterior. Biodegrad. 50, 55–59. doi:10.1016/S0964-8305(02)00067-7

Ramírez-Benítez, J.E., Muñoz-Sánchez, J.A., Becerril-Chi, K.M., Miranda-Ham, M. de L., Castro-Concha, L.A., Hernández-Sotomayor, S.M.T., 2011. Aluminum induces changes in oxidative burst scavenging enzymes in Coffea arabica L. suspension cells with differential Al tolerance. J. Inorg. Biochem. 105, 1523–1528. doi:10.1016/j.jinorgbio.2011.09.031

Reese, B.K., Mills, H.J., Dowd, S.E., Morse, J.W., 2013. Linking Molecular Microbial Ecology to Geochemistry in a Coastal Hypoxic Zone. Geomicrobiol. J. 30, 160–172. doi:10.1080/01490451.2012.659331

Richardson, C.J., Flanagan, N.E., Ho, M., Pahl, J.W., 2011. Integrated stream and wetland restoration: A watershed approach to improved water quality on the landscape. Ecol. Eng. 37, 25–39. doi:10.1016/j.ecoleng.2010.09.005

Rosegrant, M.W., Cai, X., 2002. Global Water Demand and Supply Projections: Part 2. Water Int. 27, 170–182. doi:10.1080/02508060208686990

Rosegrant, M.W., Cline, S.A., 2003. Global Food Security: Challenges and Policies. Science 302, 1917–1919. doi:10.1126/science.1092958

Routledge, 2013. The Singapore Water Story: Sustainable Development in an Urban City-State (Paperback) - Routledge [WWW Document]. URL http://www.routledge.com/books/details/9780415657839/ (accessed 7.9.13).

Saldanha, A.J., 2004. Java Treeview—extensible visualization of microarray data. Bioinformatics 20, 3246–3248. doi:10.1093/bioinformatics/bth349

Satterthwaite, D., McGranahan, G., Tacoli, C., 2010. Urbanization and its implications for food and farming. Philos. Trans. R. Soc. B Biol. Sci. 365, 2809–2820. doi:10.1098/rstb.2010.0136

Schneider, U.A., Havlík, P., Schmid, E., Valin, H., Mosnier, A., Obersteiner, M., Böttcher, H., Skalský, R., Balkovič, J., Sauer, T., Fritz, S., 2011. Impacts of population growth, economic development, and technical change on global food production and consumption. Agric. Syst. 104, 204–215. doi:10.1016/j.agsy.2010.11.003

Schütte, U.M.E., Abdo, Z., Bent, S.J., Shyu, C., Williams, C.J., Pierson, J.D., Forney, L.J., 2008. Advances in the use of terminal restriction fragment length polymorphism (T-RFLP) analysis of 16S rRNA genes to characterize microbial communities. Appl. Microbiol. Biotechnol. 80, 365–380. doi:10.1007/s00253-008-1565-4

Shade, A., Peter, H., Allison, S.D., Baho, D.L., Berga, M., Burgmann, H., Huber, D.H., Langenheder, S., Lennon, J.T., Martiny, J.B.H., Matulich, K.L., Schmidt, T.M., Handelsman, J., 2012. Fundamentals of Microbial Community Resistance and Resilience. Front. Microbiol. 3, 1–19. doi:10.3389/fmicb.2012.00417

Sheng, G.-P., Yu, H.-Q., Li, X.-Y., 2010. Extracellular polymeric substances (EPS) of microbial aggregates in biological wastewater treatment systems: A review. Biotechnol. Adv. 28, 882–894. doi:10.1016/j.biotechadv.2010.08.001

Singh, R., Paul, D., Jain, R.K., 2006. Biofilms: implications in bioremediation. Trends Microbiol. 14, 389–397. doi:10.1016/j.tim.2006.07.001

Srinivasan, V., Seto, K.C., Emerson, R., Gorelick, S.M., 2013. The impact of urbanization on water vulnerability: A coupled human–environment system approach for Chennai, India. Glob. Environ. Change 23, 229–239. doi:10.1016/j.gloenvcha.2012.10.002

Stage, J., Stage, J., Mcgranahan, G., 2010. Is urbanization contributing to higher food prices? Environ. Urban. 22, 199–215. doi:10.1177/0956247809359644

Statistics Singapore - Population and Population Structure [WWW Document], 2013. URL http://www.singstat.gov.sg/statistics/browse_by_theme/population.html (accessed 12.9.13).

Strohm, T.O., Griffin, B., Zumft, W.G., Schink, B., 2007. Growth Yields in Bacterial Denitrification and Nitrate Ammonification. Appl. Environ. Microbiol. 73, 1420–1424. doi:10.1128/AEM.02508-06

Sutherland, R.A., Tack, F.M.G., Ziegler, A.D., 2012. Road-deposited sediments in an urban environment: A first look at sequentially extracted element loads in grain size fractions. J. Hazard. Mater. 225–226, 54–62. doi:10.1016/j.jhazmat.2012.04.066

Teske, A., Durbin, A., Ziervogel, K., Cox, C., Arnosti, C., 2011. Microbial Community Composition and Function in Permanently Cold Seawater and Sediments from an Arctic Fjord of Svalbard. Appl. Environ. Microbiol. 77, 2008–2018. doi:10.1128/AEM.01507-10

Tigas, L.A., Van Vuren, D.H., Sauvajot, R.M., 2002. Behavioral responses of bobcats and coyotes to habitat fragmentation and corridors in an urban environment. Biol. Conserv. 108, 299–306. doi:10.1016/S0006-3207(02)00120-9

Tortajada, C., 2006. Water Management in Singapore. Int. J. Water Resour. Dev. 22, 227–240. doi:10.1080/07900620600691944

Tortajada, C., Joshi, Y.K., 2013. Water Demand Management in Singapore: Involving the Public. Water Resour. Manag. 27, 2729–2746. doi:10.1007/s11269-013-0312-5

Tranvik, L.J., Downing, J.A., Cotner, J.B., Loiselle, S.A., Striegl, R.G., Ballatore, T.J., Dillon, P., Finlay, K., Fortino, K., Knoll, L.B., 2009. Lakes and reservoirs as regulators of carbon cycling and climate. Limnol. Oceanogr. 54, 2298–2314.

Tu, J., 2011. Spatially varying relationships between land use and water quality across an urbanization gradient explored by geographically weighted regression. Appl. Geogr. 31, 376–392. doi:10.1016/j.apgeog.2010.08.001

United Nations, DESA (Population Division) World Urbanization Prospects: The 2007 Revision (1st February 2008) ESA/P/WP/205, n.d.

United Nations, DESA (Population Division) World Urbanization Prospects: The 2011 Revision (1st August 2012) ST/ESA/SER.A/322, n.d.

USEPA, 2013. National Recommended Water Quality Criteria [WWW Document]. URL http://water.epa.gov/scitech/swguidance/standards/criteria/current/index.cfm (accessed 12.22.13).

Varis, O., 2006a. Megacities, Development and Water. Int. J. Water Resour. Dev. 22, 199–225. doi:10.1080/07900620600648399

Varis, O., 2006b. Megacities, Development and Water. Int. J. Water Resour. Dev. 22, 199–225. doi:10.1080/07900620600648399

Varis, O., Biswas, A.K., Tortajada, C., Lundqvist, J., 2006. Megacities and Water Management. Int. J. Water Resour. Dev. 22, 377–394. doi:10.1080/07900620600684550

Villarreal, E.L., Semadeni-Davies, A., Bengtsson, L., 2004. Inner city stormwater control using a combination of best management practices. Ecol. Eng. 22, 279–298. doi:10.1016/j.ecoleng.2004.06.007

Vorosmarty, C.J., 2000. Global Water Resources: Vulnerability from Climate Change and Population Growth. Science 289, 284–288. doi:10.1126/science.289.5477.284

Vörösmarty, C.J., McIntyre, P.B., Gessner, M.O., Dudgeon, D., Prusevich, A., Green, P., Glidden, S., Bunn, S.E., Sullivan, C.A., Liermann, C.R., Davies, P.M., 2010. Global threats to human water security and river biodiversity. Nature 467, 555–561. doi:10.1038/nature09440

Wagner, P.J., 2000. Numerical Palaeobiology--Computer-based Modelling and Analysis of Fossils and their Distributions. PALAIOS 15, 364–366. doi:10.1669/0883-1351(2000)015<0364:BR>2.0.CO;2

Walker, W.J., McNutt, R.P., Maslanka, C.K., 1999. The potential contribution of urban runoff to surface sediments of the Passaic River: Sources and chemical characteristics. Chemosphere 38, 363–377. doi:10.1016/S0045-6535(98)00186-6

Walsh, C.J., 2000. Urban impacts on the ecology of receiving waters: a framework for assessment, conservation and restoration. Hydrobiologia 431, 107–114.

Wang, F., Zhou, H., Meng, J., Peng, X., Jiang, L., Sun, P., Zhang, C., Van Nostrand, J.D., Deng, Y., He, Z., 2009. GeoChip-based analysis of metabolic diversity of microbial communities at the Juan de Fuca Ridge hydrothermal vent. Proc. Natl. Acad. Sci. 106, 4840–4845.

Wang, G., Dong, J., Li, X., Sun, H., 2010. The bacterial diversity in surface sediment from the South China Sea. Acta Oceanol. Sin. 29, 98–105. doi:10.1007/s13131-010-0054-7

Ward, N.L., Challacombe, J.F., Janssen, P.H., Henrissat, B., Coutinho, P.M., Wu, M., Xie, G., Haft, D.H., Sait, M., Badger, J., Barabote, R.D., Bradley, B., Brettin, T.S., Brinkac, L.M., Bruce, D., Creasy, T., Daugherty, S.C., Davidsen, T.M., DeBoy, R.T., Detter, J.C., Dodson, R.J., Durkin, A.S., Ganapathy, A., Gwinn-Giglio, M., Han, C.S., Khouri, H., Kiss, H., Kothari, S.P., Madupu, R., Nelson, K.E., Nelson, W.C., Paulsen, I., Penn, K., Ren, Q., Rosovitz, M.J., Selengut, J.D., Shrivastava, S., Sullivan, S.A., Tapia, R., Thompson, L.S., Watkins, K.L., Yang, Q., Yu, C., Zafar, N., Zhou, L., Kuske, C.R., 2009. Three Genomes from the Phylum Acidobacteria Provide Insight into the Lifestyles of These

Microorganisms in Soils. Appl. Environ. Microbiol. 75, 2046–2056. doi:10.1128/AEM.02294-08

Weinert, N., Piceno, Y., Ding, G.-C., Meincke, R., Heuer, H., Berg, G., Schloter, M., Andersen, G., Smalla, K., 2011. PhyloChip hybridization uncovered an enormous bacterial diversity in the rhizosphere of different potato cultivars: many common and few cultivar-dependent taxa. FEMS Microbiol. Ecol. 75, 497–506. doi:10.1111/j.1574-6941.2010.01025.x

Wellington, E.M., Berry, A., Krsek, M., 2003. Resolving functional diversity in relation to microbial community structure in soil: exploiting genomics and stable isotope probing. Curr. Opin. Microbiol. 6, 295–301. doi:10.1016/S1369-5274(03)00066-3

Whitehead, P.G., Wilby, R.L., Battarbee, R.W., Kernan, M., Wade, A.J., 2009. A review of the potential impacts of climate change on surface water quality. Hydrol. Sci. J. 54, 101–123. doi:10.1623/hysj.54.1.101

Wilhelm, L., Singer, G.A., Fasching, C., Battin, T.J., Besemer, K., 2013. Microbial biodiversity in glacier-fed streams. ISME J. 1–10.

Winter, C., Hein, T., Kavka, G., Mach, R.L., Farnleitner, A.H., 2007. Longitudinal Changes in the Bacterial Community Composition of the Danube River: a Whole-River Approach. Appl. Environ. Microbiol. 73, 421–431. doi:10.1128/AEM.01849-06

Wolff, G., Gleick, P.H., 2002. The World's Water 2002–2003. Washington, DC: Island Press.

Wolman, M.G., 1967. A cycle of sedimentation and erosion in urban river channels. Geogr. Ann. Ser. Phys. Geogr. 385–395.

Wong, T.H., 2006a. Water sensitive urban design–the journey thus far. Aust. J. Water Resour. 10, 213–222.

Wong, T.H., 2006b. An overview of water sensitive urban design practices in Australia. Water Pract. Technol. 1, 1–8.

World Health Organization, 2003. Guidelines for safe recreational water environments. Volume 1, Volume 1,. World Health Organization, Geneva.

Wu, J., Yue, J., Hu, R., Yang, Z., Zhang, L., 2008. Use of caffeine and human pharmaceutical compounds to identify sewage contamination. World Acad Sci Eng Technol 44, 438–442.

Xia, X., Chen, X., Liu, R., Liu, H., 2011. Heavy metals in urban soils with various types of land use in Beijing, China. J. Hazard. Mater. 186, 2043–2050. doi:10.1016/j.jhazmat.2010.12.104

Xiang, X., Shi, Y., Yang, J., Kong, J., Lin, X., Zhang, H., Zeng, J., Chu, H., 2014. Rapid recovery of soil bacterial communities after wildfire in a Chinese boreal forest. Sci. Rep. 4. doi:10.1038/srep03829

Yanful, E., Verma, A., Straatman, A., 2000. Turbulence-Driven Metal Release from Resuspended Pyrrhotite Tailings. J. Geotech. Geoenvironmental Eng. 126, 1157–1165. doi:10.1061/(ASCE)1090-0241(2000)126:12(1157)

Yang, X., Huang, S., Wu, Q., Zhang, R., 2012. Nitrate reduction coupled with microbial oxidation of sulfide in river sediment. J. Soils Sediments 12, 1435–1444. doi:10.1007/s11368-012-0542-9

Zanaroli, G., Balloi, A., Negroni, A., Borruso, L., Daffonchio, D., Fava, F., 2012a. A Chloroflexi bacterium dechlorinates polychlorinated biphenyls in marine sediments under in situ-like biogeochemical conditions. J. Hazard. Mater. 209–210, 449–457. doi:10.1016/j.jhazmat.2012.01.042

Zanaroli, G., Balloi, A., Negroni, A., Borruso, L., Daffonchio, D., Fava, F., 2012b. A Chloroflexi bacterium dechlorinates polychlorinated biphenyls in marine sediments under in situ-like biogeochemical conditions. J. Hazard. Mater. 209–210, 449–457. doi:10.1016/j.jhazmat.2012.01.042

Zhang, H., Sekiguchi, Y., Hanada, S., Hugenholtz, P., Kim, H., Kamagata, Y., Nakamura, K., 2003. Gemmatimonas aurantiaca gen. nov., sp. nov., a Gram-negative, aerobic, polyphosphate-accumulating micro-organism, the first cultured representative of the new bacterial phylum Gemmatimonadetes phyl. nov. Int. J. Syst. Evol. Microbiol. 53, 1155–1163. doi:10.1099/ijs.0.02520-0

Zhang, Y., Lu, Z., Liu, S., Yang, Y., He, Z., Ren, Z., Zhou, J., Li, D., 2013. Geochip-based analysis of microbial communities in alpine meadow soils in the Qinghai-Tibetan plateau. BMC Microbiol. 13, 72. doi:10.1186/1471-2180-13-72

Zhao, H., Li, X., Wang, X., Tian, D., 2010. Grain size distribution of road-deposited sediment and its contribution to heavy metal pollution in urban runoff in Beijing, China. J. Hazard. Mater. 183, 203–210. doi:10.1016/j.jhazmat.2010.07.012

Zhou, J., Bruns, M.A., Tiedje, J.M., 1996a. DNA recovery from soils of diverse composition. Appl. Environ. Microbiol. 62, 316–322.

Zhou, J., Bruns, M.A., Tiedje, J.M., 1996b. DNA recovery from soils of diverse composition. Appl. Environ. Microbiol. 62, 316–322.

Appendix 1

Table A1.1: Physicochemical parameters of water samples

Land-use type	Region	Sample ID	TOC (ppm)	Temp (^{0}C)	Cond (µS/cm)	TDS (g/L)	Salinity (sal)	DO (%)	pH	ORP
Residential	Region1	R1_W	3.75 ± 0.38	25.65 ± 0.13	73.67 ± 1.53	0.05 ± 0.01	0.03 ± 0.01	74.83 ± 0.76	9.78 ± 0.03	148 ± 2.65
		R2_W	4.98 ± 0.06	25.96 ± 0.58	133.67 ± 3.21	0.08 ± 0.01	0.05 ± 0.01	93.07 ± 1.79	7.65 ± 0.01	155.23 ± 4.53
		R3_W	5.79 ± 0.26	27.25 ± 1.13	285.33 ± 5.51	0.2 ± 0.02	0.11 ± 0.02	161.7 ± 3.03	10.88 ± 0.03	134.77 ± 1.46
		R4_W	2.45 ± 0.19	26.28 ± 0.03	115 ± 3.46	0.08 ± 0.01	0.05 ± 0	73.07 ± 2.72	8.23 ± 0.03	161.1 ± 0.61
		R5_W	2.67 ± 0.08	26.58 ± 0.1	29.33 ± 0.58	0.03 ± 0.01	0.02 ± 0.01	84.33 ± 1.06	8 ± 0.1	169.73 ± 0.64
	Region2	R7_W	2.57 ± 0.27	26.93 ± 0.08	838.33 ± 32.13	0.53 ± 0.04	0.34 ± 0.03	46.33 ± 1.11	7.38 ± 0.02	141.97 ± 0.91
		R8_W	3.63 ± 0.15	27.03 ± 0.06	404.67 ± 6.81	0.24 ± 0.01	0.17 ± 0.03	67.1 ± 2.36	7.4 ± 0.09	142.53 ± 1.26
		R9_W	5.74 ± 0.38	28.03 ± 0.06	402.33 ± 4.16	0.24 ± 0.01	0.16 ± 0.01	37.97 ± 1.16	8.83 ± 0.04	137.97 ± 1.96
		R10_W	4.68 ± 0.09	26.59 ± 0.09	475 ± 9.54	0.26 ± 0.01	0.18 ± 0.03	42 ± 2.31	7.69 ± 0.17	150.61 ± 1.39
	Region3	R6_W	4 ± 0.17	26.7 ± 0.1	237.33 ± 6.81	0.19 ± 0.02	0.12 ± 0.03	70.63 ± 4.75	7.5 ± 0.02	135.83 ± 5.12
Commercial		C1_W	7.3 ± 0.7	27.43 ± 0.06	143.33 ± 1.53	0.1 ± 0.02	0.06 ± 0.02	30.83 ± 0.71	8.03 ± 0.03	155 ± 0.53
Industrial		I1_W	6.98 ± 0.34	26.07 ± 0.06	159 ± 2.65	0.12 ± 0.01	0.07 ± 0.01	75.4 ± 1.77	7.39 ± 0.1	159.8 ± 1.08
		I2_W	7.43 ± 0.37	26 ± 0.1	194 ± 3.61	0.13 ± 0.02	0.1 ± 0.02	70.3 ± 0.26	7.46 ± 0.05	159.04 ± 0.91
		I3_W	6.44 ± 0.35	27.67 ± 0.08	120.67 ± 0.58	0.09 ± 0.02	0.05 ± 0.01	32.9 ± 2.48	7.65 ± 0.06	154.73 ± 1.08
		I4_W	6.36 ± 0.33	27.53 ± 0.08	207.33 ± 6.51	0.09 ± 0.03	0.12 ± 0.04	35.13 ± 0.42	7.16 ± 0.05	156.63 ± 0.83
		I5_W	4.45 ± 0.29	25.8 ± 0.24	371.33 ± 2.52	0.2 ± 0.06	0.24 ± 0.05	63.73 ± 1.27	6.72 ± 0.04	70.67 ± 1.56
		I6_W	3.57 ± 0.35	27.04 ± 0.05	497.67 ± 12.06	0.3 ± 0.03	0.18 ± 0.04	41.27 ± 1.16	8.1 ± 0.1	152.13 ± 1.33

Forested	Region1	F1_W	2.92 ± 0.15	26.86 ± 0.03	98.67 ± 3.21	0.05 ± 0.01	0.05 ± 0.01	116.13 ± 5.56	7.06 ± 0.05	112.1 ± 1.41
	Region2	F2_W	7.06 ± 0.16	28.03 ± 0.06	159.33 ± 3.06	0.12 ± 0.03	0.07 ± 0.01	35.9 ± 0.56	7.7 ± 0.13	155.33 ± 1.33

Table A1.2a: Nutrient ions in water samples

Land-use type	Region	Sample ID	Units	NO_2^-	NO_3^-	NH_4^+	Tot N	SO_4^{-2}	PO_3^-	TOC	Na	K	Ca
Residential	Region1	R1_W	ppm	0.02 ± 0.03	0.9 ± 0.35	0.07 ± 0.04	0.98 ± 0.39	5.73 ± 0.53	N.D.	3.75 ± 0.38	2.21 ± 0.16	3.05 ± 0.15	8.04 ± 0.32
		R2_W	ppm	N.D.	0.77 ± 0.16	0.07 ± 0.03	0.84 ± 0.14	7.28 ± 0.53	N.D.	4.98 ± 0.06	1.76 ± 0.06	3.2 ± 0.18	1.71 ± 0.12
		R3_W	ppm	N.D.	3.78 ± 2.63	0.14 ± 0.06	3.93 ± 2.62	13.3 ± 0.99	N.D.	5.79 ± 0.26	3.8 ± 0.14	3.36 ± 0.07	16.41 ± 0.98
		R4_W	ppm	0.07 ± 0.11	3.87 ± 0.92	0.16 ± 0.04	4.1 ± 0.87	15.32 ± 0.57	N.D.	2.45 ± 0.19	10.12 ± 0.28	6.03 ± 0.02	16.12 ± 6.6
		R5_W	ppm	0.09 ± 0.16	25.77 ± 19.54	0.07 ± 0.02	25.94 ± 19.37	6.6 ± 0.89	N.D.	2.67 ± 0.08	3.1 ± 0.17	3.69 ± 0.07	27.95 ± 0.73
	Region2	R7_W	ppm	0.06 ± 0.1	5.11 ± 4.52	0.03 ± 0.01	5.2 ± 4.48	3.84 ± 0.44	N.D.	2.57 ± 0.27	11.43 ± 0.18	5.75 ± 0.04	15.8 ± 1.06
		R8_W	ppm	0.06 ± 0.1	2.85 ± 0.4	0.03 ± 0	2.93 ± 0.31	5.05 ± 0.48	N.D.	3.63 ± 0.15	10.21 ± 0.64	6.3 ± 0.08	23.54 ± 2.09
		R9_W	ppm	N.D.	2.25 ± 0.51	N.D.	2.25 ± 0.51	N.D.	N.D.	5.74 ± 0.38	7.67 ± 0.58	2.74 ± 0.09	63.04 ± 1.61
		R10_W	ppm	N.D.	1.66 ± 0.31	0.04 ± 0	1.7 ± 0.31	7.12 ± 0.57	N.D.	4.68 ± 0.09	19.92 ± 0.52	6.36 ± 0.05	21.39 ± 1.5
	Region3	R6_W	ppm	N.D.	19.02 ± 13.88	0.04 ± 0	19.06 ± 13.88	0.09 ± 0.01	N.D.	4 ± 0.17	4.34 ± 0.18	2.01 ± 0.01	14.1 ± 0.71
Commercial		C1_W	ppm	0.24 ± 0.29	3.18 ± 1.27	0.18 ± 0.06	3.59 ± 0.96	11.25 ± 3.55	N.D.	7.3 ± 0.7	7.28 ± 0.19	5.84 ± 0.17	15.19 ± 0.38
Industrial		I1_W	ppm	0.05 ± 0.09	4.12 ± 0.85	0.05 ± 0	4.22 ± 0.78	0.3 ± 0.08	N.D.	6.98 ± 0.34	7.13 ± 0.27	4.94 ± 0.19	16.24 ± 0.05

		I2_W	ppm	0.14 ± 0.13	2.18 ± 1.16	0.04 ± 0.01	2.35 ± 1.17	1.76 ± 0.29	N.D.	7.43 ± 0.37	13.21 ± 0.95	5.68 ± 0.1	23.31 ± 3.01
		I3_W	ppm	0.39 ± 0.27	2.1 ± 0.62	0.05 ± 0.02	2.54 ± 0.76	2.02 ± 0.18	N.D.	6.44 ± 0.35	21.91 ± 1.06	10.13 ± 0.23	23.71 ± 2.73
		I4_W	ppm	0.38 ± 0.07	1.67 ± 0.08	0.16 ± 0.03	2.21 ± 0.09	18.39 ± 0.26	N.D.	6.36 ± 0.33	20.43 ± 1.63	10.95 ± 1.05	25.71 ± 0.64
		I5_W	ppm	0.12 ± 0.21	1.04 ± 0.35	0.05 ± 0	1.21 ± 0.57	10.52 ± 0.26	N.D.	4.45 ± 0.29	14.82 ± 1.06	6.56 ± 0.08	23.91 ± 3.37
		I6_W	ppm	0.35 ± 0.31	2.13 ± 1.05	0.17 ± 0.22	2.65 ± 1.14	12.07 ± 0.53	N.D.	3.57 ± 0.35	32.33 ± 1.14	16.38 ± 0.14	16.97 ± 0.93
Forested	Region1	F1_W	ppm	N.D.	2.58 ± 1.04	0.06 ± 0.02	2.64 ± 1.04	4.53 ± 0.32	N.D.	2.92 ± 0.15	5.27 ± 0.19	3.09 ± 0.07	13.41 ± 0.45
	Region2	F2_W	ppm	N.D.	4.49 ± 1.28	0.13 ± 0.06	4.62 ± 1.25	11.46 ± 2.43	N.D.	7.06 ± 0.16	9.98 ± 0.26	3.31 ± 0.11	24.57 ± 0.86

Table A1.2b: Nutrient ions in sediment samples

Land-use type	Region	Sample ID	Units	NO_2^-	NO_3^-	NH_4^+	Tot N	SO_4^{-2}	PO_4^{-3}	TOC	Na	K	Ca
Residential	Region1	R1_S	µg/gm	N.D.	N.D.	0.17 ± 0	0.17 ± 0	2.58 ± 0.22	N.D.	2.76 ± 0.21	0.28 ± 0.01	1.04 ± 0.03	3.32 ± 0.12
		R2_S	µg/gm	0.02 ± 0.04	N.D.	1.23 ± 0	1.25 ± 0.04	7.12 ± 0.36	N.D.	3.12 ± 0.22	N.D.	0.22 ± 0	3.93 ± 0
		R3_S	µg/gm	N.D.	N.D.	0.99 ± 0.01	0.99 ± 0.01	5.9 ± 0.3	N.D.	1.55 ± 0.01	0.23 ± 0.03	0.4 ± 0.04	2.84 ± 0.25
		R4_S	µg/gm	0.02 ± 0.04	0.21 ± 0.37	N.D.	0.23 ± 0.35	6.16 ± 0.62	N.D.	2.02 ± 0.03	0.06 ± 0	0.03 ± 0	1.65 ± 0
		R5_S	µg/gm	N.D.	1.08 ± 0.94	0.07 ± 0	1.15 ± 0.94	0.31 ± 0.54	N.D.	4.24 ± 0.28	0.06 ± 0.01	0.06 ± 0.01	0.36 ± 0.04
	Region2	R7_S	µg/gm	N.D.	N.D.	0.06 ± 0	0.06 ± 0	3.32 ± 0.21	N.D.	6.65 ± 0.13	0.22 ± 0	0.1 ± 0	2.76 ± 0
		R8_S	µg/gm	0.06 ± 0.1	0.02 ± 0.03	1.17 ± 0	1.25 ± 0.09	2.22 ± 0.1	N.D.	2.12 ± 0.12	0.21 ± 0	0.74 ± 0	6.95 ± 0

		R9_S	µg/gm	0.02 ± 0.03	N.D.	0.23 ± 0	0.25 ± 0.03	0.68 ± 0.59	N.D.	2.97 ± 0.09	0.14 ± 0	0.41 ± 0	5.66 ± 0
		R10_S	µg/gm	N.D.	0.25 ± 0.22	0.45 ± 0	0.7 ± 0.22	2.28 ± 0.15	N.D.	3.92 ± 0.09	0.12 ± 0	0.28 ± 0	3.5 ± 0
	Region3	R6_S	µg/gm	N.D.	0.44 ± 0.76	0.05 ± 0	0.49 ± 0.76	0.08 ± 0.14	N.D.	2.71 ± 0.33	0.47 ± 0	0.26 ± 0	0.33 ± 0
Commercial		C1_S	µg/gm	N.D.	N.D.	0.21 ± 0	0.21 ± 0	1.72 ± 0.09	N.D.	7.04 ± 0.13	0.15 ± 0	0.14 ± 0	3.27 ± 0
Industrial		I1_S	µg/gm	N.D.	N.D.	0.19 ± 0	0.19 ± 0	1.11 ± 0.18	N.D.	3.41 ± 0.14	0.06 ± 0	0.23 ± 0	2.34 ± 0
		I2_S	µg/gm	N.D.	N.D.	0.75 ± 0	0.75 ± 0	4.15 ± 4.3	N.D.	8.41 ± 0.34	0.14 ± 0	0.27 ± 0	4.74 ± 0
		I3_S	µg/gm	0.03 ± 0.05	0.13 ± 0.22	N.D.	0.16 ± 0.28	1.14 ± 1.01	N.D.	2.95 ± 0.15	0.07 ± 0	0.1 ± 0	1.54 ± 0
		I4_S	µg/gm	N.D.	0.38 ± 0.35	0.06 ± 0.01	0.43 ± 0.35	4.04 ± 0.17	N.D.	1.01 ± 0.04	0.07 ± 0	0.09 ± 0.01	0.29 ± 0.02
		I5_S	µg/gm	0.02 ± 0.04	N.D.	0.91 ± 0	0.94 ± 0.04	9.33 ± 0.69	N.D.	2.81 ± 0.25	0.13 ± 0	0.13 ± 0	3.68 ± 0
		I6_S	µg/gm	N.D.	0.37 ± 0.64	0.36 ± 0	0.73 ± 0.64	0.82 ± 0.3	N.D.	1.72 ± 0.15	0.11 ± 0	0.17 ± 0	3.2 ± 0
Forested	Region1	F1_S	µg/gm	N.D.	N.D.	0.04 ± 0	0.04 ± 0	0.68 ± 0.48	N.D.	1.4 ± 0.23	0.05 ± 0	0.04 ± 0	1.3 ± 0
	Region2	F2_S	µg/gm	N.D.	N.D.	N.D.	N.D.	1.55 ± 0.23	N.D.	3.43 ± 0.11	0.06 ± 0	0.04 ± 0	0.57 ± 0

Table A1.3a: Metals in water samples

Land-use type	Region	Sample ID	Units	Al	As	Cd	Cr	Co	Cu	Pb	Mg	Hg	Ni	Se	Ag	Zn
Residential	Region1	R1_W	ppb	153.87 ± 7.22	0.33 ± 0.38	0.06 ± 0.01	0.83 ± 0.61	0.1 ± 0.03	15.06 ± 3.6	0.22 ± 0.08	224.45 ± 15.32	0.01 ± 0.01	0.44 ± 0.04	0.58 ± 0.06	0.02 ± 0.02	196.31 ± 7.13
		R2_W	ppb	42.73 ± 5	3.33 ± 0.3	0.06 ± 0.02	0.65 ± 0.45	0.12 ± 0.06	1.09 ± 0.47	0.26 ± 0.06	1318.02 ± 40.95	0.02 ± 0	0.32 ± 0.06	0.72 ± 0.03	0.09 ± 0.07	260.92 ± 12.53
		R3_W	ppb	821.14 ± 7.44	2.51 ± 0.59	0.01 ± 0.01	6.5 ± 0.24	0.02 ± 0.02	29.42 ± 1.76	0.19 ± 0.05	1143.87 ± 43.6	0.06 ± 0	0.08 ± 0.07	0.85 ± 0.05	0.14 ± 0.04	202.53 ± 38.08
		R4_W	ppb	73.89 ± 7.8	1.2 ± 0.67	0.05 ± 0.02	0.5 ± 0.56	0.06 ± 0.02	6.11 ± 0.94	0.43 ± 0.05	1281.08 ± 39.23	0.05 ± 0.01	0.03 ± 0.03	1.53 ± 0.07	0.11 ± 0.06	1157.79 ± 42.09
		R5_W	ppb	12.01 ± 5.82	0.64 ± 0.61	0.04 ± 0.01	0.24 ± 0.39	0.03 ± 0.02	0.31 ± 0.53	0.28 ± 0.02	58.78 ± 9.73	0.03 ± 0	0.11 ± 0.04	0.97 ± 0.04	0.07 ± 0.06	197.17 ± 37.2
	Region2	R7_W	ppb	12.96 ± 7.07	1.5 ± 0.36	0.02 ± 0.01	0.36 ± 0.48	0.08 ± 0.04	6.35 ± 2.09	0.44 ± 0.01	3193.36 ± 29.69	0.05 ± 0.01	0.16 ± 0.02	1.35 ± 0.03	0.15 ± 0.07	190.15 ± 40.52
		R8_W	ppb	17.34 ± 5.29	0.34 ± 0.26	0.01 ± 0.01	0.4 ± 0.49	0.62 ± 0.01	0.19 ± 0.33	0.51 ± 0.08	2919.21 ± 24.38	0.02 ± 0	2.21 ± 0.05	1.24 ± 0.02	0.18 ± 0.08	189.77 ± 65.04
		R9_W	ppb	915.32 ± 12.03	1.95 ± 0.12	0.05 ± 0.01	2.1 ± 0.57	0.14 ± 0.06	1.95 ± 1.68	0.42 ± 0.02	3028.26 ± 36.78	0.05 ± 0.01	1.09 ± 0.06	0.71 ± 0.01	0.11 ± 0.03	204.62 ± 18.43
		R10_W	ppb	77.63 ± 8.11	1.56 ± 0.66	0.06 ± 0.01	0.13 ± 0.21	0.09 ± 0.05	0.08 ± 0.13	0.44 ± 0.05	2803.92 ± 27.72	0.05 ± 0	0.37 ± 0.06	0.85 ± 0.07	0.19 ± 0.04	211.88 ± 46
	Region3	R6_W	ppb	35.58 ± 2.43	0.34 ± 0.39	0.06 ± 0.01	0.46 ± 0.47	0.1 ± 0.04	9.73 ± 0.68	0.72 ± 0.04	1574.85 ± 34.27	0.2 ± 0.34	1.08 ± 0.05	0.05 ± 0.04	0.04 ± 0.02	245.69 ± 20.09
Commercial		C1_W	ppb	91.75 ±	0.8 ± 0.63	0.02 ± 0.02	1.45 ± 0.6	0.04 ±	2.18 ±	0.22 ±	787 ± 28.33	0.08 ±	0.63 ±	0.7 ± 0.02	0.17 ±	195.94 ±

				2.95				0.03	1.89	0.07		0.73	0.04		0.05	39.08
Industrial		I1_W	ppb	51.15 ± 2.44	1.05 ± 0.12	0.05 ± 0.01	0.78 ± 0.61	0.1 ± 0.07	7.42 ± 1.98	0.14 ± 0.03	1700.41 ± 28.86	1.98 ± 0.7	0.73 ± 0.05	0.32 ± 0.09	0.19 ± 0.01	216.75 ± 12.52
		I2_W	ppb	40.94 ± 7.41	1.48 ± 0.31	0.08 ± 0	1.25 ± 0.5	0.78 ± 0.05	4.56 ± 2.09	0.21 ± 0.02	2033.02 ± 12.54	1.44 ± 0.6	1.22 ± 0.05	0.98 ± 0.02	0.02 ± 0.02	378.62 ± 47.52
		I3_W	ppb	51.21 ± 3.46	1.08 ± 0.43	0.01 ± 0.01	0.52 ± 0.5	0.69 ± 0.03	0.41 ± 0.29	0.3 ± 0	1998.46 ± 17.82	0.99 ± 0.23	1.48 ± 0.06	1.01 ± 0.07	0.05 ± 0.05	292.79 ± 38.8
		I4_W	ppb	104.27 ± 2.42	0.57 ± 0.5	0.04 ± 0.01	0.77 ± 0.08	0.02 ± 0.01	0.11 ± 0.19	0.22 ± 0.06	736.68 ± 19.54	0.22 ± 0.51	0.04 ± 0.03	1.09 ± 0.04	0.03 ± 0.04	217.46 ± 12.74
		I5_W	ppb	8.5 ± 4.63	0.38 ± 0.42	0.06 ± 0.01	0.38 ± 0.43	2.52 ± 0.05	2.6 ± 0.43	0.47 ± 0.05	3649.03 ± 31.48	0.9 ± 0.49	3.99 ± 0.05	0.07 ± 0.06	0.07 ± 0.06	254.42 ± 35.97
		I6_W	ppb	69.23 ± 5.52	1.2 ± 0.55	0.03 ± 0	0.04 ± 0.05	0.01 ± 0.01	1.25 ± 1.31	0.44 ± 0.09	2826.96 ± 28.28	0.76 ± 0.32	0.6 ± 0.04	0.57 ± 0.02	0.12 ± 0.07	218.22 ± 34.71
Forested	Region1	F1_W	ppb	1.74 ± 1.43	0.15 ± 0.61	0.12 ± 0.01	0.54 ± 0.45	0.24 ± 0.01	2.25 ± 0.98	0.37 ± 0.03	1512.73 ± 23.86	3.86 ± 0.28	0.11 ± 0.07	0.61 ± 0.06	0.8 ± 0.01	253.05 ± 34.48
	Region2	F2_W	ppb	91.82 ± 2.16	1.32 ± 0.37	0.02 ± 0.01	0.81 ± 0.42	0.05 ± 0.03	2.39 ± 1.1	0.07 ± 0.04	871.13 ± 20.21	0.52 ± 0.41	0.87 ± 0.02	0.45 ± 0.06	0.1 ± 0.05	193.67 ± 22.6

Table A1.3b: Metals in sediment samples

Land-use type	Region	Sample ID	Units	Al	As	Cd	Cr	Co	Cu	Pb	Mg	Hg	Ni	Se	Ag	Zn
Residential	Region1	R1_S	ng/gm	6.9 ± 1.48	0.28 ± 0.06	0.01 ± 0	ND	0.01 ± 0.01	0.33 ± 0.06	0.01 ± 0.01	70.22 ± 5	0.72 ± 0.04	0.23 ± 0.06	0.13 ± 0.01	0.03 ± 0	0.25 ± 0.08
		R2_S	ng/gm	11.59 ± 2.64	0.3 ± 0.05	0.01 ± 0	ND	0.02 ± 0	0.41 ± 0.06	0.03 ± 0.01	54.03 ± 2.08	0.58 ± 0.07	0.33 ± 0.08	0.09 ± 0.01	0.03 ± 0.01	0.31 ± 0.07
		R3_S	ng/gm	6.72 ± 0.67	0.03 ± 0.02	N.D.	ND	N.D.	0.22 ± 0.06	0.01 ± 0	37.28 ± 4.04	0.01 ± 0	0.23 ± 0.08	N.D..01	N.D.	0.39 ± 0.1
		R4_S	ng/gm	19.41 ± 1.75	0.04 ± 0.04	N.D.	ND	N.D.	0.03 ± 0.07	N.D.	4.8 ± 0.6	0.1 ± 0.05	0.24 ± 0.06	0.03 ± 0	N.D.	0.02 ± 0.02
		R5_S	ng/gm	100.9 ± 5.29	0.27 ± 0.05	N.D.	ND	N.D.	0.2 ± 0.04	0.02 ± 0.01	5.09 ± 0.31	0.51 ± 0.08	0.24 ± 0.07	0.07 ± 0	0.01 ± 0.01	1.43 ± 0.07
	Region2	R7_S	ng/gm	12.54 ± 0.59	0.22 ± 0.09	N.D.	ND	0.02 ± 0	0.15 ± 0.06	0.02 ± 0	40.8 ± 1	0.04 ± 0.06	0.5 ± 0.04	0.04 ± 0	0.09 ± 0.01	0.75 ± 0.04
		R8_S	ng/gm	2.42 ± 0.99	0.2 ± 0.04	N.D.	ND	0.06 ± 0	0.5 ± 0.09	0.01 ± 0.01	73.36 ± 5.51	0.03 ± 0.06	0.6 ± 0.08	0.05 ± 0.01	0.04 ± 0.01	0.76 ± 0.07
		R9_S	ng/gm	4.16 ± 0.55	0.13 ± 0.02	N.D.	ND	0.02 ± 0	0.41 ± 0.08	N.D.	118 ± 5.51	0.02 ± 0.03	0.54 ± 0.06	0.02 ± 0.01	0.03 ± 0.01	0.73 ± 0.08
		R10_S	ng/gm	11.22 ± 2.06	0.07 ± 0.02	N.D.	ND	0.01 ± 0	0.15 ± 0.05	0.01 ± 0.01	50.93 ± 3.22	0.03 ± 0.04	0.52 ± 0.04	0.02 ± 0.01	0.02 ± 0.01	0.34 ± 0.05
	Region3	R6_S	ng/gm	106.23 ± 6.06	0.13 ± 0.07	N.D.	0.066 ± 0.01	N.D.	0.19 ± 0	0.02 ± 0	3.18 ± 0.57	0.03 ± 0.03	0.24 ± 0.02	0.01 ± 0.01	N.D.	0.87 ± 0.06

Commercial		C1_S	ng/gm	3.29 ± 1.12	0.07 ± 0.04	N.D.	ND	0.01 ± 0	0.13 ± 0.08	0.01 ± 0.01	27.28 ± 1.74	N.D.	0.51 ± 0.09	0.01 ± 0.01	0.01 ± 0	0.3 ± 0.02
Industrial		I1_S	ng/gm	6.86 ± 1.01	0.11 ± 0.06	N.D.	ND	0.05 ± 0	0.52 ± 0.04	0.02 ± 0.01	18.82 ± 6.03	0.05 ± 0.04	0.41 ± 0.02	0.02 ± 0.01	N.D.	1.21 ± 0.05
		I2_S	ng/gm	7.01 ± 1.04	0.09 ± 0.07	N.D.	ND	0.08 ± 0	0.92 ± 0.04	0.01 ± 0.01	55.32 ± 5.57	0.03 ± 0	0.43 ± 0.04	0.03 ± 0	N.D.	4.3 ± 0.06
		I3_S	ng/gm	18.84 ± 1.77	0.03 ± 0.01	N.D.	ND	N.D.	0.18 ± 0.02	0.01 ± 0.01	19.98 ± 1	0.18 ± 0.08	0.21 ± 0.07	0.02 ± 0.01	N.D.	0.09 ± 0.06
		I4_S	ng/gm	45.99 ± 6.99	0.15 ± 0.05	N.D.	0.067 ± 0.011	0.01 ± 0	0.14 ± 0.03	0.01 ± 0.01	3.68 ± 0.1	0.33 ± 0.05	0.27 ± 0.07	0.04 ± 0.01	0.01 ± 0.01	1.26 ± 0.06
		I5_S	ng/gm	1.12 ± 0.58	0.03 ± 0.05	N.D.	ND	0.07 ± 0	0.4 ± 0	0.01 ± 0	49.11 ± 3	0.04 ± 0.03	0.44 ± 0.08	0.02 ± 0.01	N.D.	0.66 ± 0.01
		I6_S	ng/gm	1.65 ± 0.29	0.09 ± 0.05	N.D.	ND	0.22 ± 0	0.7 ± 0.06	N.D.	91.12 ± 7.55	0.02 ± 0	0.49 ± 0.04	0.01 ± 0	N.D.	0.81 ± 0.05
Forested	Region1	F1_S	ng/gm	3.52 ± 0.54	N.D..06	N.D.	ND	N.D.	0.04 ± 0.05	N.D.	8.55 ± 1.15	0.1 ± 0.06	0.2 ± 0.05	0.02 ± 0.01	0.01 ± 0.01	0.04 ± 0.04
	Region2	F2_S	ng/gm	3.72 ± 0.54	0.05 ± 0.05	0 ± 0	ND	0 ± 0	0.06 ± 0.05	0.01 ± 0	3.73 ± 0.5	0.04 ± 0.06	0.23 ± 0.01	0 ± 0.01	0 ± 0.01	0.19 ± 0.06

Table A1.4a: Organics in water samples

Land-use type	Region	Sample ID	Unit	Toluene	m+p Xylene	Styrene	O-xylene	Pinene	Limonene	Naphthalene	Fluorene	Atrazine	Lindane	Anthracene	Pen G	Chloramphenicol	Nalidixic Acid
Residential	Region1	R1_W	ppb	45.97 ± 7.09	0.02 ± 0.01	0.01 ± 0	0.01 ± 0	N.D.	0.11 ± 0.02	0.88 ± 0	0.87 ± 0	0.28 ± 0.01	0.02 ± 0.01	0.47 ± 0.01	N.D.	N.D.	N.D.
		R2_W	ppb	29.06 ± 2.05	0.02 ± 0	0.01 ± 0	0.01 ± 0.01	N.D.	N.D.	0.82 ± 0.01	0.59 ± 0	0.06 ± 0	0.01 ± 0.01	0.31 ± 0	N.D.	N.D.	N.D.
		R3_W	ppb	1.56 ± 0.19	0.02 ± 0.01	0.02 ± 0.01	0.02 ± 0.01	N.D.	N.D.	0.09 ± 0	0.06 ± 0.01	0.13 ± 0	N.D.	0.06 ± 0.01	N.D.	0.08 ± 0	N.D.
		R4_W	ppb	11.61 ± 0.62	N.D.	0.01 ± 0	N.D.	N.D.	N.D.	N.D.	N.D.	N.D.	N.D.	0.02 ± 0	N.D.	N.D.	N.D.
		R5_W	ppb	31.52 ± 2.09	0.55 ± 0.01	0.31 ± 0.01	0.05 ± 0.01	0.08 ± 0	0.4 ± 0.09	0.42 ± 0.01	0.93 ± 0	0.02 ± 0.01	0.05 ± 0.01	0.46 ± 0.01	0.02 ± 0	0.08 ± 0.01	0.14 ± 0.02
	Region2	R7_W	ppb	31.22 ± 1.03	0.02 ± 0.01	0.02 ± 0.01	0.02 ± 0.01	N.D.	N.D.	0.48 ± 0	0.33 ± 0.01	0.03 ± 0	0.01 ± 0.01	0.23 ± 0	0.03 ± 0.01	N.D.	N.D.
		R8_W	ppb	0.41 ± 0.32	N.D.	N.D.	N.D.	N.D.	N.D.	0.02 ± 0.01	N.D.	0.01 ± 0.01	N.D.	0.04 ± 0	N.D.	N.D.	N.D.
		R9_W	ppb	N.D.	N.D.	N.D.	N.D.	N.D.	N.D.	N.D.	N.D.	0.03 ± 0	N.D.	N.D.	N.D.	0.07 ± 0	0.16 ± 0
		R10_W	ppb	0.45 ± 0.14	N.D.	N.D.	N.D.	N.D.	N.D.	N.D.	N.D.	0.01 ± 0	N.D.	N.D.	0.26 ± 0.04	N.D.	0.17 ± 0.01
	Region3	R6_W	ppb	35.11 ± 7.04	0.02 ± 0.01	0.01 ± 0	0.02 ± 0.01	N.D.	N.D.	0.12 ± 0	0.04 ± 0.01	0.02 ± 0	N.D.	0.11 ± 0.01	N.D.	N.D.	0.11 ± 0
Commercial		C1_W	ppb	1.39 ± 0.55	0.02 ± 0.01	0.01 ± 0	0.01 ± 0.01	0.49 ± 0.08	N.D.	N.D.	0.03 ± 0.01	0.08 ± 0.01	N.D.	0.02 ± 0.01	N.D.	0.09 ± 0.01	0.13 ± 0

Industrial		I1_W	ppb	N.D.	N.D.	N.D.	N.D.	N.D.	N.D.	0.01 ± 0	N.D.	0.03 ± 0	N.D.	0.03 ± 0	N.D.	0.13 ± 0.02	0.2 ± 0.01
		I2_W	ppb	0.54 ± 0.12	N.D.	0.01 ± 0.01	0.01 ± 0.01	N.D.	N.D.	N.D.	N.D.	0.01 ± 0	N.D.	0.02 ± 0.01	N.D.	N.D.	N.D.
		I3_W	ppb	0.51 ± 0.05	N.D.	0.01 ± 0.01	0.01 ± 0	N.D.	N.D.	N.D.	N.D.	0.02 ± 0.01	N.D.	0.05 ± 0	N.D.	N.D.	N.D.
		I4_W	ppb	4.48 ± 1.07	N.D.	N.D.	N.D.	N.D.	N.D.	N.D.	N.D.	0.01 ± 0.01	N.D.	N.D.	0.01 ± 0	N.D.	0.26 ± 0.1
		I5_W	ppb	0.47 ± 0.02	0.02 ± 0.01	0.02 ± 0.01	0.02 ± 0	N.D.	N.D.	0.15 ± 0.01	0.13 ± 0.01	0.02 ± 0.01	0.01 ± 0.01	0.19 ± 0	N.D.	0.09 ± 0.01	N.D.
		I6_W	ppb	22.78 ± 2.67	0.02 ± 0.01	0.02 ± 0.01	0.03 ± 0	N.D.	N.D.	0.04 ± 0.01	N.D.	0.03 ± 0	N.D.	0.05 ± 0.01	N.D.	N.D.	0.13 ± 0.02
Forested	Region1	F1_W	ppb	0.38 ± 0.39	0.01 ± 0	0.01 ± 0.01	N.D.	N.D.	N.D.	N.D.	0.03 ± 0.01	0.01 ± 0	N.D.	0.04 ± 0.01	N.D.	N.D.	N.D.
	Region2	F2_W	ppb	1.48 ± 0.04	0.01 ± 0	0.01 ± 0	0.02 ± 0.01	0.37 ± 0.03	N.D.	N.D.	0.01 ± 0.01	0.08 ± 0	N.D.	0.01 ± 0	0.02 ± 0	0.08 ± 0.01	0.13 ± 0.01

Table A1.4b: Organics in sediment samples

Land-use type	Region	Sample ID	Units	Toluene	m+p Xylene	Styrene	O-xylene	Pinene	Limonene	Naphthalene	Fluorene	Atrazine	Lindane	Anthracene	Pen G	Chloramphenicol	Nalidixic Acid
Residential	Region1	R1_S	ng/gm	0.04 ± 0.01	0.02 ± 0.01	0.01 ± 0	N.D.	N.D.	N.D.	N.D.	0.12 ± 0	N.D.	0.02 ± 0	0.04 ± 0	N.D.	0.18 ± 0	N.D.
		R2_S	ng/gm	0.05 ± 0.01	0.02 ± 0	N.D.	N.D.	N.D.	N.D.	0.03 ± 0	N.D.	N.D.	0.03 ± 0	N.D.	N.D.	0.29 ± 0	N.D.
		R3_S	ng/gm	N.D.	0.02 ± 0.01	0.02 ± 0.01	0.02 ± 0	N.D.	N.D.	0.02 ± 0	N.D.	0.04 ± 0	0.03 ± 0	0.03 ± 0	0.06 ± 0	0.09 ± 0.01	N.D.
		R4_S	ng/gm	N.D.	0.03 ± 0.01	0.05 ± 0	N.D.	N.D.	N.D.	0.03 ± 0	N.D.	N.D.	0.04 ± 0.01	0.03 ± 0.01	N.D.	N.D.	N.D.
		R5_S	ng/gm	N.D.	0.02 ± 0.01	0.01 ± 0	N.D.	N.D.	N.D.	N.D.	N.D.	N.D.	0.02 ± 0	0.03 ± 0	N.D.	0.09 ± 0	N.D.
	Region2	R7_S	ng/gm	N.D.	0.03 ± 0	0.02 ± 0.01	N.D.	N.D.	N.D.	N.D.	0.07 ± 0	0.17 ± 0.01	0.05 ± 0.01	0.06 ± 0.01	N.D.	0.32 ± 0.01	0.27 ± 0.01
		R8_S	ng/gm	N.D.	N.D.	0.02 ± 0.01	N.D.	N.D.	N.D.	N.D.	N.D.	0.16 ± 0	0.06 ± 0	N.D.	N.D.	0.1 ± 0	N.D.
		R9_S	ng/gm	N.D.	N.D.	0.03 ± 0.01	0.02 ± 0.01	N.D.	0.02 ± 0.01	0.01 ± 0	0.03 ± 0.01	N.D.	N.D.	N.D.	0.06 ± 0	N.D.	N.D.
		R10_S	ng/gm	N.D.	0.03 ± 0.01	N.D.	N.D.	N.D.	N.D.	0.01 ± 0	0.04 ± 0.01	0.16 ± 0.01	0.06 ± 0.01	N.D.	0.13 ± 0.01	0.28 ± 0	0.22 ± 0
	Region3	R6_S	ng/gm	N.D.	0.01 ± 0	0.05 ± 0	0.02 ± 0	N.D.	0.02 ± 0.01	N.D.	0.02 ± 0	N.D.	0.05 ± 0	N.D.	0.1 ± 0.01	N.D.	N.D.
Commercial		C1_S	ng/gm	N.D.	N.D.	0.03 ± 0	0.05 ± 0.01	N.D.	N.D.	N.D.	0.03 ± 0	0.2 ± 0.01	N.D.	N.D.	0.2 ± 0.01	0.22 ± 0.01	0.17 ± 0

Industrial		I1_S	ng/gm	N.D.	N.D.	0.06 ± 0.01	N.D.	N.D.	0.03 ± 0	0.02 ± 0	0.09 ± 0.01	0.06 ± 0.01	N.D.	0.02 ± 0	0.27 ± 0	0.1 ± 0.01	0.26 ± 0.01
		I2_S	ng/gm	N.D.	N.D.	N.D.	N.D.	N.D.	N.D.	N.D.	N.D.	0.07 ± 0.01	0.04 ± 0.01	0.02 ± 0.01	N.D.	0.18 ± 0	N.D.
		I3_S	ng/gm	N.D.	0.03 ± 0	N.D.	N.D.	N.D.	N.D.	N.D.	N.D.	N.D.	0.05 ± 0	0.03 ± 0.01	N.D.	N.D.	0.16 ± 0.01
		I4_S	ng/gm	N.D.	0.03 ± 0	N.D.	N.D.	N.D.	N.D.	N.D.	N.D.	N.D.	0.05 ± 0	0.03 ± 0.01	N.D.	0.08 ± 0.01	N.D.
		I5_S	ng/gm	0.04 ± 0.01	N.D.	N.D.	N.D.	0.02 ± 0.01	N.D.	N.D.	N.D.	0.08 ± 0.01	0.05 ± 0	0.02 ± 0.01	0.04 ± 0	N.D.	N.D.
		I6_S	ng/gm	N.D.	0.02 ± 0	0.07 ± 0	N.D.	0.06 ± 0	0.03 ± 0.01	0.03 ± 0.01	0.02 ± 0.01	N.D.	N.D.	0.05 ± 0.01	0.09 ± 0.01	N.D.	0.27 ± 0.01
Forested	Region1	F1_S	ng/gm	N.D.	0.04 ± 0.01	N.D.	N.D.	N.D.	N.D.	0.03 ± 0	N.D.	0.03 ± 0	0.03 ± 0.01	0.03 ± 0	N.D.	N.D.	N.D.
	Region2	F2_S	ng/gm	N.D.	0.02 ± 0	0.08 ± 0.01	N.D.	0.04 ± 0	N.D.	0.03 ± 0	N.D.	0.11 ± 0	N.D.	N.D.	N.D.	0.33 ± 0.01	N.D.

Table A1.5a: Kendal Tau correlation coefficients among environmental variables in water samples. Underline numbers represent –ve correlation. *: p<0.1; **:p<0.05 and ***: p<0.01

Temp													
Cond													
TDS			0.9 **										
Salinity			0.9 **	0.8 **									
DO	0.3 *	0.4 *											
pH													
ORP													
$N0_2^-$			0.3 *		0.3 *	0.4 **							
$N0_3^-$													
NH_4^+			0.4 **	0.3 **	0.4 **								
TotN										0.9 **			
$S0_4^+$			0.3 *		0.3 *						0.6 **		
Na						0.5 **			0.5 **				

K			0.3**	0.3*	0.4**	0.4**			0.6**				0.3**	0.7**																	
Ca		0.3*				0.3*								0.3**																	
Al		0.3*					0.6**																								
As																	0.3*														
Cd		0.5**				0.3*																									
Cr	0.5**													0.3*	0.3*		0.4**														
Co							0.3**				0.5**		0.4**				0.3*		0.3**												
Cu						0.3*				0.3*		0.3*		0.3*	0.3**	0.3*															
Pb	0.5**							0.4**			0.3*						0.3*			0.5**										
Mg								0.4**			0.5**			0.4**							0.4**		0.4**								
Hg	0.3*		0.3**	0.3*	0.4**		0.3**																								
Ni						0.3*					0.4**		0.4**								0.5**			0.4**						
Se															0.3*							0.3*				0.3*				
Ag																															

Zn																			0.4 **						0.4 **			
	TOC	**Temp**	**Cond**	**TDS**	**Salinity**	**DO**	**pH**	**ORP**	**$N0_2^-$**	**$N0_3^-$**	**NH_4^+**	**Tot N**	**$S0_4^+$**	**Na**	**K**	**Ca**	**Al**	**As**	**Cd**	**Cr**	**Co**	**Cu**	**Pb**	**Mg**	**Hg**	**Ni**	**Se**	**Ag**

Table A1.5b: Kendal Tau correlation coefficients among environmental variables in sediment samples. Underline numbers represent –ve correlation. *: p<0.1; **:p<0.05 and ***: p<0.01

$N0_3^-$											
NH_4^+											
Tot N	0.4 **		0.8 **								
$S0_4^+$			0.6 **								
TOC											
Na											
K							0.5 **				
Ca	0.6 **	0.5 **	0.7 **					0.6 **			
Al		0.8 **							0.6 **		
As								0.4 *			
Co											

Cu			0.5 **	0.4 *					0.6 **			0.7 **							
Pb										0.4 *	0.6 **								
Mg			0.4 *					0.6 **	0.8 **	0.5 **		0.5 **	0.6 **						
Hg											0.7 **			0.4 *					
Ni									0.8 **			0.5 **	0.5 **		0.7 **	0.4 *			
Se								0.6 **			0.8 **					0.9 **			
Ag											0.6 **						0.4 *	0.4 *	
Zn													0.7 **						
	$N0_2^-$	**$N0_3^-$**	**NH_4^+**	**Tot N**	**$S0_4^+$**	**TOC**	**Na**	**K**	**Ca**	**Al**	**As**	**Co**	**Cu**	**Pb**	**Mg**	**Hg**	**Ni**	**Se**	**Ag**

Appendix 2

Table A 2.1: Number of sub-families from individual phylum detected in the catchment

Phylum	Number of sub-families
Proteobacteria	620
Firmicutes	343
Bacteroidetes	247
Unclassified	226
Chloroflexi	111
Planctomycetes	95
Cyanobacteria	91
Actinobacteria	89
Acidobacteria	85
Verrucomicrobia	42
Others	155

Table A 2.2: Gene variants detected in the catchment as a percent of number of probes present on GeoChip.

	All genes	Varying genes	Top 10% (based on abundance)
Antibiotic resistance	49.06	4.55	5.98
Organic remediation	48.46	6.08	4.79
Metal resistance	44.11	6.98	5.34
Phosphorus cycling	39.73	5.84	4.17
Energy processes	38.58	2.76	2.36
Sulfur cycling	36.50	4.85	3.59
Carbon cycling	36.34	4.62	2.98
Nitrogn cycing	35.64	5.08	2.79
Gyrase B	29.59	5.54	3.41

Table A2.3: PERMANOVA and ANOSIM Tables for testing differences between functional genes from two major land-use type groups and sediment/water pahse

PERMANOVA based on Bray–Curtis similarity measure for square root transformed relative abundances of functional gene abundance				
Source	df	MS	Pseudo-F	P(perm)
Land-use	1	2244.5	2.2105	0.0157
Res	16	1015.4		

PERMANOVA based on Jaccard similarity measure for sub-family presence/absence				
Source	df	MS	Pseudo-F	P(perm)
Phase	1	6886.5	2.6168	0.0001
Res	24	2631.7		

One way ANOSIM on residential and industrial dominated groups of functional gene abundance	
Mean rank within groups	58.19
Mean rank between groups	93.72
R	0.464
p (same)	0.0004
Bonferroni corrected p value	0.0009

One way ANOSIM on sediment and water groups of sub-family presence/absence	
Mean rank within groups	138.4
Mean rank between groups	186
R	0.2925
p (same)	0.0003
Bonferroni corrected p value	0.0003

Appendix 3

Table A3.1. PERMANOVAs based on Bray–Curtis similarity measure for square root transformed relative abundances of Bacteria and Archaea genus

A

		Relative abundance		
Source	*df*	MS	pseudo*F*	*p*(perm)
La	1	395.51	1.9168	0.18
Pr	1	201.15	1.2813	0.38
Ra	1	278.31	0.61444	0.61
Lo(La)	2	248.41	0.54843	0.77
LaxPr	1	44.928	0.91281	0.56
LaxRa	1	194.23	0.42882	0.71
PrxRa	1	148.13	1.6909	0.27
PrxLo(La)	2	77.232	0.8816	0.57
RaxLo(La)	2	452.95	45.551	*<0.01*
LaxPrxRa	1	67.959	0.77574	0.51
PrxRaxLo(La)	2	87.605	8.8099	*<0.01*
Res	32	9.9438		

B

Contrasts (Pre vs Post rain)	
Group	*p* (MC)
E1R1	*<0.01*
E1R2	*0.01*
E2R1	0.07
E2R2	*0.01*
E1I1	*<0.01*
E1I2	*0.02*
E2I1	0.09
E2I2	*<0.01*

Table A3.2. PERMANOVAs based on Jaccard similarity for presence/absence of Bacteria and Archaea genus

		Relative abundance		
Source	*df*	MS	pseudo*F*	*p*(perm)
La	1	33.661	1.9101	0.17
Pr	1	11.194	1.0053	0.50
Ra	1	17.173	0.56268	0.65
Lo(La)	2	16.542	0.54201	0.78
LaxPr	1	5.4164	0.67992	0.70
LaxRa	1	17.059	0.55894	0.65
PrxRa	1	8.2606	1.2792	0.36
PrxLo(La)	2	9.2985	1.4399	0.31
RaxLo(La)	2	30.52	4.7387	*<0.01*
LaxPrxRa	1	8.1656	1.2645	0.38
PrxRaxLo(La)	2	6.4577	1.0027	*0.40*
Res	32	6.4404		

Table A3.3. PERMANOVAs based on Bray–Curtis similarity measure for square root transformed relative abundances of all species

A

		Relative abundance		
Source	*df*	MS	pseudo*F*	*p*(perm)
La	1	419.9	1.736	0.18
Pr	1	208.49	1.4608	0.31
Ra	1	328.18	0.69074	0.57
Lo(La)	2	277.81	0.58472	0.77
LaxPr	1	97.215	1.4793	0.32
LaxRa	1	237.76	0.50042	0.68
PrxRa	1	159.49	0.93436	0.48
PrxLo(La)	2	100.08	0.58632	0.75
RaxLo(La)	2	475.12	12.687	*<0.01*
LaxPrxRa	1	81.018	0.47463	0.67
PrxRaxLo(La)	2	170.7	4.5581	*<0.01*
Res	32	37.449		

B

Contrasts (Pre vs Post rain)	
Group	*p* (MC)
E1R1	*0.22*
E1R2	*0.02*
E2R1	0.09
E2R2	*0.05*
E1I1	*0.02*
E1I2	*0.03*
E2I1	0.13
E2I2	*0.09*

Table A3.4. PERMANOVAs based on Jaccard similarity for presence/absence of all species

		Relative abundance		
Source	*df*	MS	pseudo*F*	*p*(perm)
La	1	267.48	1.2172	0.30
Pr	1	189.51	1.2848	0.36
Ra	1	228.64	0.82407	0.55
Lo(La)	2	279.77	1.0084	0.47
LaxPr	1	108.14	1.0795	0.46
LaxRa	1	167.92	0.60524	0.66
PrxRa	1	113.12	0.72306	0.57
PrxLo(La)	2	156.15	0.99806	0.51
RaxLo(La)	2	277.45	2.8854	*<0.01*
LaxPrxRa	1	88.954	0.56858	0.65
PrxRaxLo(La)	2	156.45	1.627	0.10
Res	32	96.156		

Table A3.5. PERMANOVAs based on Bray–Curtis similarity measure for square root transformed relative abundances of all Genus

A

		Relative abundance		
Source	*df*	MS	pseudo*F*	*p*(perm)
La	1	445.77	1.8289	0.18
Pr	1	188.08	1.4171	0.31
Ra	1	291.33	0.60969	0.62
Lo(La)	2	269.35	0.56369	0.78
LaxPr	1	78.688	1.4305	0.33
LaxRa	1	235.66	0.49319	0.67
PrxRa	1	148.74	0.99816	0.45
PrxLo(La)	2	89.131	0.59816	0.75
RaxLo(La)	2	477.83	17.152	*<0.01*
LaxPrxRa	1	70.045	0.47007	0.68
PrxRaxLo(La)	2	149.01	5.3489	*<0.01*
Res	32	27.858		

B

Contrasts (Pre vs Post rain)	
Group	*p* (MC)
E1R1	0.21
E1R2	*0.01*
E2R1	0.08
E2R2	0.04
E1I1	*<0.01*
E1I2	*0.02*
E2I1	0.10
E2I2	0.06

Table A3.6. PERMANOVAs based on Jaccard similarity for presence/absence of all Genus

		Relative abundance		
Source	*df*	MS	pseudo*F*	*p*(perm)
La	1	48.933	1.37	0.28
Pr	1	28.396	1.2664	0.37
Ra	1	41.854	0.83467	0.51
Lo(La)	2	36.169	0.72129	0.69
LaxPr	1	29.828	1.2405	0.40
LaxRa	1	36.15	0.72091	0.55
PrxRa	1	17.138	0.61923	0.63
PrxLo(La)	2	27.14	0.98065	0.52
RaxLo(La)	2	50.145	2.8574	*0.01*
LaxPrxRa	1	19.215	0.6943	0.55
PrxRaxLo(La)	2	27.676	1.5771	0.13
Res	32	17.549		

Table A3.7. PERMANOVAs based on Bray–Curtis similarity measure for square root transformed relative abundances of metabolism level KEEG functions (Level2)

		Relative abundance		
Source	*df*	MS	pseudo*F*	*p*(perm)
La	1	34.768	1.2753	0.34
Pr	1	6.6875	0.71338	0.63
Ra	1	20.59	1.8236	0.26
Lo(La)	2	18.608	1.647	0.25
LaxPr	1	8.8073	0.9528	0.52
LaxRa	1	17.519	1.5516	0.30
PrxRa	1	7.3952	3.6994	0.12
PrxLo(La)	2	4.7835	2.3923	0.20
RaxLo(La)	2	11.298	8.873	*<0.01*
LaxPrxRa	1	6.5606	3.2819	0.14
PrxRaxLo(La)	2	1.9996	1.5704	0.18
Res	27	1.2733		

Table A3.8. PERMANOVAs based on Bray–Curtis similarity measure for square root transformed relative abundances of pathway level KEEG functions (Level3)

A

		Relative abundance		
Source	*df*	MS	pseudo*F*	*p*(perm)
La	1	80.055	1.5245	0.27
Pr	1	17.03	0.98979	0.51
Ra	1	103.83	2.9092	0.15
Lo(La)	2	42.379	1.1866	0.37
LaxPr	1	15.01	0.85796	0.56
LaxRa	1	33.572	0.94066	0.45
PrxRa	1	13.905	1.8933	0.25
PrxLo(La)	2	10.726	1.4598	0.35
RaxLo(La)	2	35.713	11.759	*<0.01*
LaxPrxRa	1	15.334	2.0879	0.25
PrxRaxLo(La)	2	7.3475	2.4193	*0.04*
Res	27	3.0371		

B

Contrasts (Pre vs Post rain)	
Group	*p* (MC)
E1R1	*0.01*
E1R2	0.30
E2R1	0.27
E2R2	*0.02*
E1I1	*0.02*
E1I2	0.05
E2I1	0.07
E2I2	*0.04*

Table A3.9. PERMANOVAs based on Bray–Curtis similarity measure for square root transformed relative abundances of KO level KEEG functions (Last level)

A		Relative abundance			B	Contrasts (Pre vs Post rain)	
Source	*df*	MS	pseudo*F*	*p*(perm)		Group	*p* (MC)
La	1	124.17	1.6262	0.21		E1R1	*0.04*
Pr	1	42.775	1.1589	0.41		E1R2	0.10
Ra	1	138.42	1.3122	0.34		E2R1	0.19
Lo(La)	2	94.05	0.89099	0.61		E2R2	*0.03*
LaxPr	1	24.132	1.0358	0.47		E1I1	0.05
LaxRa	1	47.238	0.44781	0.71		E1I2	0.05
PrxRa	1	33.484	1.1902	0.39		E2I1	0.10
PrxLo(La)	2	27.715	0.9846	0.50		E2I2	*0.05*
RaxLo(La)	2	105.56	11.948	*<0.01*			
LaxPrxRa	1	22.756	0.80885	0.53			
PrxRaxLo(La)	2	28.148	3.1861	*<0.01*			
Res	27	8.8346					

Table A3.10. PERMANOVAs based on Bray–Curtis similarity measure for square root transformed relative abundances of metabolism level SEED functions (Level2)

A		Relative abundance			B	Contrasts (Pre vs Post rain)	
Source	*df*	MS	pseudo*F*	*p*(perm)		Group	*p* (MC)
La	1	37.537	1.5579	0.23		E1R1	*0.01*
Pr	1	6.6332	1.0154	0.50		E1R2	0.08
Ra	1	8.7745	0.43485	0.71		E2R1	0.28
Lo(La)	2	24.401	1.2085	0.39		E2R2	0.06
LaxPr	1	3.8365	0.86408	0.58		E1I1	*0.04*
LaxRa	1	12.662	0.6275	0.61		E1I2	0.10
PrxRa	1	5.639	1.071	0.42		E2I1	0.34
PrxLo(La)	2	6.0825	1.1546	0.44		E2I2	*0.01*
RaxLo(La)	2	20.192	14.742	*<0.01*			
LaxPrxRa	1	4.4544	0.84598	0.50			
PrxRaxLo(La)	2	5.2683	3.8463	*<0.01*			
Res	27	1.3697					

Table A3.11. PERMANOVAs based on Bray–Curtis
measure for square root transformed relative
es of pathway level SEED functions (Level3)

A		Relative abundance			B	Contrasts (Pre vs Post rain)	
Source	*df*	MS	pseudo*F*	*p*(perm)		Group	*p* (MC)
La	1	82.282	1.7413	0.20		E1R1	*0.02*
Pr	1	25.135	1.1745	0.42		E1R2	0.05
Ra	1	33.747	0.49991	0.68		E2R1	0.21
Lo(La)	2	55.034	0.81467	0.63		E2R2	*0.04*
LaxPr	1	9.0702	0.87673	0.57		E1I1	*0.05*
LaxRa	1	31.024	0.45957	0.69		E1I2	0.05
PrxRa	1	19.078	1.3423	0.34		E2I1	0.21
PrxLo(La)	2	14.433	1.0149	0.48		E2I2	*0.02*
RaxLo(La)	2	67.553	18.613	*<0.01*			
LaxPrxRa	1	12.131	0.85355	0.50			
PrxRaxLo(La)	2	14.221	3.9183	*<0.01*			
Res	27	3.6293					

Table A3.12. PERMANOVAs based on Bray–Curtis similarity measure for square root transformed relative abundances of KO level SEED functions (Last level)

A		Relative abundance			B	Contrasts (Pre vs Post rain)	
Source	*df*	MS	pseudo*F*	*p*(perm)		Group	*p* (MC)
La	1	122.61	1.6473	0.20		E1R1	*0.03*
Pr	1	44.399	1.1913	0.41		E1R2	0.06
Ra	1	60.874	0.54018	0.65		E2R1	0.16
Lo(La)	2	87.01	0.77158	0.66		E2R2	*0.05*
LaxPr	1	15.905	0.9505	0.53		E1I1	*0.04*
LaxRa	1	55.894	0.49599	0.68		E1I2	0.05
PrxRa	1	35.749	1.3986	0.33		E2I1	0.17
PrxLo(La)	2	22.987	0.89883	0.57		E2I2	*0.04*
RaxLo(La)	2	112.77	16.281	*<0.01*			
LaxPrxRa	1	20.65	0.80788	0.53			
PrxRaxLo(La)	2	25.574	3.6924	*<0.01*			
Res	27	6.9263					

Symbol	Interpretation	Levels
La	Land-use	Residential (R); Industrial (I)
Pr	Before & after rain	Pre rain (Pr); Post rain (Po)
Ra	Rain event	Event1 (E1); Event2 (E2)
Lo	Location	Location1 (1); Location2 (2)

Land-use and Pre/Post rain were fixed with two levels; Rain event and Location were random. Location was nested in land-use, with two levels and Rain event was orthogonal with two levels. The samples were collected from five spots at a location and pooled (n = 3). P values were calculated using 9,999 permutations under a reduced model. Italicised values are those statistically significant with significance level alpha=0.05 (i.e. those with $p < 0.05$)

Appendix 4

Table A6.1: PERMANOVA table of results: Main test

Source	df	SS	MS	Pseudo-F	P(perm)	Unique perms
La	2	5968.2	2984.1	1.7496	0.0503	2469
Day	9	222270	24697	17.366	0.0001	9870
Re (La)	6	10234	1705.7	4.4911	0.0001	9860
LaxDay	18	32321	1795.6	1.2624	0.0215	9729
Re(La)xDay	54	76854	1423.2	3.7473	0.0001	9589
Residual	179	67985	379.8			
Total	268	414240				

Land-use: La, Reactor: Re

Table A6.2: Pairwise tests: Term 'Re(La)xDa' for pairs of levels of factor 'Day'. Sums of squares type: Type III (partial). Fixed effects sum to zero for mixed terms. Permutation method: Permutation of residuals under a reduced model. Number of permutations: 9999

Reactor 1	Industrial			
Groups	t	P(perm)	Unique perms	P(MC)
30, 16	1.8418	0.1007	10	0.068
12, 16	1.9057	0.0947	10	0.0566
12, 20	1.6266	0.1006	10	0.1348
12, 25	1.6652	0.1041	10	0.1121
Reactor 2	Industrial			
30, 16	1.2914	0.1029	10	0.2075
0, 4	1.5654	0.0967	10	0.1307
Reactor 3	Industrial			
30, 16	1.3616	0.1	10	0.1645
0, 4	2.1749	0.1018	10	0.0516
Reactor 4	Mixed			
30, 12	2.0241	0.1006	10	0.0596
30, 16	1.6331	0.2009	10	0.1223
0, 12	2.2023	0.1029	10	0.0521
1, 3	1.8022	0.1035	10	0.079
1, 12	1.7432	0.0996	10	0.0907
3, 12	1.9296	0.0999	10	0.0716
8, 12	2.2981	0.0991	10	0.0525
12, 16	2.178	0.1019	10	0.0531
12, 20	2.19	0.099	10	0.0503

12, 25	2.2042	0.101	10	0.0501
Reactor 5	Mixed			
30, 12	2.0241	0.1006	10	0.0596
30, 16	1.7236	0.0937	10	0.0672
0, 4	1.7685	0.1009	10	0.1012
Reactor 6	Mixed			
30, 16	1.6698	0.0979	10	0.0714
8, 16	1.7247	0.1022	10	0.0737
Reactor 7	Residential			
0, 1	1.7507	0.099	10	0.0678
0, 3	1.4265	0.2011	10	0.1696
0, 4	1.4987	0.0994	10	0.1521
1, 3	1.6291	0.0971	10	0.1168
Reactor 8	Residential			
30, 8	1.8351	0.0994	10	0.0697
0, 4	1.3768	0.1019	10	0.1941
Reactor 9	Residential			
30, 16	1.7809	0.1004	10	0.0591
8, 16	1.7107	0.0932	10	0.0691

Table A6.3 ANOSIM table for global and pairwise tests of differences between days across all sediment type groups using TRF peak height data.

Global Test

Sample statistic (Global R)	0.749
Significance level of sample statistic	0.01%
Number of permutations	9999
Number of permuted statistics greater than or equal to Global R	0

Pairwise Tests

Days	R Statistic	Significance Level %	Actual Permutations	Number >= Observed
30, 0	0.824	0.01	9999	0
30, 1	0.869	0.01	9999	0
30, 3	0.901	0.01	9999	0
30, 4	0.981	0.01	9999	0
30, 8	0.782	0.01	9999	0
30, 12	0.661	0.01	9999	0

30, 16	0.691	0.01	9999	0
30, 20	0.937	0.01	9999	0
30, 25	0.822	0.01	9999	0
0, 1	0.708	0.01	9999	0
0, 3	0.609	0.01	9999	0
0, 4	0.534	0.01	9999	0
0, 8	0.743	0.01	9999	0
0, 12	0.724	0.01	9999	0
0, 16	0.82	0.01	9999	0
0, 20	0.985	0.01	9999	0
0, 25	0.85	0.01	9999	0
1, 3	0.569	0.01	9999	0
1, 4	0.847	0.01	9999	0
1, 8	0.775	0.01	9999	0
1, 12	0.701	0.01	9999	0
1, 16	0.821	0.01	9999	0
1, 20	0.947	0.01	9999	0
1, 25	0.782	0.01	9999	0
3, 4	0.841	0.01	9999	0
3, 8	0.83	0.01	9999	0
3, 12	0.706	0.01	9999	0
3, 16	0.873	0.01	9999	0
3, 20	0.984	0.01	9999	0
3, 25	0.837	0.01	9999	0
4, 8	0.948	0.01	9999	0
4, 12	0.726	0.01	9999	0
4, 16	0.989	0.01	9999	0
4, 20	1	0.01	9999	0
4, 25	0.848	0.01	9999	0
8, 12	0.679	0.01	9999	0
8, 16	0.859	0.01	9999	0
8, 20	0.996	0.01	9999	0
8, 25	0.853	0.01	9999	0
12, 16	0.659	0.01	9999	0
12, 20	0.32	0.01	9999	0
12, 25	0.386	0.01	9999	0
16, 20	0.94	0.01	9999	0
16, 25	0.847	0.01	9999	0
20, 25	0.523	0.01	9999	0

Table A6.4 ANOSIM table for pairwise tests of differences between sediment types within all time-points (days) using TRF peak height data.

Day	Land use	R	Significance Level %	Possible Permutations	Actual Permutations	Number >= Observed
Day0	I, M	0.064	13.4	24310	9999	1334
	I, R	0.178	0.7	24310	9999	70
	M, R	0.019	31.6	24310	9999	3160
Day1	I, M	0	40.2	24310	9999	4018
	I, R	0.147	1.6	24310	9999	155
	M, R	0.011	38.9	24310	9999	3889
Day3	I, M	0.249	0.2	24310	9999	22
	I, R	0.349	0.02	24310	9999	1
	M, R	0.16	1.6	24310	9999	157
Day4	I, M	0.223	0.1	24310	9999	13
	I, R	0.381	0.01	24310	9999	0
	M, R	0.249	0.07	24310	9999	6
Day8	I, M	0.375	0.01	24310	9999	0
	I, R	0.64	0.01	24310	9999	0
	M, R	0.468	0.01	24310	9999	0
Day12	I, M	0.085	9.2	24310	9999	923
	I, R	0.33	0.2	24310	9999	17
	M, R	0.203	1.2	24310	9999	115
Day16	I, M	0.041	25.6	24310	9999	2558
	I, R	0.23	0.5	24310	9999	46
	M, R	0.225	1.1	24310	9999	108
Day20	I, M	0.26	0.3	24310	9999	29
	I, R	0.522	0.01	24310	9999	0
	M, R	0.478	0.01	24310	9999	0
Day25	I, M	0.339	0.05	24310	9999	4
	I, R	0.482	0.02	24310	9999	1
	M, R	0.702	0.02	24310	9999	1
Day30	I, M	0.165	4	24310	9999	396
	I, R	0.217	2.6	24310	9999	258
	M, R	-0.004	42.1	24310	9999	4213

Table A6.5 correlation between mRNA abundance and metals levels in 36 sediment samples from residential and industrial sediment type and 6 time-points

	Mg	Al	Cr	Fe	Co	Ni	Cu	Zn	As	Cd	Hg	Pb
Pearson's r	-0.29	0.7	0.78	-0.08	0.32	0.85	-0.06	0.01	0.62	0.72	0.1	0.26
pvalue	0.36	0.01	0	0.8	0.32	0	0.86	0.98	0.03	0.01	0.75	0.42